REDUCING THE EFFECT OF BALL VARIATION IN BAT PERFORMANCE MEASUREMENTS

By

WARREN LELAND FABER

A thesis submitted in partial fulfillment of
the requirements for the degree of

MASTERS OF SCIENCE IN MECHANICAL ENGINEERING

WASHINGTON STATE UNIVERSITY
Department of Mechanical and Materials Engineering

DECEMBER 2010

To the Faculty of Washington State University:

The members of the Committee appointed to examine the thesis of WARREN LELAND FABER find it satisfactory and recommend that it be accepted.

_____

Lloyd V. Smith, Ph.D., Chair

_____

Jow-Lian Ding, Ph.D.

_____

Alan M. Nathan, Ph.D.

ACKNOWLEDGMENT

I would first like to thank my family, especially my parents Kent and Lelia Faber, for the continued support I have received throughout my academic career. Without their encouragement I would not have made it this to this point.

Then, I would like to thank Dr. Lloyd Smith for giving me an opportunity to continue my education and making this research possible. I would like to thank Dr. Alan Nathan for his support and ideas. I would like to thank Dr. Jow-Lian Ding for being on my research committee and being there if I needed help with numerical analysis.

I thank the faculty and staff at WSU in the department of Mechanical and Materials Engineering, namely, Bob, Jan, Gayle, Mary, Shandi, Michelle, and Annette, their dedication was vital to the wellbeing of the lab.

I would also like to thank all of my colleagues Andy Bryson, Jeff Kensrud, Jason Martin, Steve Edburg, Jeff Burke, Chris Detzel, Brian Edgmon and everyone who came before me, thanks for laying the ground work and showing me the way. Thanks to everyone that worked in the lab (past and present), Nick, Ryan, Chris, Peter, Tj, and Anthony.

Lastly, I would like to thank all of my friends I have met over the 6 years I have been at WSU. I could always count on them to distract me and help me relax when school or research was frustrating and stressful, at least for a little while. Go Cougs.

REDUCING THE EFFECT OF BALL VARIATION IN BAT

PERFORMANCE MEASUREMENTS

Abstract

by Warren Leland Faber, M.S.
Washington State University
December 2010

Chair: Lloyd V. Smith

The performance of softball bats depend on the properties of the ball. Three of these ball properties are the weight, elasticity and stiffness. They vary with the type of material used in the manufacturing. It is desired to remove these properties from standardized testing.

Previous work has shown that weight dependence is readily accounted for in bat performance measurements. Attempts to remove elasticity and stiffness dependence have not been successful. The following analyzes a method to determine bat performance, independent of the ball. Elasticity of the ball was accounted for through a cylindrical coefficient of restitution (CCOR). Ball stiffness (k_T) was found from a high speed impact and calculated using four different techniques. All four approaches maintained relatively the same trend.

Three bats varying in performance were compared with a large range of different ball types. In some cases the normalizing technique eliminated the ball properties from the bat performance however, in other cases it did not. The procedure for removing CCOR worked for a wider range of balls than k_T. Overall, with the different ball models a medium performance bat had a range in Batted Ball Speed (BBS) from 104 mph to 93 mph. The range in the normalized BBS reduced to from 98 mph to 92 mph. Balls with low k_T and balls with a combined low CCOR and high k_T provided the largest range in BBS.

A numerical model was developed and analyzed bat-ball impacts in more detail than was possible experimentally. In the model the BBS of a medium performance bat had a range from 105 mph to 92 mph, the normalized BBS had a range from 99 mph to 94 mph (similar to the experimental results). It was found that during impact the effective bat stiffness changed with k_T and the bat was not elastic (a common assumption). A technique was developed to account for the changes in bat stiffness that reduced the range in normalized BBS to between 97 mph and 95 mph. The improvement demonstrated that the effect of the ball in the bat stiffness is the primary limitation of normalizing bat performance.

TABLE OF CONTENTS

LIST OF TABLES

LIST OF FIGURES

Dedication

To those who dedicate their lives trying to understand the laws of nature and to those who spend their lives playing games governed by them.

CHAPTER ONE

INTRODUCTION

Advancements in technology in the past several decades have significantly improved the performance of baseball and softball bats. Baseball and softball bats began as wood clubs. As players desired to hit the ball faster and farther bat manufactures started to experiment with other materials. Using metal to make a bat can be traced back as far as the early as the 1920's [1.1] but did not get implemented until the late 1960's and early 1970's [1.2]. Using a hollow double wall aluminum bat greatly improved the distance of batted balls due to the elastic properties and relative light weight of the material. The 90's saw bats made out of titanium, these bats were so successful in increasing performance they were temporarily outlawed [1.3].

Bat performance may be measured a number of different ways. Different methods of determining bat performance are subject to experimental error, depending on the type of test and the method of quantifying the data. There is interest to improve the accuracy and repeatability of these methods.

Softball bats today are made primarily from wood, aluminum, titanium and composite materials. The high performance bats are hollow and have multiple walls, and in general have lower barrel stiffness than their low performing counterparts. The reduction in barrel stiffness causes the bat to absorb some of the bat-ball impact force reducing the deformation of the ball upon impact. The reduction in ball deformation allows the ball to retain its energy. Wood bats are solid and do not deform much when hit with a baseball or softball. However, hollow aluminum, titanium, and composite bats will deform when hit with a baseball or softball much

like when a tennis racket contacts a tennis ball. The bat absorbs this energy and returns it back to the ball after impact resulting in higher rebound speed, this is commonly referred to as the trampoline effect [1.4]. While other factors contribute in bat performance the trampoline effect dominates. Bat performance is dependent on the properties of the ball. The ball, in turn, has variation inherent in its manufacturing process. To improve the repeatability of bat performance measurements, it is desirable to remove the ball dependence. Three properties of the ball, namely weight, stiffness, and elasticity have been shown to effect bat performance. The following will evaluate the effectiveness of the methods that reduce the effect of the ball in bat performance measurements.

Bat performance is a joint property of the bat and ball. A baseball is made from wrapped yarned wrapped around a rubber pill with leather or synthetic covering. The response of a baseball is affected by the properties of the rubber pill and yarn tension. A softball is made from a polyurethane core and leather or synthetic cover. The response of a softball is affected by the formulation of the polyurethane. These advancements in technology increased the level of offense in play. In an effort to keep offense and defense sides of play fair, regulating agencies have placed limits on the performance of the bats and balls. Each league that a player participates in is subject to its own regulation.

The bat performance test can be modeled using numerical methods. By carefully choosing the properties of the bat and ball the numeric models do an excellent job in describing the bat performance test [1.5]. The following uses a numeric model to study bat-ball impact forces and displacements that cannot be measured experimentally. The results help explain limitations in removing the effect of the ball in bat performance measurements.

REFERENCES

[1.1] **Hill, Bob.** *The Louisville Slugger Story.* Champaign : Sports Publishing Inc., 2000.

[1.2] **Shroyer, William.** *Baseball Bat. 1499128* US, May 27, 1922.

[1.3] **Dickson, Paul.** *The Worth Book Of Softball: A Celebration Of America's True National Pastime.* New York : Facts On File, Inc, 1994.

[1.4] **A Nathan, D. Russel, L. Smith.** *The Physics of the Trampoline Effect in Baseball and Softball Bats.* Davis : s.n., 2004. The Engineering of Sport 5th International Conference. Vol. 2, pp. 33-44.

[1.5] **Duris, J. G.** Experimental and Numerical Characterization of Softballs. *Master's Thesis, Washington State University.* 2004.

CHAPTER TWO

LITERATURE REVIEW

2.1 Ball Performance Metrics

To determine bat performance, it is necessary to understand the properties of the ball. Baseballs are made from yarn wrapped around a rubber or cork core with a synthetic or leather cover that is sown together. Softballs are made from polyurethane with a synthetic or leather as seen in figure 2.1. Both types of balls are non-linear by their geometry and material and are subject to manufacturing variations.

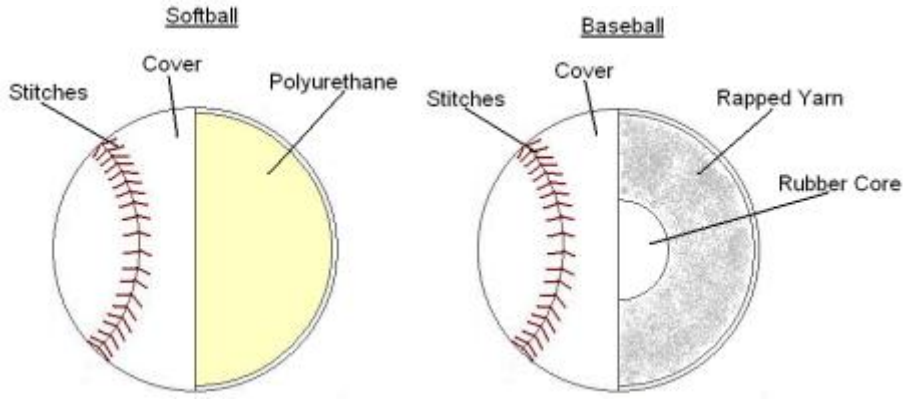

Figure 2.1: Softball showing the polyurethane and baseball showing the rapped yarn and rubber core.

Three properties of a ball that affect bat performance are: weight, stiffness, and elasticity. A heaver ball will rebound off a bat slower than a lighter ball due to its mass. The elasticity of the ball affects the amount of energy lost from the impact. The more energy lost the slower the ball will rebound off of the bat. Ball stiffness affects the performance of hollow bats through the

trampoline effect that will be described in section 2.2.1. The following section describes standardized tests to measure each of these properties.

2.1.1. Coefficient of Restitution

The elasticity of the ball is measured from its coefficient of restitution (COR), e_0, which describes the amount of energy loss from an impact between two objects. It can be defined as "the negative of the ratio of the relative normal velocity after impact to that before impact [2.1]." It can be given as,

$$\boldsymbol{e_0 = -\frac{v_1 - v_2}{V_1 - V_2}} \qquad (2.1)$$

where, $v_1 - v_2$ is the relative velocity of the objects immediately after collision and $V_1 - V_2$ is the relative velocity of the objects immediately before collision. For a perfectly elastic collision where there would be no energy loss, $e_0 = 1$, and for a perfectly inelastic collision where all the energy is dissipated, and $e_0 = 0$. For a collision where the second object is fixed, i.e. $v_2 = V_2 = 0$, equation 2.1 reduces to,

$$\boldsymbol{e = -\frac{v_1}{V_1}} \qquad (2.2)$$

ASTM F 1887-02 describes a standardized method to measure ball COR using equation 2.2. Softballs are tested at 60 mph and pass through electronic speed monitors to record the incoming and rebound velocities from impact with a rigid wall. A diagram of the COR testing apparatus is shown in figure 2.2.

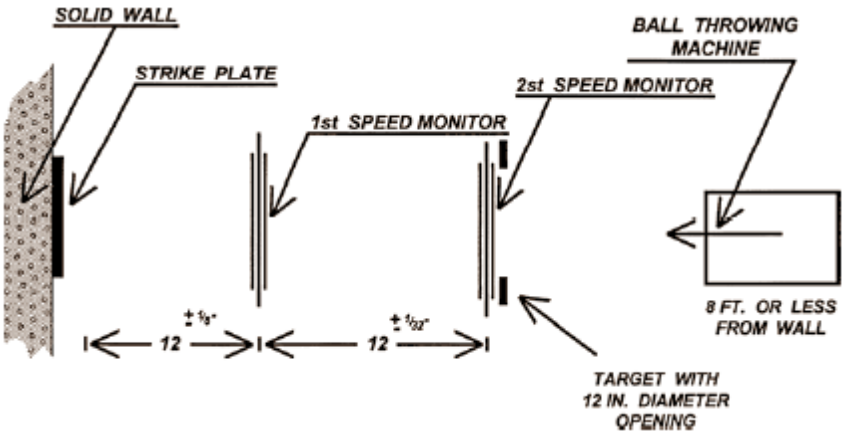

Figure 2.2: Diagram of ball COR test apparatus

2.1.2. Static Compression

Ball stiffness can be measured dynamically or quasi-statically. The quasi-static test, termed compression and is done by compressing a ball ¼ inch between two flat plates and measuring the peak force. ASTM F 1888-02 describes the standardized method to measure ball compression [2.2]. A picture of the compression testing apparatus is shown in figure 2.3.

Figure 2.3: Testing apparatus to measure ball compression

Quasi-static compression can only compare balls of similar size and material makeup. As the ball diameter increases, for instance, the contact area will also increase. Thus, for two balls that differ only in diameter, the larger ball will have higher compression. This result is often used incorrectly to claim that softballs are harder than baseballs [2.3].

2.1.3. Dynamic Stiffness and Cylindrical Coefficient of Restitution

The ball compression test of ASTM F-1888 uses a displacement rate that is about 10,000 times slower than occurs in play [2.3][2.4]. Because softballs are non-linear and have strain-rate dependence the stiffness found from compression is not be an accurate description of the ball in application to bat performance testing.

Previous studies have shown that the dynamic properties of baseballs and softballs can be accurately measured from impact tests [2.5][2.6][2.7][2.8]. Hendee, Greenwald, and Crisco tried unsuccessfully to correlate the compression of baseballs with their dynamic properties. The dynamic properties were found by firing baseballs from an air cannon at a rigidly mounted force plate. They found that energy losses during quasi-static compression differed from the dynamic energy losses [2.6]. Chauvin and Carlson used pressure sensitive film to record the impact pressure distribution of baseballs and softballs. They showed no correlation between compression and dynamic impact pressure. Smith used an air cannon and load cells mounted on the back of a half cylinder to find the dynamic stiffness (DS) of softballs. The dynamic stiffness was found by equating the initial kinetic energy of the ball to the potential energy at maximum displacement of the ball during impact.

The dynamic stiffness test was intended to describe the ball's response on a bat. Compression and COR do not take into account the non-linear geometry effects of a sphere impacting a cylinder [2.8]. ASTM F 2845 describes a standardized method to measure dynamic stiffness [2.9]. An apparatus of the dynamic stiffness test is depicted in figure 2.4

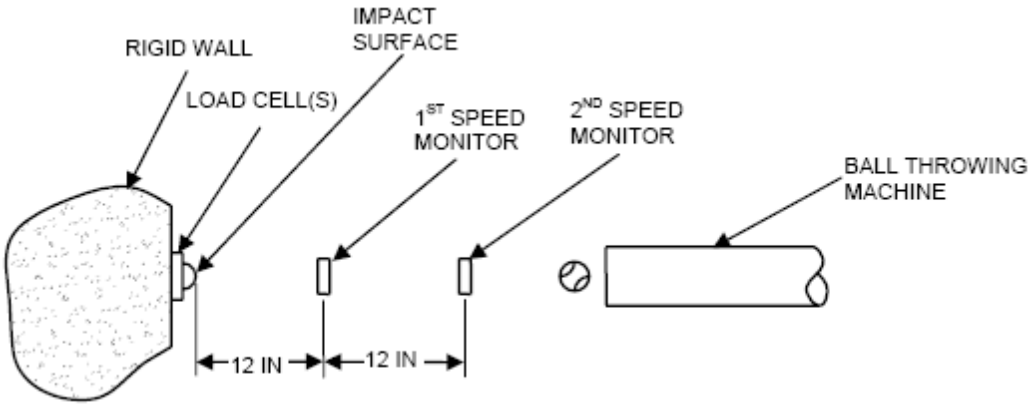

Figure 2.4: Schematic of the dynamic stiffness test apparatus

The ratio of outgoing and incoming velocities on a cylinder is called the cylindrical coefficient of restitution (CCOR) [2.8]. CCOR is less than COR because there is more energy loss during a collision with a cylinder than a flat plate. The COR and CCOR are a function of incoming velocity [2.1][2.4][2.10][2.11]. For the CCOR to describe a bat-ball collision, the incoming velocity must result in mimicking a recoiling bat impact condition. Smith tested the dynamic stiffness of a ball with a rigid half cylinder and with free cylinders of differing mass that recoil as they were impacted. When the speeds were matched correctly Smith found that the force-displacement curves were similar [2.8]. The relationship between the incoming ball speeds for the recoiling and fixed impact conditions is,

$$\boldsymbol{v_r = v_f \left(1 + \frac{m_b}{m_c}\right)^{1/2}} \tag{2.3}$$

where v_r, and v_f are the incoming ball speeds for the recoiling and fixed impact conditions respectively, and m_b and m_c are the mass of the ball and recoiling cylinders, respectively [2.7]. A dynamic stiffness test speed of 95 mph and 115 mph were found to represent a relative speed of 110 mph and 140 mph for softball and baseball, respectively [2.3].

2.2 Bat Performance

2.2.1. Trampoline Effect

In order to determine the performance of a bat the physics of a bat-ball collision must be understood. Cross examined tennis racket and tennis ball collisions with balls of varying COR. Cross showed that the elastic properties of the racket strings can increase the rebound speed of the tennis ball even if the tennis ball has a low COR. This is because the strings in a tennis racket absorb most of the impact energy and then return the energy back to the ball [2.10]. Nathan, Russell and Smith applied Cross's work to baseball and softball bats [2.12]. The collision may be described as colliding point masses, where the bat and ball have stiffness k_{bat} and k_{ball}, respectively, as shown in figure 2.5 [2.12].

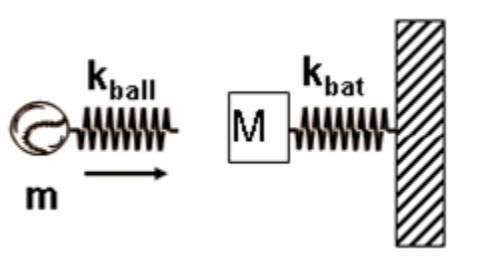

Figure 2.5: Illustration showing the bat and ball spring model

If the bat is hollow (aluminum bat) it acts like a spring and upon collision the bat and ball mutually compress each other, so some of the ball's initial energy goes into compressing the bat instead of the ball. Therefore less energy gets stored and dissipated in the ball and the compressional energy stored in the bat is returned to the ball resulting in a higher rebound speed than with a wood bat [2.12]. This is analogous to what happens with a trampoline and appropriately, it is called the trampoline effect. This is why hollow bats have increased performance compared with a wood bat.

2.2.2. Barrel Stiffness

Given the importance of bat stiffness, it is helpful to compare the stiffness of bat barrels. Although the barrel stiffness is not an official measure of bat performance it provides an idea of how the bat will behave. For example, the lower the barrel stiffness the more the bat will compress during a ball impact and increase the trampoline effect resulting in a higher ball exit velocity.

A schematic of a bat barrel compression test can be seen in figure 2.6. The test is similar to ball compression where a force is recorded from a given displacement. It is therefore referred to as barrel compression.

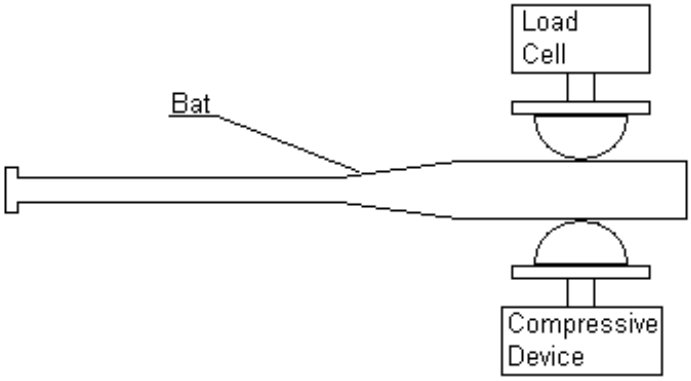

Figure 2.6: A Schematic showing the bat barrel compression test.

According to ASTM F 2884, the barrel compression is determined by compressing the barrel of a bat between two solid cylindrical surfaces with 1.93 inch radii (equivalent to that of a softball) at 6 inches from the end of the barrel to 0.050 inch defection and recording the force load that is reached. Then the bat is rotated 90° and the force and defection is recorded again. The barrel compression is the average between the two locations [2.13]. For softball bats, barrel compression can range from 300 lb to 500 lb [2.14].

2.2.3. Impact location

There is a so called "sweet spot" on the barrel that is at the location of highest performance. A common misconception is that the sweet spot of a hollow bat is at the bat's center of percussion (COP) [2.15]. The sweet spot is the result of the harmonic motion of the bat's natural oscillation and the distance from the axis of rotation [2.16]. The farther up the barrel the highest node of natural oscillation is, the higher performing the bat will be due to the increased bat velocity [2.17]. There are two types of vibration modes: flexural and hoop modes.

Flexural modes describe the bending along the perpendicular axis of the bat, while hoop modes describe the radial oscillation in the bat [2.18][2.19]. An illustration of the first and second bending modes can be seen in figure 2.7.

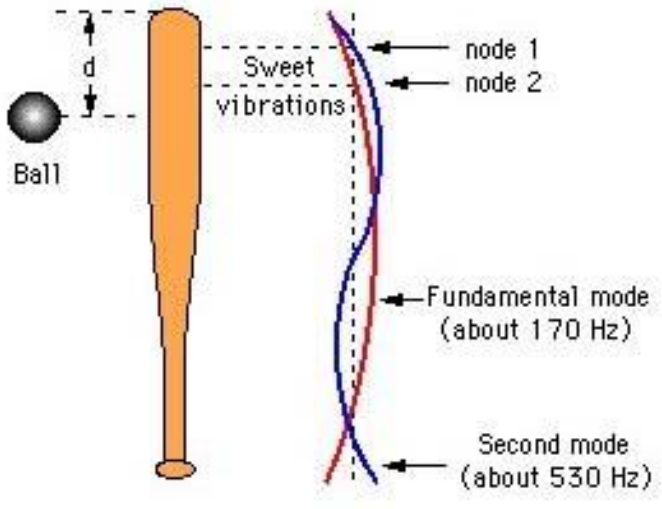

Figure 2.7: The first and second vibration modes of a baseball bat (from Cross [1.19]).

The effect bat velocity has on the impact location will be described in section 2.2.8.

2.2.4. Performance Testing

Bats have been tested a number of ways. Up until 2005 the NCAA used a complex machine that involved a swinging bat and a pitched ball [2.20]. Other testing machines have a moving bat and stationary ball. Currently, all certification processes involve firing a ball with a pneumatic cannon at a stationary bat placed on a pivot [2.3]. An example of a bat performance measurement test apparatus is seen in figure 2.8.

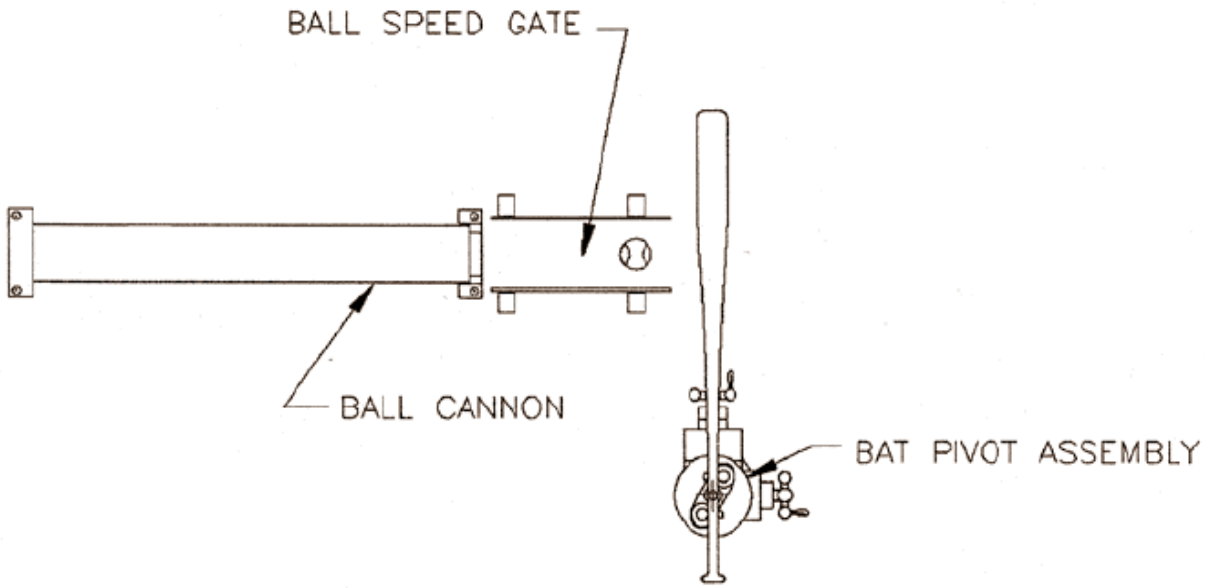

Figure 2.8: Apparatus of bat testing machine with pneumatic air cannon, ball speed gate and bat pivot assembly.

2.2.5. Bat-Ball Coefficient of Restitution

Some regulating agencies use the bat-ball coefficient of restitution (BBCOR), *e*, as a measure of bat performance [2.21]. The BBCOR is found through an angular momentum balance as [2.3],

$$-\boldsymbol{mv_i Q} + \frac{\boldsymbol{IV_i}}{\boldsymbol{Q}} = \boldsymbol{mv_r Q} + \frac{\boldsymbol{IV_r}}{\boldsymbol{Q}} \tag{2.4}$$

where, m is the mass of the ball, v_i and v_r are the incoming and rebound velocity of the ball respectively, Q is the distance from the pivot location to the impact point, V_i and V_r are the incoming and rebound velocity of the bat respectively, and I is the combined mass moment of inertia of the bat and pivot. All speeds are taken to be positive. For cases with the bat initially at rest, $V_i = 0$ and the rebound bat speed is found from,

$$\boldsymbol{V_r = (v_i + v_r) r_b} \tag{2.5}$$

where,

$$\boldsymbol{r_b = \frac{mQ^2}{I}} \tag{2.6}$$

The equation for *e* is,

$$\boldsymbol{e = \frac{v_r + V_r}{v_i}} \tag{2.7}$$

Substituting equation 2.5 for V_r in equation 2.7, *e* becomes,

$$\boldsymbol{e = \frac{v_r}{v_i} + \frac{r_b}{v_i I}(v_i + v_r)} \tag{2.8}$$

2.2.6. Ball Exit Speed Ratio

The NCAA uses the ball exit speed ratio (BESR) to measure bat performance. The BESR is found from the collision efficiency which is defined for a bat initially at rest by,

$$\boldsymbol{e_A \equiv \frac{v_r}{v_i}} \tag{2.9}$$

The BESR is then found by [2.22],

$$\boldsymbol{BESR = e_A + 0.5} \tag{2.10}$$

The NCAA and the National Federation of State High School Association (NFHS) use the BESR to regulate baseball bat performance.

2.2.7. Bat Performance Factor

The Bat Performance Factor (BPF) is an attempt to account for variation in the inherent elastic properties of the ball. The BPF however, does not account for the trampoline effect and assumes *e* is a property of the bat alone and independent of ball COR (e_0) which has been shown only to be true in wood and low performance bats [2.23]. The BPF is found from [2.24],

$$\boldsymbol{BPF} = \frac{\boldsymbol{e}}{\boldsymbol{e_0}} \tag{2.11}$$

The United States Specialty Sports Association (USSSA), the National Softball Association (NSA), and Little League Baseball use BPF to regulate bat performance. Studies have shown that it over-corrects for ball COR in medium to high performance bats [2.3] (i.e. those of most reliance in bat performance testing).

2.2.8. Bat Recoil Factor

The collision efficiency, e_A can also be derived by the conservation of momentum. The BBCOR, *e* and collision efficiency are not independent but related by the bat recoil factor r_b according to [2.21],

$$\boldsymbol{e_A} = \left(\frac{\boldsymbol{e}-\boldsymbol{r_b}}{\boldsymbol{1}+\boldsymbol{r_b}}\right) \tag{2.12}$$

The bat recoil factor depends on the inertial properties of the bat and ball [2.21]. Looking at the energy of the bat-ball collision, when the bat recoil factor is small, less energy is transferred to the bat and more energy is retained by the ball. The bat recoil factor gets smaller as the bat mass moment of inertia gets larger. In other words the more massive the bat is, the less it recoils from the collision, until the bat gets to a point where it is so massive it acts like a rigid object. As an

illustration of the implication of the bat recoil factor, suppose the bat MOI becomes very large then the bat recoil factor will become very small and the collision efficiency will become equal to *e*. On the other end of the spectrum if the bat MOI is very small the bat recoil factor becomes very large and the collision efficiency approaches -1. If the collision efficiency is -1 then the ball will pass through the bat and retain all of its kinetic energy.

2.2.9. Batted Ball Speed

The Batted Ball Speed (BBS) performance measure is intended to represent the speed a ball when hit in field conditions. The American Softball Association (ASA) has performed multiple field studies to determine the factors that affect slow and fast pitch softball in the field of play.

It was found that swing speed is independent of bat weight and dependent on the MOI. An idealized model that compares the rotational swing speeds of two bats (V_1 and V_2) having different MOI (I_1 and I_2) is given by,

$$\boldsymbol{V_1 = V_2 \left(\frac{I_2}{I_1}\right)^n} \tag{2.13}$$

The exponent, *n*, represents different idealized assumptions. For $n = 0$ the speed is constant and not affected by MOI. For $n = 1$ the angular momentum of the bat does not change with MOI [2.25]. The exponent for the MOI was 0.25 and 0.2 for the men's slow pitch and women's fast pitch respectively. To calculate the linear swing speed from the angular swing velocity the distance from the impact to the pivot point or center of rotation is needed. It was found in the field studies that the center of rotation of the bat during impact is close to the center of the

batter's lower wrist. The average location of the center of rotation of men's slow pitch and women's fast pitch is given in figure 2.9.

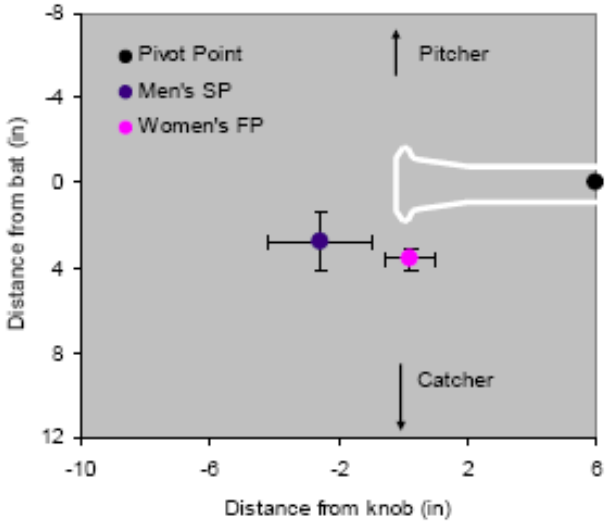

Figure 2.9: Average center of rotation from men's slow pitch and women's fast pitch field studies.

From equation 2.13 the swing speed is found from,

$$v_{bat} = 85\left(\frac{Q+8.5}{30.5}\right)\left(\frac{9000}{I}\right)^{1/4} \tag{2.14}$$

The BBS is then found from,

$$\boldsymbol{BBS = v_r = e_A v_{ball} + (1 + e_A) v_{bat}} \tag{2.15}$$

The BBS is a representation of the batted ball speed during field play. The limit that the ASA has placed on the BBS is 98 mph. NCAA softball and the International Softball Federation (ISF) has also incorporated the ASA protocol for bat testing, but they use a 100 mph limit.

2.3 Normalizing Bat Performance Measurements

Normalizing is an attempt to eliminate or reduce the ball dependence on bat performance measurements. The three properties of the ball that effect bat performance are: weight, elasticity, and stiffness.

2.3.1. Weight Normalizing

While e is independent of weight, e_A is not. Since e_A is typically measured in bat performance measurements weight normalization made in e_A.

$$\boldsymbol{e_A = \left(\frac{e - r_b}{1 + r_b}\right)} \tag{2.16}$$

The collision efficiency is normalized by weight if a nominal ball weight (rather than the test ball weight) is used for m in equation 2.6. The results from normalizing for weight can be seen in figure 2.10 [2.3].

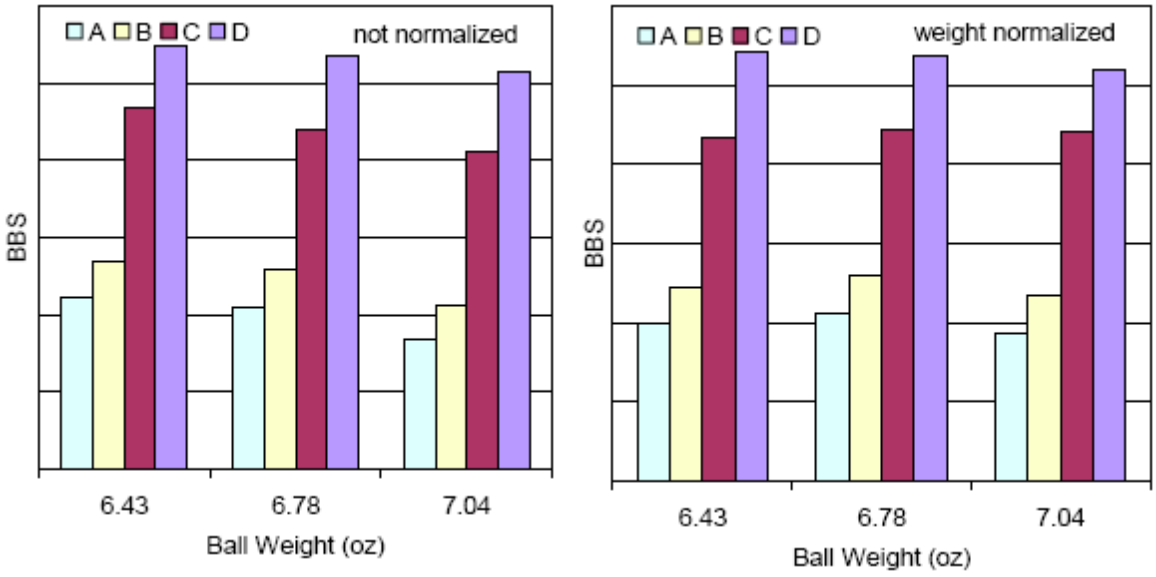

Figure 2.10: Comparison of normalizing on the performance of four bats as a function of test ball weight

Not surprisingly the normalization was more dramatic for the low performance bats because the trampoline effect in the high performance bats outweighs the effect of ball mass.

2.3.2. Normalizing for ball CCOR and Stiffness

Recently, Smith and Nathan used a two spring model to relate the bat-ball coefficient of restitution (BBCOR = e) to the ball cylindrical coefficient of restitution (CCOR = e_0) and dynamic stiffness (k). Their approach was similar to that used by Cross for tennis rackets [2.23] [2.10]. The bat and ball were modeled after masses on linear lossy springs, with spring constants k_1 and k_2 respectively. Upon impact the two springs will mutually compress each other, converting the initial kinetic energy into potential energy. The simplified two-spring model for the bat-ball collision is represented in figure 2.11.

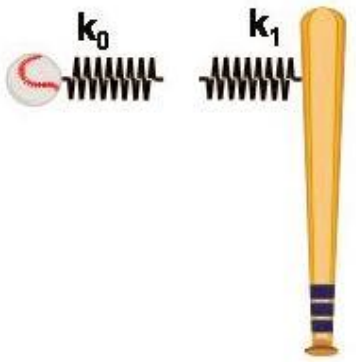

Figure 2.11: Simplified two-spring model for the bat-ball collision.

The fundamental equation for the energy dissipated in the collision is,

$$\mathbf{1} - \boldsymbol{e}^{\mathbf{2}} = (\mathbf{1} - \boldsymbol{e_0}^{\mathbf{2}})\boldsymbol{f_0} + (\mathbf{1} - \boldsymbol{e_1}^{\mathbf{2}})\boldsymbol{f_1} \qquad (2.17)$$

where, f_0 and f_1 are the fraction of the initial center of mass energy stored in the ball and bat, respectively; e_1 is the COR of the bat; the quantities $(1 - e_0^2)$ and $(1 - e_1^2)$ are the fraction of stored energy that is dissipated in the ball and bat respectively and $(1 - e^2)$ is the fraction of total center of mass energy that is dissipated in the collision. The fraction of energy loss can be defined as the loss in kinetic energy divided by the initial kinetic energy. The fraction of the initial energy stored in the ball (f_0), and the fraction stored in the bat (f_1) can be expressed as,

$$\boldsymbol{f_0 = \frac{k_1}{(k_1+k_0)}} \tag{2.18}$$

$$\boldsymbol{f_1 = \frac{k_0}{(k_1+k_0)}} \tag{2.19}$$

Equation 2.16 can be simplified by defining,

$$\boldsymbol{r \equiv \frac{k_1}{k_0}} \tag{2.20}$$

And solving for e, as,

$$\boldsymbol{e^2 = \frac{re_0^2+e_1^2}{1+r}} \tag{2.21}$$

If the bat is elastic (approximately true for impacts near the sweet spot $e_1 = 1$) equation 2.21 becomes [2.23],

$$\boldsymbol{e^2 = \frac{re_0^2+1}{1+r}} \tag{2.22}$$

For wood or low performing hollow aluminum bats $r >> 1$ or $k_1 >> k_0$ all the energy is stored in the ball and e is independent of r. On the other end of the spectrum where $r << 1$ or $k_1 << k_0$ the bat absorbs all the energy of the ball and returns it to the ball upon rebound. Bats and balls in play usually have an r of around 100 for low performing bats and 5 for high performing bats.

Solving for r in equation 2.20 we obtain,

$$\boldsymbol{r = \frac{1-e^2}{e^2-{e_0}^2}} \tag{2.23}$$

Suppose that from a bat performance measurement test we obtain the BBCOR = e_T, for a particular bat from a test ball with known CCOR = e_{0T}, and dynamic stiffness, k_T. To obtain the BBCOR from a standard or "normalizing" ball, NBBCOR = e_N, we choose a normalizing ball with CCOR = e_{0N} and dynamic stiffness k_N. The dimensionless parameter r and is normalized by it by the ratio of dynamic stiffness of the test ball, k_T, and the normalizing ball, k_N, as,

$$\boldsymbol{r_N = \frac{k_1}{k_0}\frac{k_T}{k_N} = \frac{k_T}{k_N}\frac{1-{e_T}^2}{{e_T}^2-{e_{0T}}^2}} \tag{2.24}$$

The normalized, NBBCOR = e_N, is obtained by [2.23],

$$\boldsymbol{{e_N}^2 = \frac{r_N\,{e_{0N}}^2+1}{1+r_N}} \tag{2.25}$$

Currently there has been no comprehensive study to determine if this normalizing procedure is valid, which is an aim of this work.

2.4 Finite Element Modeling

By numerically modeling baseball and softball bats with different elastic moduli a wide range of bats can be analyzed. Sports balls are typically analyzed numerically three ways; using elastic, visco-elastic, or hyper-elastic properties. Baseballs and softballs are difficult to analyze experimentally due to the nonlinear nature of the materials used to manufacture the ball. In finite element programs it is possible to model the ball as a visco-elastic or hyper-elastic material and typically FEA studies model the ball in this way.

Tanank, Oodaira, Teranishi, Sato, and Ujihashi modeled a golf ball in FE with multiple layers with using a hyper-elastic Mooney-Rivlin model for the cover and a visco-elastic model for the core of the golf ball [2.26]. The Mooney-Rivlin model represents the elastic response of rubber-like material, in this case it fits a golf ball with a relatively high COR. Mustone and Sherwood used FE to model bat-ball impacts. Using a FE program LS-DYNA, Mustone and Sherwood modeled an ash wood bat and a hollow C405 aluminum bat. A Mooney-Rivlin model was used to model the baseball. The ball model was impacted against a stationary wood block to calibrate it to known COR values. The bat-ball modeled a 70-70 mph impact, in which the bat rotated at 70 mph relative to the impact surface and the ball was pitched at 70 mph. The bat was pinned a 6 inches from the handle to simulate the experimental bat test. They found that the Mooney-Rivin model was over-damping the aluminum bat model, to overcome this they added mass damping to the wood bat model. The results were that the COR was higher than the accepted values from the experimental data. Mustone and Sherwood concluded that an improved ball model would yield better results [2.27].

Shenoy, Smith and Axtell used the power law to describe the response of a baseball [2.28]. The power law visco-elasticity model is defined by,

$$\boldsymbol{G(t) = G_\infty + (G_0 - G_\infty)e^{-\beta t}} \tag{2.26}$$

where, G_∞ and G_0 are the long term and instantaneous shear moduli, respectively, t is time, and β is the decay constant. In the Power Law model stiffness is governed by the long term modulus during long time durations and by the instantaneous modulus at short time durations. The decay constant (β) determines how quickly the modulus changes between the two moduli. If the decay constant is very large then time dependent shear modulus ($G(t)$) is controlled by the long term

modulus (G_∞). If the decay constant is zero then the time dependent shear modulus is controlled by the instantaneous modulus (G_0). If the long term and instantaneous shear moduli are equal the shear modulus becomes time independent. The bulk modulus, *k*, is constant, producing a time dependent Poisson's ratio, ν, and is defined by,

$$\boldsymbol{\nu(t)} = \frac{\boldsymbol{3k-2G(t)}}{\boldsymbol{6k+2G(t)}} \tag{2.27}$$

Typically, the constants are found by adjusting the values until the numerical model matches experimental data. Shenoy, Smith, and Axtell used a homogeneous synthetic ball and the long term modulus was found from the quasi-static compressive stress-strain response of the ball. They found that the long term modulus was too low and that the dynamic properties needed to be addressed [2.28]. Nicholls, Miller and Elliott also used the power law for the response of a baseball. A Quasi-static uniaxial compression test was conducted to obtain the experimental force-displacement data, and implicit FEA was used to fit a value for G_∞ to the data from the stiffest baseball. G_0 was obtained through simulation of the impact of a ball on a vertical rigid wall with velocities ranging from 13.2 to 40.2 m/s and comparing the COR to experimental results. Nicholls argued that the decay constant should be set to the approximate duration of the bat-ball impact [2.29]. Sandmeyer used the power law to model the ball and found the properties through trial and error. Experimentally the ball COR was found by impacting a ball with initial velocity of 58 mph into a 2.5 in. thick northern white ash plank bolted to a rigid wall. Douglas fir properties were substituted for the ash in the FEA model [2.30]. With all the different ways to get to model the properties of the ball, it is difficult to determine if the FEA models are describing dynamic response of the ball correctly.

Another method is to model a visco-elastic material using a series of Voigt elements called the Prony-series based on a spring-damper system. The Prony-series visco-elastic model to describe the shear modulus is defined as,

$$\boldsymbol{G(t) = \sum_{i=1}^{N} g_i e^{-\beta_i t}} \quad (2.28)$$

Where, g_i and β_i are the shear modulus and decay constant, respectively, as seen in figure 2.12 [2.31].

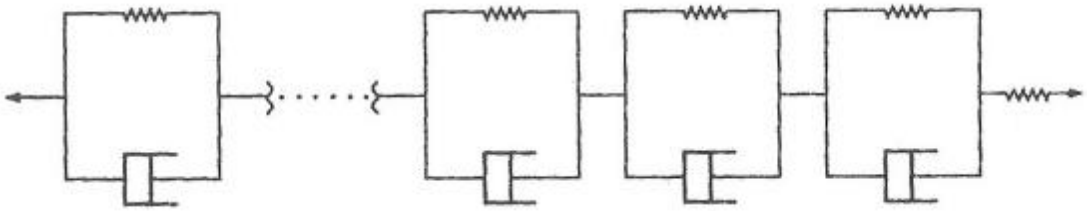

Figure 2.12: Spring-damper model in a series of Voigt elements that represents the Prony-series

Smith and Duris compared the simple power law to a six element Prony-series model. For the Prony-series the shear modulus, g_i and decay constant, β_i values were determined through dynamic mechanical analysis testing of a sample of a polyurethane softball core. They also used a power law where the coefficients were found deterministically by modeling the dynamic stiffness test. Smith and Duris used LS-DYNA to model bat-ball collisions and they concluded that the simpler power law (obtained from more realistic ball deformation) did a better job in describing the dynamic response of the ball [2.32]. Also by varying the constants a wide range of balls could be analyzed. It is possible for instance to obtain balls with constant CCOR's and varying DS or vice-versa. To demonstrate how the visco-elastic model corresponds with experimental results the force-time and force-displacement curves that Smith and Duris found in

the FEA model were plotted against experimental data as seen in figure 2.13 and figure 2.14 respectively.

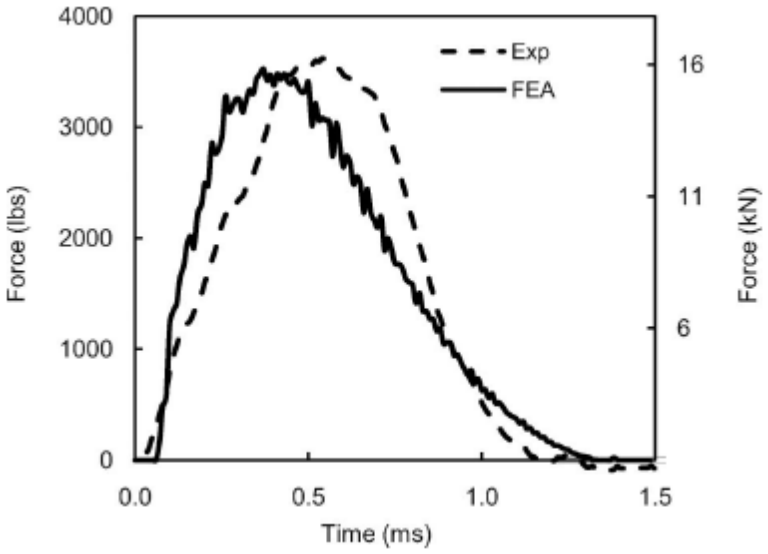

Figure 2.13: Representative force-time curve for a ball impacting a solid cylinder.

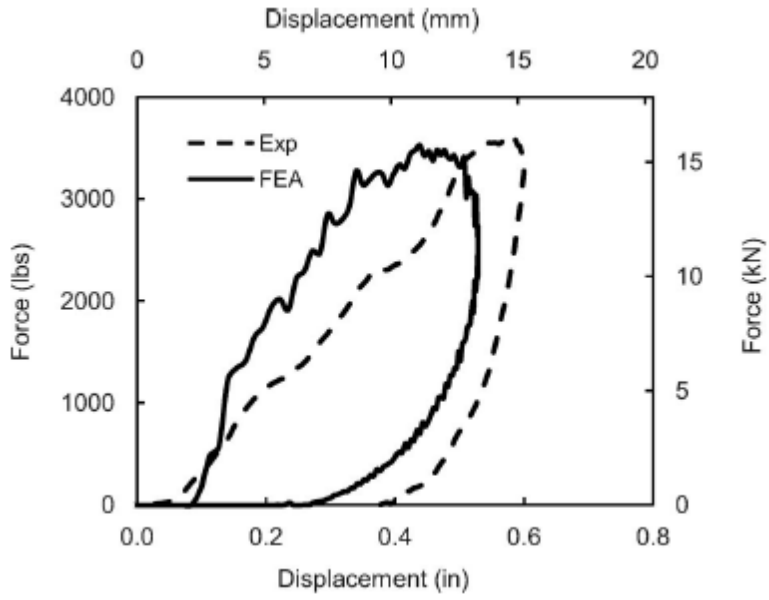

Figure 2.14: Representative force-displacement curve for a ball impacting a solid cylinder.

The force-time curve and the force displacement curve correspond to a dynamic stiffness test at 80 mph [2.30]. The Power Law (equation 2.26) was used in the FEA model with k = 0.80 Msi, G_0 = 28 ksi, G_∞ = 1.5 ksi and $\beta = 6.8 \times 10^4$. Smith and Duris determined that the power law was a sufficient model for dynamic stiffness in numerical analysis [2.32].

2.5 Summary

Bat performance is highly dependent on the properties of the ball. Normalizing is an attempt to eliminate or reduce the ball dependence in bat performance measurements. Theoretical models have been developed to normalize for the ball weight, elasticity and stiffness.

Modeling the bat-ball collision numerically in finite elements can be useful if the physical characteristics of the bat and ball can be modeled correctly. Past studies show that visco-elastic models in FE can describe the ball accurately, and an elastic model can describe a hollow metal bat. The numeric model will be used to obtain displacements and forces that cannot be measured experimentally.

Normalizing for weight has been shown to be an appropriate way to eliminate the variation in ball weight on bat performance measurements. However, currently there has been no comprehensive study to eliminate the bat's dependence on the ball's stiffness and elastic properties. This study will look at the factors and assumptions used in normalizing, to validate the procedure or identify it's shortcomings. The study will use experimental and numerical results to explore ball normalizing.

REFERENCES

[2.1] **Barnes, G.***Study of collisions.* 1957, American Journal of Physics, pp. 5-12.

[2.2] **F1888-02, ASTM.** Test Method for Compression-Displacement of Baseballs and Softballs. West Conshohocken, PA : s.n., January 2003.

[2.3] **Smith, L V.** A White Paper on Bat and Ball Test Methods and Performance Characteristics. 2007.

[2.4] **Duris, J and Smith, L.** *Evaluating Test Methods Used to Characterize Softballs.* Davis, CA : The Engineering of Sport 5th International Conference, 2004. Vol. 2, pp. 80-86.

[2.5] **Giacobbe, Peter A., Scarton, H. A., and Lee, Y.-S,.** *Dynamic Hardness (SDH) of Baseballs and Softballs, ASTM STP 1313.* 1997. Earl F. Hoerner and Francis A. Cosgrove, EDS, American Society for Testing and Materials.

[2.6] **Hendee, S. P., Greenwald, R. M., and Crisco, J. J.** *Static and Dynamic Properties of Various Baseballs.* 1998, Journal of Applied Biomechanics, Vol. 14, pp. 390-400.

[2.7] **Smith, L. V. and Duris, J.** *The Dependence of bat Performance on Ball Properties.* St. Louis, MO : s.n., 2006. IMAC-XXIV.

[2.8] **Smith, L. V.** *Measuring the Hardness of Softballs.* Orlando, FL : s.n., 2008. IMAC-XXVI.

[2.9] **F2845, ASTM.** Measuring the Dynamic Stiffness (DS) and Cylinderical Coefficient of Restitution (CCOR) of Baseballs and Softballs.

[2.10] **Cross, R.** *The coefficient of restitution for collisoins of happy balls, unhappy balls, and tennis balls.* 2000, American Journal of Physics, pp. 1025-1031.

[2.11] **Coaplen, J., Stronge, W. J. and Ravani, B.** *Work equivalent composite coefficient of restitution.* s.l. : International Journal of Impact Engineering, 2004, Vol. 30, pp. 581-591.

[2.12] **Nathan, A. M., Russell, D. A. and Smith, L. V.** *The Physics of the Trampoline Effect in Baseball and Softball Bats.* Davis, CA : s.n., 2004. The Engineering of Sport 5th International Conference. Vol. 2, pp. 38-44.

[2.13] **F2884, ASTM.** Test Method for Compression-Displacement of Baseball and Softball Barrels.

[2.14] **Cruz, C. M.** Characterizing Softball Bat Modifications and Their Resulting Performance Effects. s.l. : MS Thesis, Washington State University, May 2005.

[2.15] **Lloyd Smith, James Sherwood.** *Engineering Our Favorite Pastime.* s.l. : Mechanical Engineering, the Magazine of ASME, 2010, Vol. 132.4, pp. 44-48.

[2.16] **House, Gale C.** Baseball and Softball Bats. [book auth.] Mark A. Smith Ellen Kreighbaum. *Sports and Fitness Equipment Design.* s.l. : Human Kinetics, Health and Fitness, 1996, 10, pp. 117-125.

[2.17] **Brody, H.** *The Sweet Spot of A Baseball Bat.* 7, s.l. : American Journal of Physics, 1986, Vol. 54.

[2.18] **Russell, D. A.** *Hoop frequency as a predictor of performance for softball bats.* 2004. Proceeding of ISEA2004.

[2.19] **Cross, Rod.** *The sweet spot of a baseball bat.* s.l. : Am. J. Phys., 1998, Vol. 66, pp. 772-779.

[2.20] **Smith, L. V. and Axtell, I. T.** *Mechanical Testing of Baseball Bats.* 3, 2003, Journal of Testing and Evaluation, Vol. 31, pp. 210-214.

[2.21] **Nathan, A.** *Characterizing the Performance of Baseball Bats.* 2002, American Journal of Pysics, Vol. 71, pp. 134-143.

[2.22] **F2219-07, ASTM.** Standard Test Methods for Measuring High-Speed Bat Performance. West Conshohocken, PA : s.n., November 2007.

[2.23] **Nathan, A. M. and Smith, L. V.** *Effect of Ball Properties on the Ball-Bat Coefficient of Restitution.* Honolulu, Hawaii : s.n., 2009. 4th Asia-Pacific Congress on Sports Technology.

[2.24] **ASTM F 1881-05.** Standard Test Method for Measuring Baseball bat Performance Factor. *2005.* West Conshohocken, PA : s.n., October.

[2.25] **Smith, L. V., Broker, J. and Nathan, A.** *A Study of Softball Player Swing Speed.* [ed.] P. Trivailo, and F. Alam, RMIT University A. Subic. Melbourne Australia : s.n., 2003. Sports Dynamic Discovery and Application. pp. 12-14.

[2.26] **Tanaka, K., et al.** *Experimental and Finite-Element Analysis of a Golf Ball Colliding With Simplified Clubheads.* [ed.] F. K. Fuss, A. Subic and S. Ujihashi. 2008, The Impact of Technology on Sport, pp. 235-340.

[2.27] **Mustone, T. and Sherwood, J.** *Using LS-DYNA to develop a baseball bat performance and design tool.* Detroit, MI : s.n., 2000. Proceedings of 6th international LS-DYNA users Conference.

[2.28] **Shenoy, M. M., Smith, L. V. and Axtell, J. T.** *Performance Assessment of Wood, Metal, and Composite Baseball Bats.* 2001, Composite Structures, Vol. 52, pp. 397-404.

[2.29] **Nicholls, Rochelle L., Miller, Karol and Elliott, Bruce C.** *numerical analysis of maximal bat performance in baseball.* 2006, Journal of Biomechanics, Vol. 39, pp. 1001-1009.

[2.30] **Sandmeyer, B. J.** Simulation of bat/ball impacts using finite element analysis. *Masters Thesis, Oregon State University.* 1994.

[2.31] **Duris, J. G.** Experimental and Numerical Characterization of Softballs. *Master's Thesis, Washington State University.* 2004.

[2.32] **Smith, Lloyd V. and Duris, Joseph G.** *Progress and challenges in numerically modelling solid sports balls with application to softballs.* February 15, 2009, Journal of Sports Sciences, pp. 353-360.

Chapter Three

Experimental Results

3.1. Introduction

There was desire to eliminate the dependence of the ball's COR and stiffness on bat performance. The following will evaluate a technique to normalize bat performance for ball COR and stiffness.

All the Experimental testing was completed at the Sports Science Laboratory at Washington State University. The testing was done in a Stability Environment, Inc. environmentally controlled walk-in chamber model number 1332401. The environmental chamber was 429 square feet and 8'-10" high, large enough to both store the balls and carry out the bat performance test [3.1][3.2]. A picture of the outside of the walk-in environmental chamber can be seen in figure 3.1.

Figure 3.1: Outside of the environmental chamber

By controlling the environment, the effect that temperature and relative humidity has on the balls was constant. The testing standard required the balls to be placed in the controlled environment for at least 14 days before testing with the temperature maintained at 72 ± 4 °F and the relative humidity maintained at 50 ± 10% R.H. [3.3]. The environmental chamber was fitted with Watlow PID controllers for the temperature and humidity controls. The temperature and humidity was recorded on a Honeywell chart recorder, as seen in the figure 3.2.

Figure 3.2: Honeywell chart recorder with the red pin recording the humidity and the blue pin recording the temperature.

In addition, the temperature and humidity was tracked by HOBO U14 LCD data loggers placed around the room to insure the temperature and humidity was consistent throughout the environmental chamber. The HOBO data logger was able to record the instantaneous temperature and humidity as seen in figure 3.3.

Figure 3.3: Hobo data logger showing the temperature (°F) and relative humidity.

The environmental conditions can be exported to an excel file where an electronic readout of the temperature and humidity over time can be plotted as seen in the figures 3.4 and 3.5 respectively. The figures show that once the environmental chamber was installed the temperature (figure 3.4) and humidity (figure 3.5) in the lab was more consistent then without it.

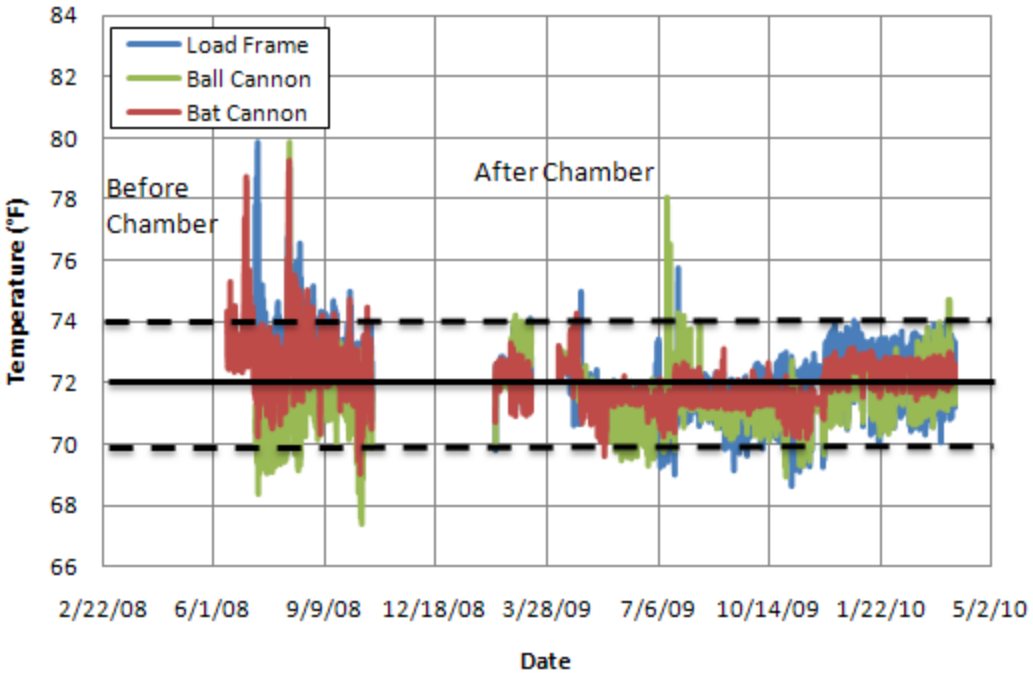

Figure 3.4: Temperature before and after the environmental chamber was installed. The data was taken from the data loggers placed around the lab.

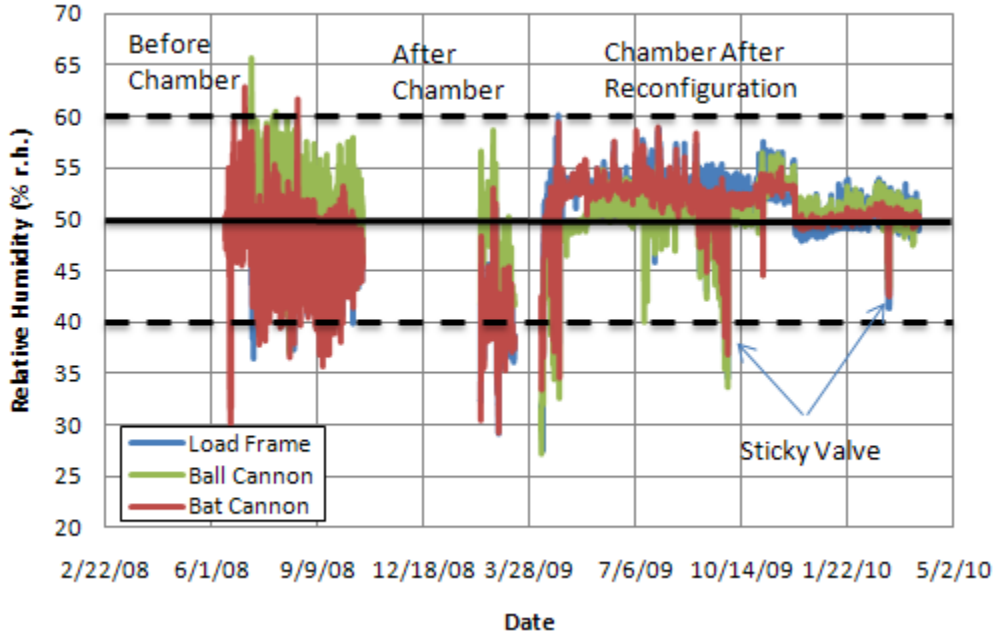

Figure 3.5: The humidity before and after the environmental chamber was installed. The data was taken from the data loggers placed around the room.

After the chamber was calibrated for a period of almost a full year (4/15/2009-3/29/10) the average temperature in the lab was 71.9 °F with a standard deviation of 0.8 °F, and the average relative humidity was 51.3 % R.H. with a standard deviation of 2.1 % R.H., taken from all three data loggers.

3.2. Ball Testing

Softballs are made with a polyurethane foam core and a leather or synthetic cover. The cover was in two parts and stitched together by string laces as shown in figure 3.6. Polyurethane is a visco-elastic material that is temperature, humidity, and strain rate dependent.

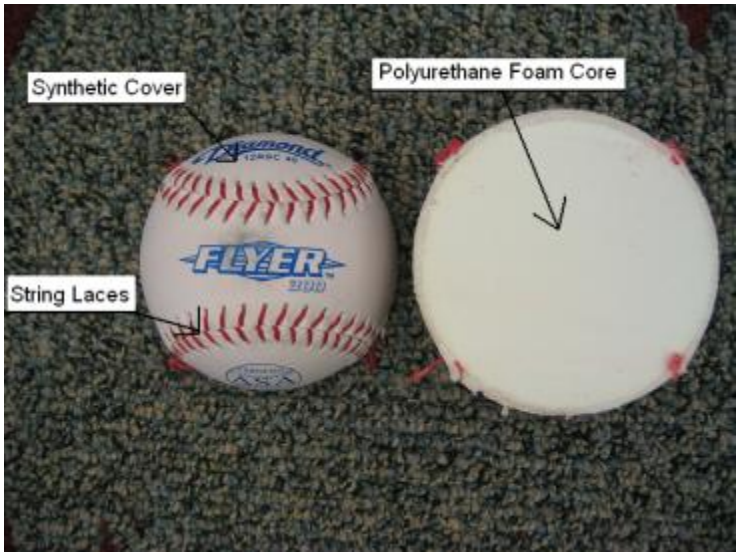

Figure 3.6: Typical Softball cut in half showing the polyurethane core and cover.

3.2.1. Ball Compression

A load frame was used to test the compression or hardness of the softballs and complied with the standardized method ASTM F 1888-02 [3.3]. The displacement was controlled by a

MTS controller that was connected to a computer and controlled through LabView version 9.0. The ball compression test apparatus is shown in figure 3.7.

Figure 3.7: Ball compression apparatus

3.2.2. CCOR and Dynamic Stiffness.

The ball cannon was used to determine the ball's COR and dynamic stiffness. It had been shown that the cylindrical COR (CCOR = e_0) gives a better approximation of the energy loses in a bat-ball impact then the flat plate COR and this study used the CCOR as the measure of ball energy loss [3.4]. The ball dynamic stiffness test was a representation of the forces acting on the ball that were involved in the bat-ball collision. The ball's CCOR and dynamic stiffness were found by firing a ball from a pneumatic cannon at a rigid half cylinder. The incoming and rebound speed of the ball was measured by light gates as the ball passed through them. The half cylinder was attached to an array of load cells that recorded the impulse force. The pneumatic cannon minimized the variability in pitch speed, impact location, and spin on the ball. The testing apparatus of the ball cannon is shown in Figure 3.8.

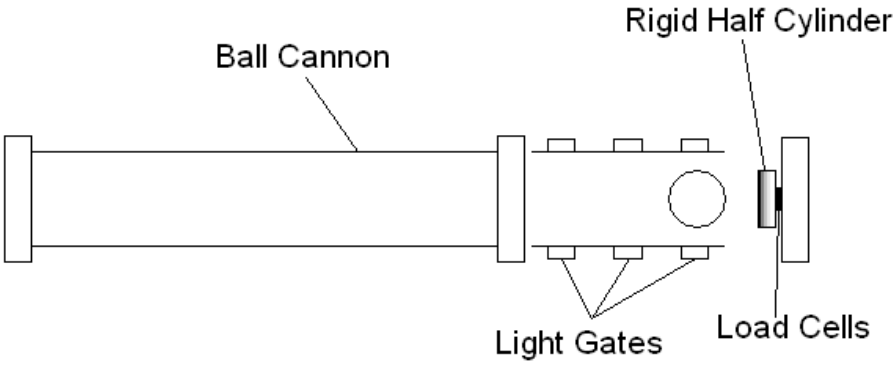

Figure 3.8: Testing apparatus of the ball cannon, light box, rigid half cylinder, and load cells.

The light gates and load cells were connected to a desktop computer. A large air accumulator was connected to the ball cannon and controlled by a regulating valve connected to the computer. The pitch speed was regulated by adjusting the air pressure in the accumulator tank. Figure 3.9 shows ball cannon setup.

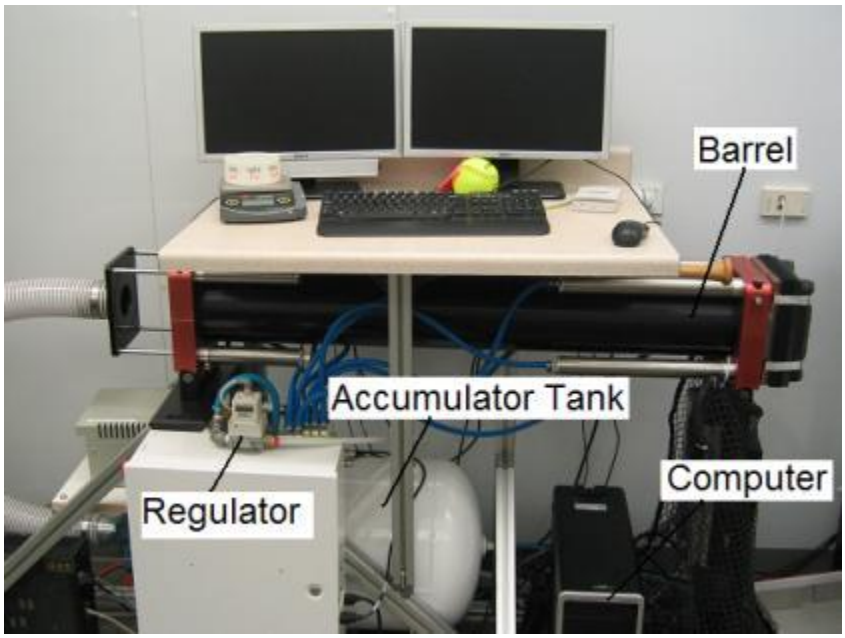

Figure 3.9: Cannon regulator, accumulator tank, computer, and barrel.

The ball was placed in a holder called a sabot and placed in the breach end of the barrel. The sabot was made from polycarbonate and was used to center the ball and ensured that the ball did not rotate when fired as seen in figure 3.10. This allowed for consistent and repeatable shots.

Figure 3.10: The sabot and softball

At the breach end of the barrel pneumatic cylinders were used to close the breach plate so when the air was released the full pressure was behind the ball; this ensured consistent velocities. The breach plate and pneumatic cylinders can be seen in figure 3.11.

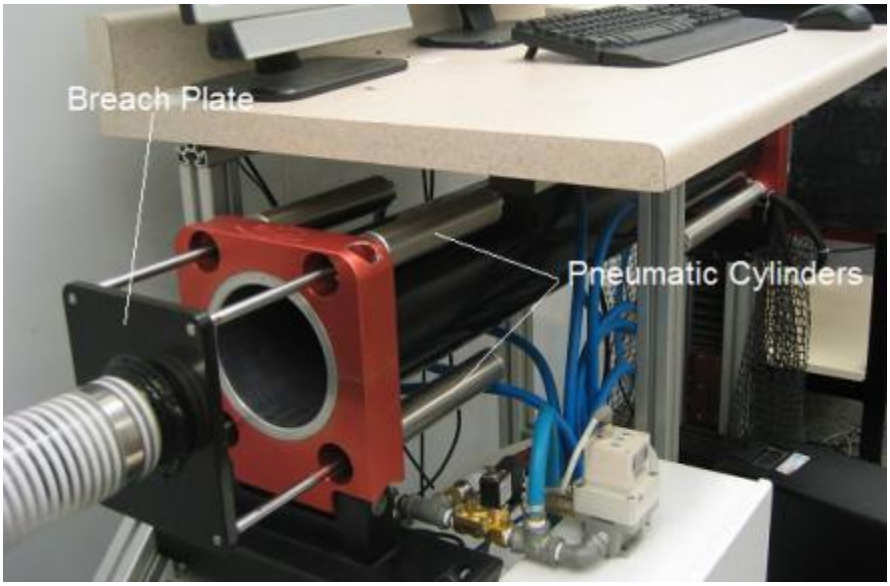

Figure 3.11: Breach plate and pneumatic cylinders.

Once the ball was fired a pneumatically controlled arrestor plate was simultaneously triggered and "caught" the sabot while allowing the ball to continue through the light gates and on to the rigid half cylinder. A figure of the arrestor plate can be seen in figure 3.12.

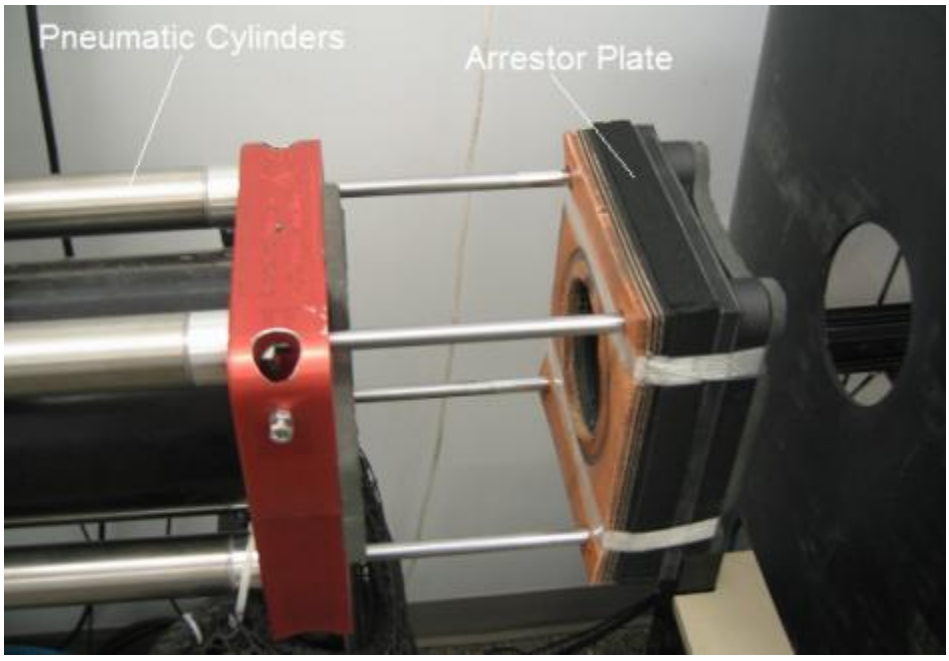

Figure 3.12: Open arrestor plate and pneumatic cylinders.

The ball passed through three pairs of ADC iBeam light gates, impacted the rigid half cylinder, and rebounded back through the light gates. The light gates, rigid half cylinder and load cells are shown in figure 3.13. The load cells were PCB Model 208C05 and arranged in an equilateral triangle with two inch spacing between each cell.

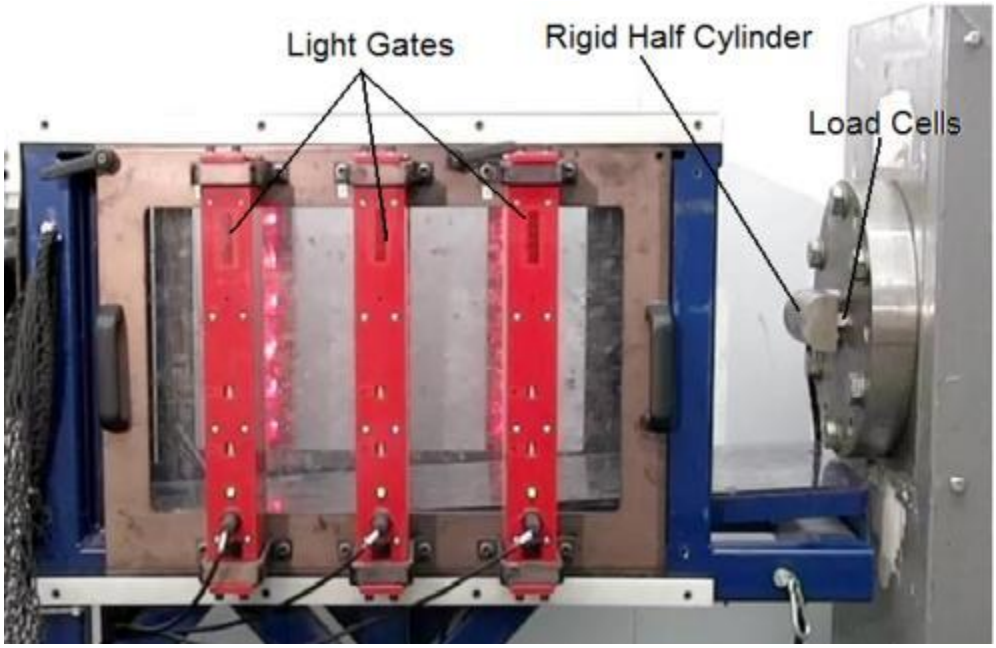

Figure 3.13: Light box with light gates, rigid half cylinder, and load cells.

The ball was fired at a target velocity of 95 ± 1 mph and only rebounds that were within ±5 degrees of the inbound path were considered valid impacts [3.1]. National Instruments' Lab View version 9.0 was used to record and control the test. The incoming and rebound speeds and the force of the impact were recorded through Lab View.

3.2.3. Ball Results

To magnify the effect of the ball on bat performance, balls with large differences in cylindrical coefficient of restitution (CCOR) and stiffness were needed. Balls were tested that ranged in both CCOR and dynamic stiffness from multiple manufacturers.

The CCOR and dynamic stiffness were found simultaneously. The CCOR of the ball was found by,

$$\boldsymbol{e_0 = -\frac{v_r}{v_i}} \tag{3.1}$$

where, v_r and v_i were the rebound and incoming velocity of the ball respectively.

Dynamic stiffness, *k*, can be found multiple ways. This study focused on four ways to find *k*.

The ball was assumed to behave like a linear spring according to,

$$\boldsymbol{F = kx} \tag{3.2}$$

where, *F* and *x*, were the force and displacement respectively. Solving for *k* equation 3.2 becomes,

$$\boldsymbol{k_x = \frac{F}{x}} \tag{3.3}$$

The maximum displacement was taken for *x* and used with the corresponding force, *F*, this k_x was the slope of the force-displacement curve. The maximum displacement was found by dividing the force by the mass of the ball and integrating twice or,

$$\boldsymbol{\frac{d^2x}{dt^2} = \frac{F(t)}{m_b}} \tag{3.4}$$

The ball stiffness was also found using energy. Equating the initial kinetic energy of the ball to the potential energy at maximum defection we have,

$$\frac{1}{2}m_b v_i^2 = \frac{1}{2}kx^2 \tag{3.5}$$

where, m_b was the mass of the ball and v_i was the initial velocity of the incoming ball. Solving for k equation 3.4 becomes,

$$k_v = m_b\left(\frac{v_i}{x}\right)^2 \tag{3.6}$$

where, $F(t)$ was the measured force as a function of time t, and d^2x/dt^2 was the acceleration.

The dynamic stiffness was found from the peak force and velocity by combining equation 3.2 and equation 3.6

$$k_F = \frac{1}{m_b}\left(\frac{F_p}{v_i}\right)^2 \tag{3.7}$$

The dynamic stiffness was found from the force signal, by fitting it to a sine function as,

$$F(t) = F_p sin\left(\frac{t}{t_0}\pi\right) \tag{3.8}$$

where, t_0 was the contact time. Combing equation 3.8 and equation 3.4 and integrating twice, the maximum displacement became,

$$x = \frac{F_p}{m_b}\left(\frac{t_0}{\pi}\right)^2 \tag{3.9}$$

Rearranging the stiffness, k, became,

$$k_t = m_b\left(\frac{\pi}{t_0}\right)^2 \tag{3.10}$$

The sine function was fit using a solver function in Excel. A representative force curve is shown in figure 3.14 and the force-displacement curve is shown in figure 3.15. A representative force-time curve and the sine fit from equation 3.8 is shown in figure 3.16.

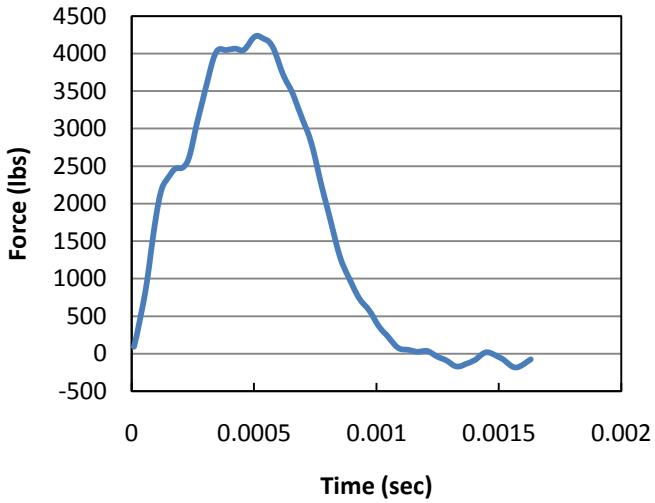

Figure 3.14: Force curve for a DeMarini A9044ASAWR ball impacting a fixed half cylinder traveling at 95 mph.

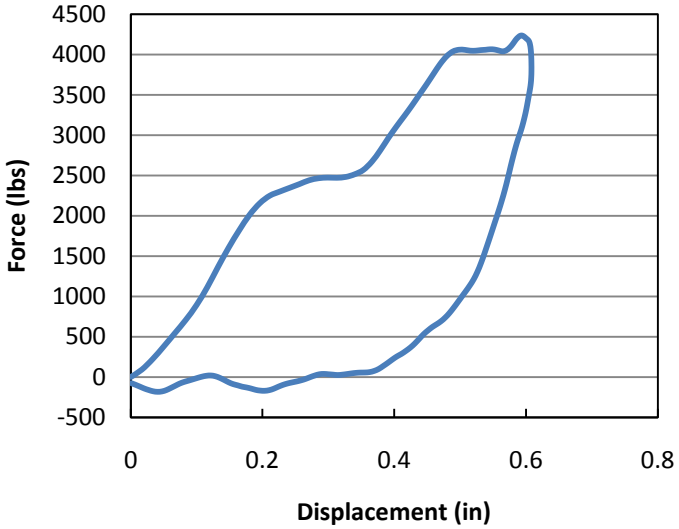

Figure 3.15: Representative force-displacement curve for a DeMarini A9044ASAWR ball impacting a fixed half cylinder traveling at 95 mph.

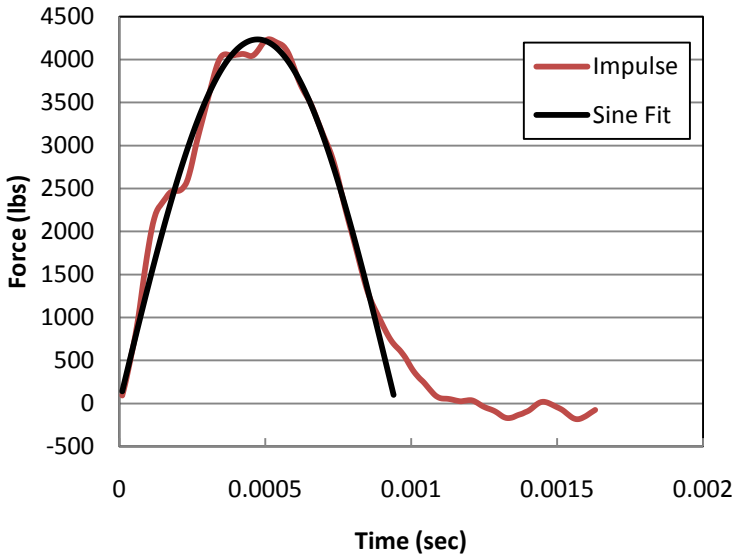

Figure 3.16: Force-time curve for a DeMarini A9044ASAWR ball impacting a fixed half cylinder traveling at 95 mph and the sine fit.

The visco-elastic response fluctuated with different ball models. Five ball models of varying properties were tested using the dynamic stiffness procedure. Figure 3.17 compares the force displacement curves of the five ball models. From the force-displacement curve (Fig 3.17) it was observed that the loading phase of all balls was relatively linear.

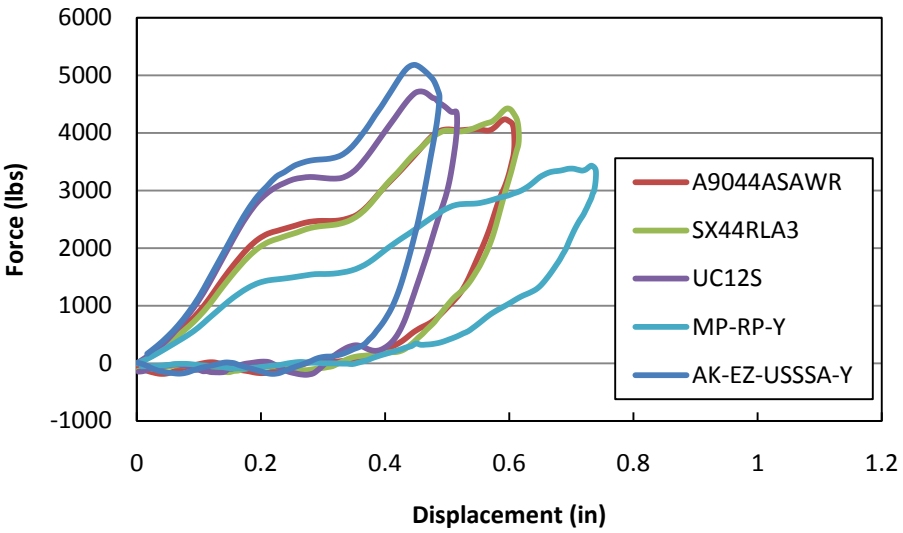

Figure 3.17: Representative force-displacement curve for 5 different balls impacting a fixed half cylinder traveling at 95 mph.

Figure 3.18 shows that contact time varied with dynamic stiffness, for high stiffness balls the contact time was ~0.7 ms and for low stiffness balls the contact time was ~1.2 ms.

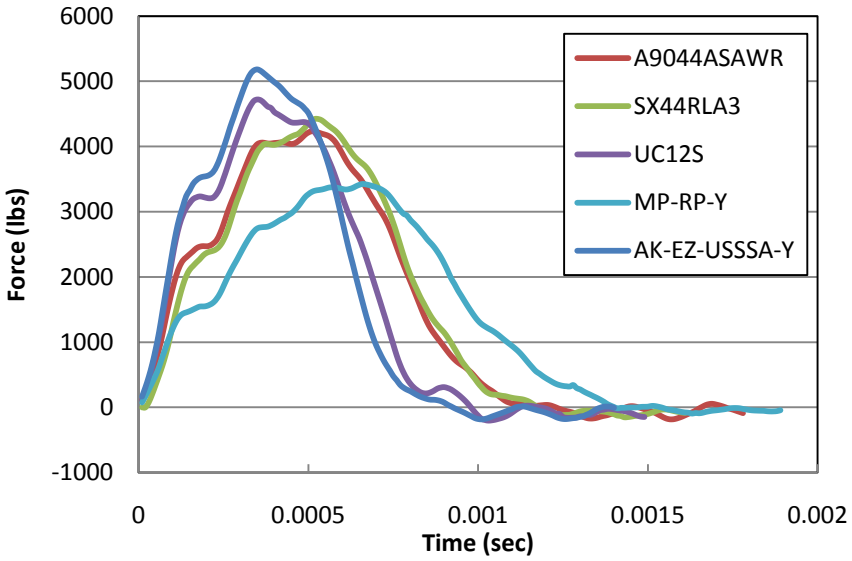

Figure 3.18: Representative force-time curve for 5 different balls impacting a fixed half cylinder traveling at 95 mph from the dynamic stiffness test.

The four ways of determining dynamic stiffness were compared in figure 3.19 and table 3.1

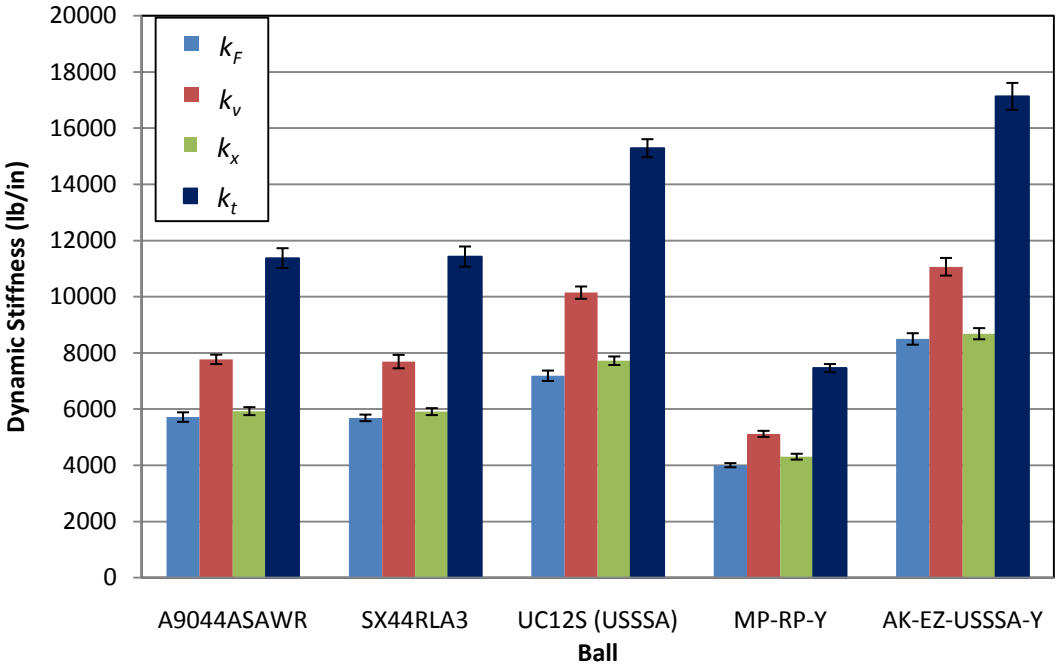

Figure 3.19: Comparing the four ways to find the ball. The figure shows the average of six balls of the same model with standard deviation.

Table 3.1: Comparing the ways to find the ball stiffness

			Average Dynamic Stiffness (lb/in)			
Model	CCOR	Compression (lbs)	k_F	k_v	k_x	k_t
A9044ASAWR*	0.373	370	5716	7770	5928	11374
SX44RLA3*	0.371	357	5687	7691	5911	11428
UC12S (USSSA)	0.322	359	7187	10145	7722	15286
MP-RP-Y	0.442	283	4003	5117	4307	7459
AK-EZ-USSSA-Y	0.327	326	8497	11066	8684	17130

*** Standard Ball**

The trends of the four ways to find dynamic stiffness were compared as slopes on a force-displacement curve, as seen in figure 3.20.

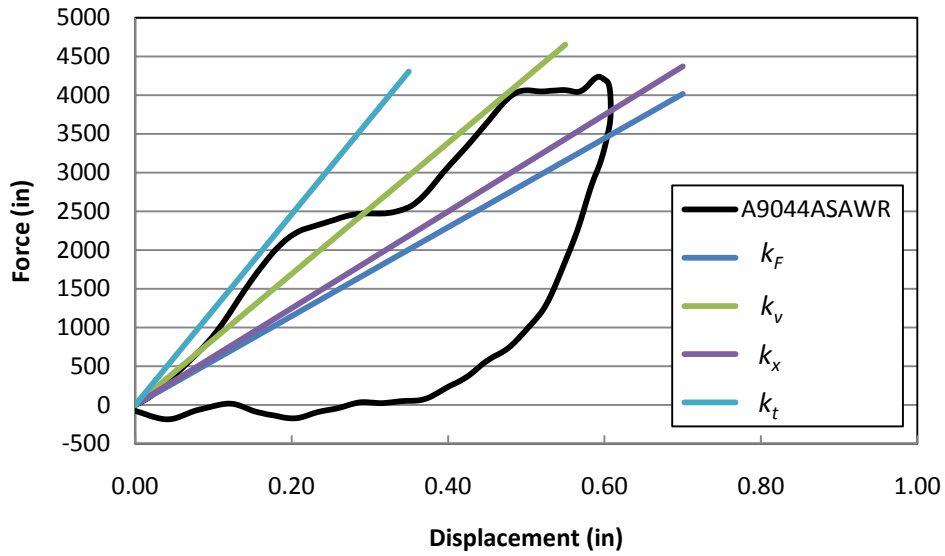

Figure 3.20: Comparing the four ways to find dynamic stiffness as slopes on the force-displacement curve.

For the five balls tested the percent difference between k_F and k_v ranged from 28% to 41%, the difference between k_F and k_x was 2% to 8%, and the difference between k_F and k_t was 86% to 113%. The relative difference between the four ways to find dynamic stiffness was about the same as seen in figure 3.19. Since the peak force was easier to obtain than the slope of the force-displacement curve and k_F (equation 3.7) was within 8% of k_x (equation 3.3), k_F was used to find ball stiffness throughout this thesis. Not coincidentally k_F is used to find dynamic stiffness in the ASTM standard F 2845 [3.5].

3.3. Bat Testing

3.3.1. Testing Apparatus: Moment of Inertia (MOI)

To calculate the MOI, the bat weight and balance point had to be measured. The weight and balance point were found simultaneously by placing the bat on a level stand with two supports that were 6 inches and 24 inches from the knob. The fixture was then placed on scales and zeroed out, then the bat was placed on the fixture as shown in figure 3.21.

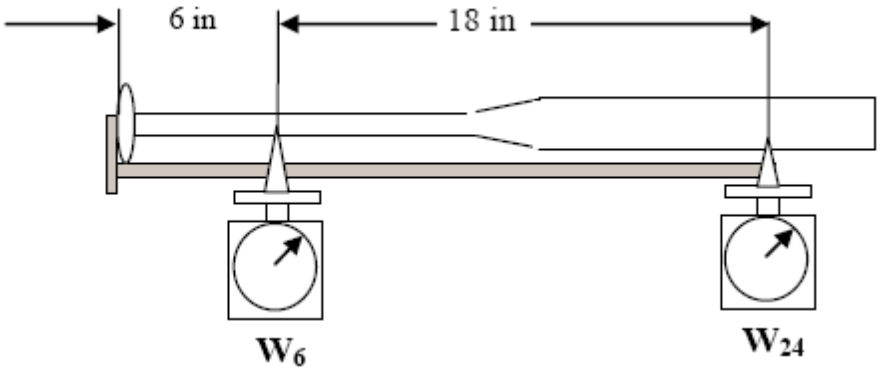

Figure 3.21: Schematic of the stand that measures the weight of the bat and balance point.

The weight (*W*) and balance point (*BP*) were calculated as,

$$\boldsymbol{W = W_6 + W_{24}} \tag{3.11}$$

$$\boldsymbol{BP = \frac{6W_6 + 24W_{24}}{W_6 + W_{24}}} \tag{3.12}$$

where, W_6 and W_{24} were the weights at 6 inches and 24 inches from the knob respectively.

The MOI of a bat was found by ASTM F2398-04 [3.6] using a pivot point 6 inches from the end of the handle [3.7]. The bat swings freely and a light gate recorded the oscillation

period. The setup of the computer and test apparatus to measure the MOI of a softball bat is shown in figure 3.22.

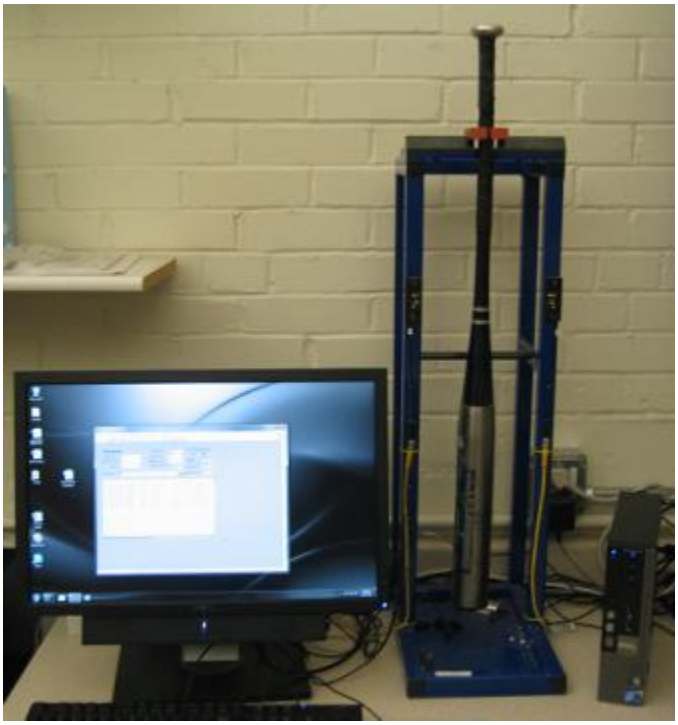

Figure 3.22: Setup of the computer and test apparatus to test the bat's MOI

The MOI was found from the average of the oscillation periods as,

$$\boldsymbol{MOI = Wa\left(\frac{t}{2\pi}\right)^2} \tag{3.13}$$

where, *a* was the distance from the balance point to the pivot point and *t* was the average period [3.6].

3.3.2. Testing Apparatus: Bat Cannon

A pneumatic bat cannon was used to test the performance of softball bats. The bat testing apparatus was similar to the ball test but the rigid wall and dynamic stiffness fixture were replaced by a bat pivot assembly as seen in figure 3.23.

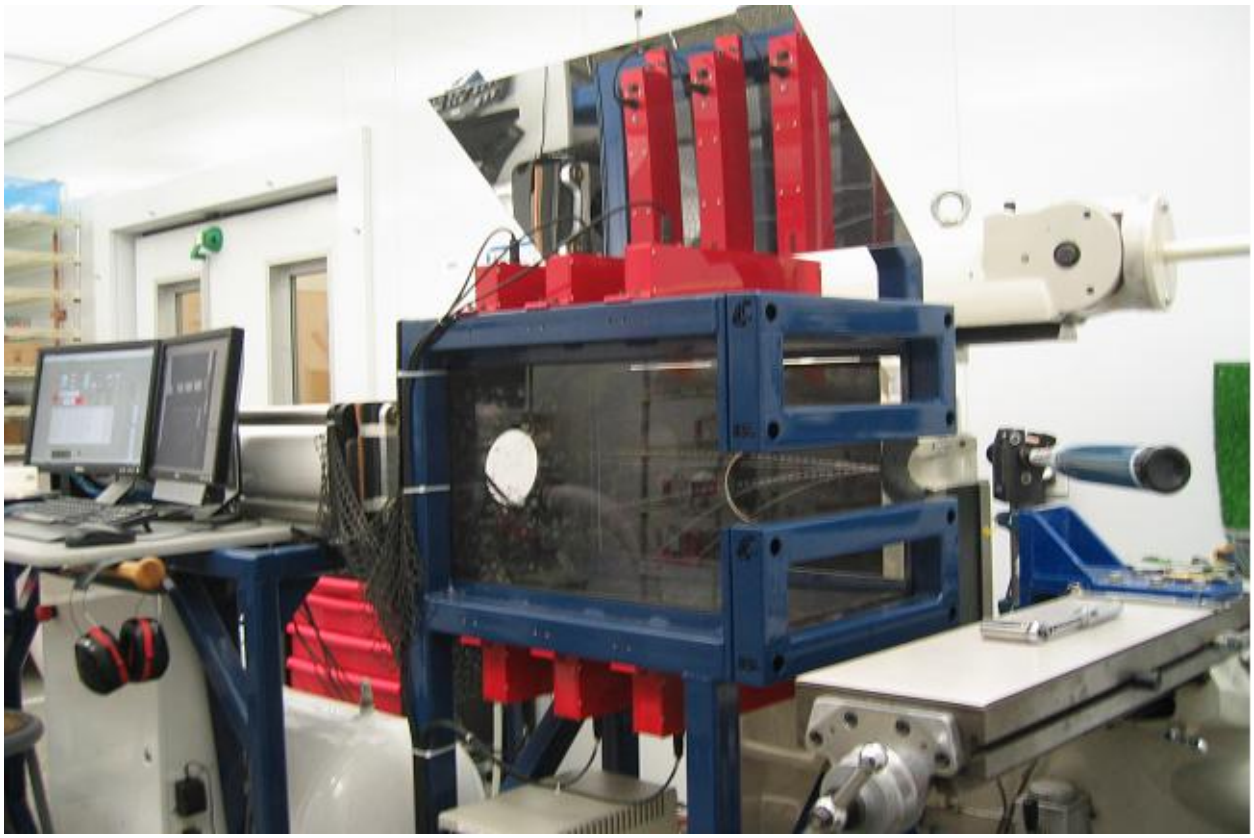

Figure 3.23: The bat cannon and bat pivot assembly

The bat pivot assembly was connected to a mill base allowing three degrees of freedom to control the impact location on the bat. A digital encoder was connected to the bat pivot assembly to measure the angular velocity of the bat. Figure 3.24 shows the bat pivot assembly on the mill base.

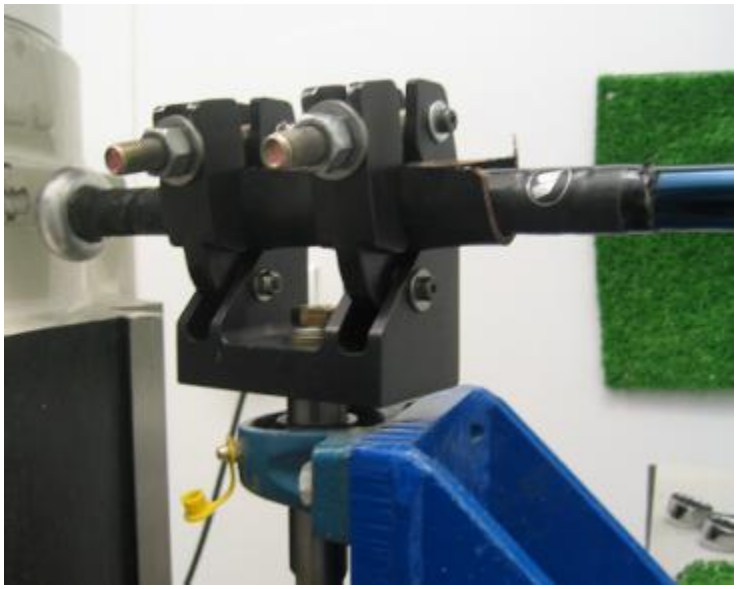

Figure 3.24: Bat pivot

The ball was fired at 110±1 mph. Only rebounds that were within ± 5 degrees of the inbound path were considered valid impacts [3.8]. National Instruments' Lab View version 9.0 was used to record and control the test. The incoming and rebound speeds and angular velocity of the bat from the ball impact were recorded through Lab View.

3.4. Bat Testing and Normalizing Results

The normalized collision efficiency = e_{AN} was found from the normalized BBCOR = e_N (equation 2.25) through,

$$\boldsymbol{e_{AN} = \frac{e_N - r_{bN}}{1 + r_{bN}}} \tag{3.14}$$

where, r_{bN} was the normalized bat recoil factor (equation 2.6) with m = 6.75 ounces. Bat performance can then be found from equation 2.15, in terms of e_{AN},

$$\boldsymbol{NBBS = e_{AN} v_{ball} + (1 + e_{AN}) v_{bat}} \tag{3.15}$$

3.4.1. The Effect of Normalizing With The Standard Ball

If the nominal values for CCOR (e_{0N}) and dynamic stiffness (k_N) were chosen appropriately, normalizing with standard balls should have little to no effect on performance. In this case the batted ball speed would equal the normalized batted ball speed or,

$$\boldsymbol{NBBS = BBS} \tag{3.16}$$

From a sample of 114 balls, the standard test ball had an average CCOR of 0.372 and average dynamic stiffness of 5,755 lb/in with standard deviation of 0.003 and 166 lb/in respectively (Appendix 1). Accordingly, normalizing values for CCOR and dynamic stiffness were chosen as $e_T \approx 0.37 = e_{0N}$ and $k_T \approx 5{,}800$ lb/in $= k_N$ respectively. The balls had a range in CCOR of 0.365-0.378 and dynamic stiffness of 5,435-6,182 lb/in. To observe the effect of small changes in the ball on normalized bat performance, 77 bats were compared for BBS (equation 2.15) and NBBS (equation 3.15). Figure 3.25 shows NBBS – BBS.

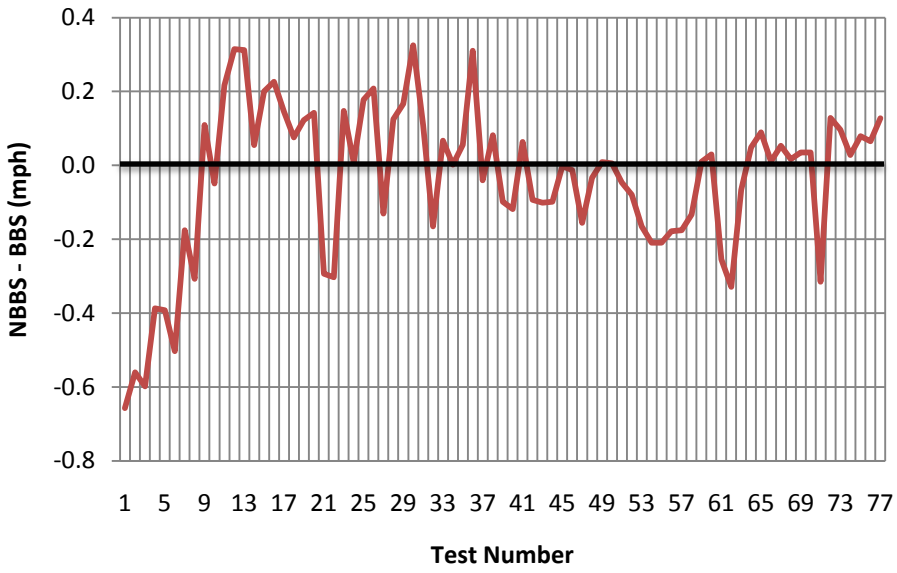

Figure 3.25: The correction from the normalizing procedure with nominal ball values of e_{0T} = 0.37 and k_T = 5800lb/in.

The average correction in BBS was -0.04 mph well within the experimental error of the BBS test. The variation in figure 3.25 was due to the variation of CCOR and dynamic stiffness of the individual balls used in the test. For example, test 1 used balls with an average CCOR of 0.376 and average dynamic stiffness of 6,043 lb/in, as a consequence the BBS had a correction of -0.66 mph. This indicated the correction was going in the right direction, because for balls with high CCOR or high dynamic stiffness the correction will be negative and vice-versa.

Figure 3.26 shows the correlation between the dynamic stiffness and CCOR for the standard test ball.

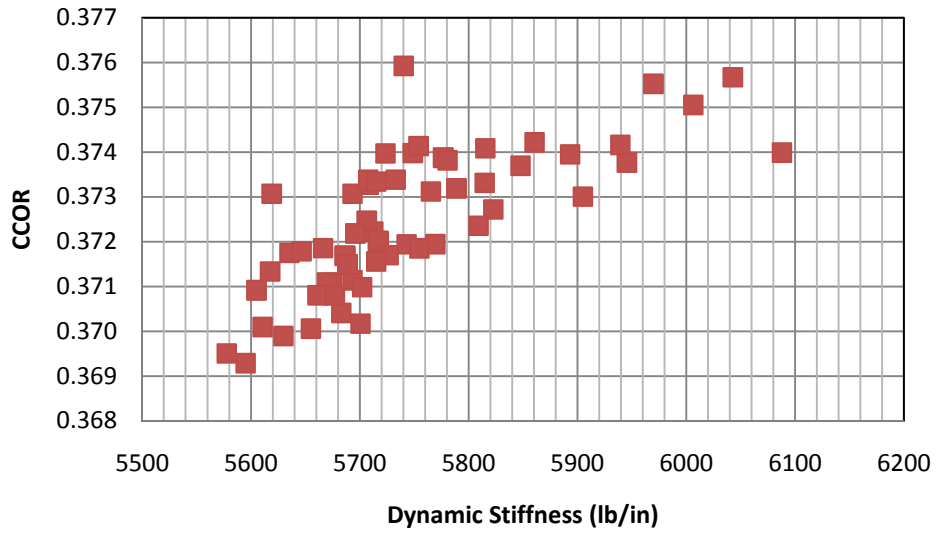

Figure 3.26: The correlation of dynamic stiffness and CCOR for the standard test ball, of the balls used in the certification test.

As seen in figure 3.26 the trend of the standard balls was linear, as the CCOR increased so did the dynamic stiffness. For this reason it was not clear whether the COR or dynamic stiffness had more effect in the correction.

The standardized bat performance test obtains 6 valid impacts at the sweet spot and at 0.5 inches on either side of the sweet spot [3.8]. Normalizing will be the most effective at the sweet spot, where $e_1 \approx 1$. To determine if the normalizing procedure was appropriate for impacts away from the sweet spot, the performance of the 77 bats were tested and normalized ± 0.5 inches away from the sweet spot. If the impact location does not matter the difference between the normalized values at and away from the sweet spot will be the same (i.e. if equation 2.25 reduced the bat performance 2 mph at the sweet spot it would also reduced the performance 2 mph away from the sweet spot). Figure 3.27 shows an example of what equation 2.25 does to impacts away from the sweet spot.

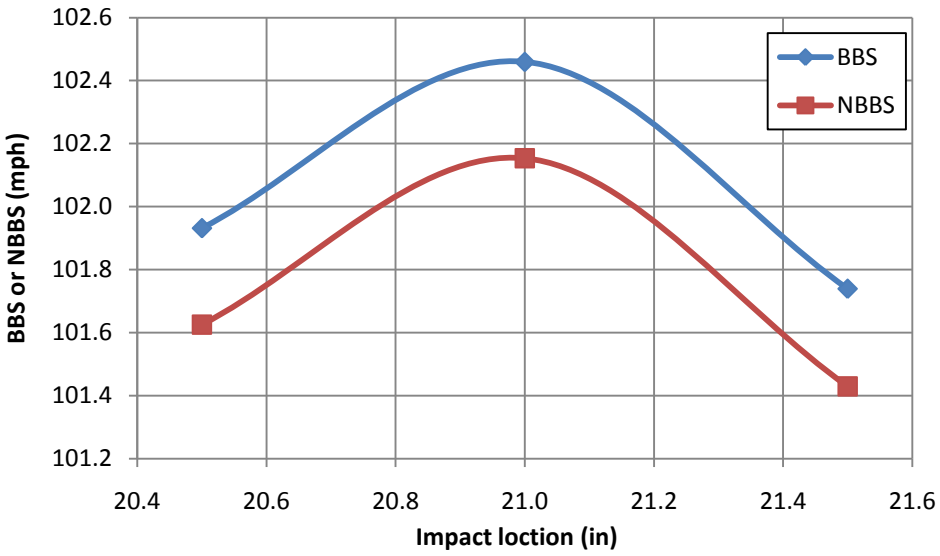

Figure 3.27: Normalizing at and away from the sweet spot.

There was a slight difference in the correction values at and ± 0.5 inches away from the sweet spot (i.e. for this bat equation 2.25 reduced the bat performance 0.306 mph at the sweet spot, it reduced the performance 0.310 mph + 0.5 inches away from the sweet spot). The difference of the corrected values at the sweet spot and the corrected values ± 0.5 inches away from the sweet spot can be seen in figure 3.28.

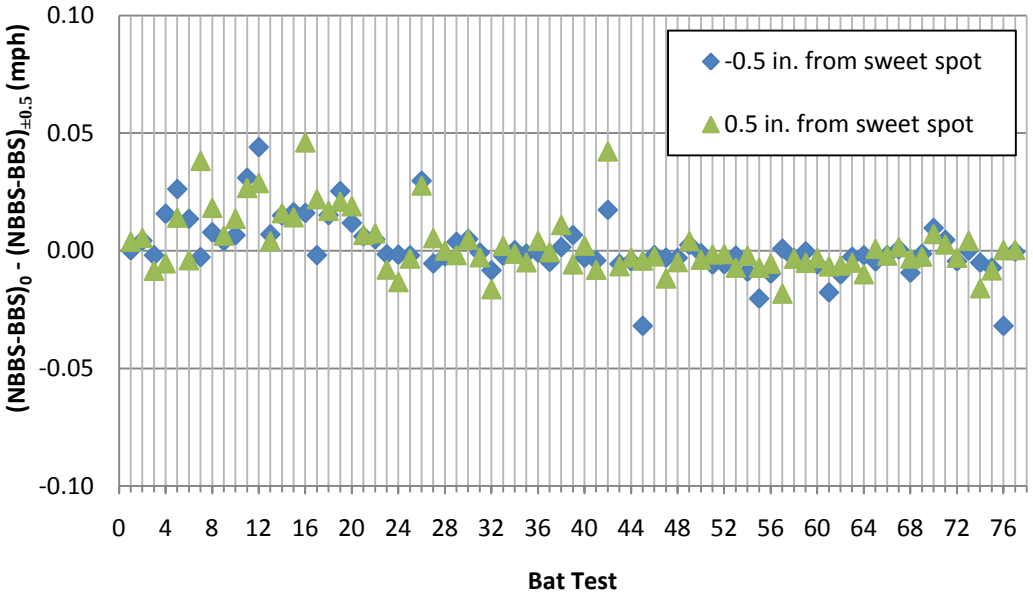

Figure 3.28: The difference between normalized performance at and away from the sweet spot ((NBBS – BBS)$_0$ – (NBBS – BBS)$_{\pm 0.5}$).

The difference in the corrected values in BBS at and away from the sweet spot was very small (less than 0.05 mph) as seen in figure 3.28. Because the relative difference in correction from the sweet spot was small for BBS and NBBS the normalizing procedure was appropriate for bat certification tests with impacts at and near the sweet spot.

3.4.2. The Effect of Normalizing

Equation 2.25 suggested that the effect of ball COR and stiffness will depend on the bat stiffness. The normalizing equations should reflect this ball property effect. The performance of a low, medium, and high performing bat were compared using equation 2.25 with differing e_{0N} and k_N. The properties of these bats can be seen in table 3.2.

Table 3.2: The properties of the low, medium, and high performing bats.

Performance	Code	Manufacturer	Model	Length (in)	Weight (oz)	MOI (oz-in^2)	e_T	BBS (mph)
Low	MW15	BamBooBat	HNBB34	34.0	30.5	10303	**0.380**	**87.9**
Medium	BS48	Worth	M7598	33.9	27.8	8860	**0.479**	**95.0**
High	NC197	Miken	Ultra 2	33.9	30.7	9096	**0.605**	**105.1**

The range for CCOR and dynamic stiffness represented commercially available balls. The results can be seen in figures 3.29 and 3.30 for varying nominal CCOR (e_{0N}) and dynamic stiffness (k_N) in equation 2.25 respectively.

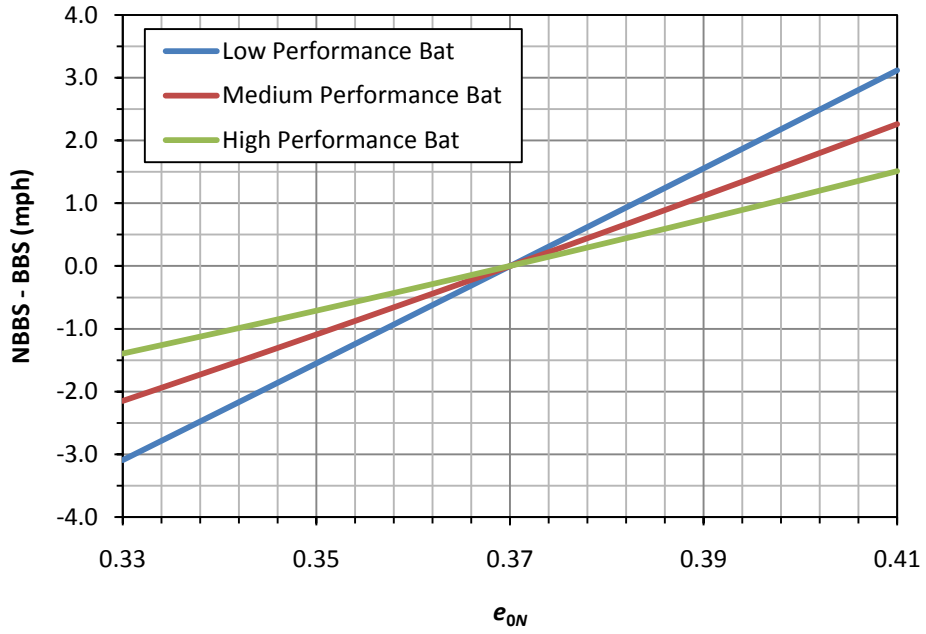

Figure 3.29: Varying nominal ball CCOR (e_{0N}) on the low, medium, and high performing bats.

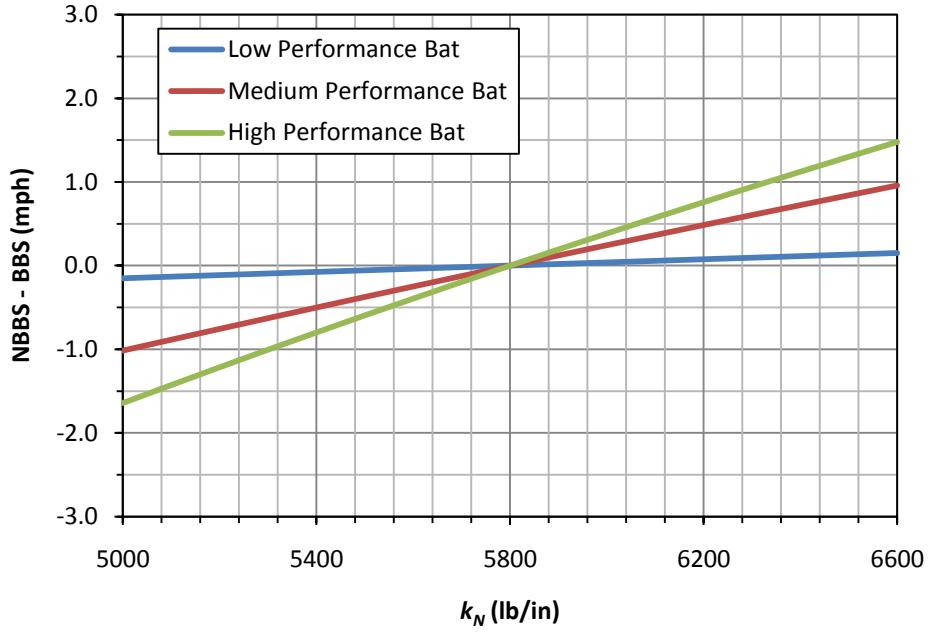

Figure 3.30: Varying nominal ball dynamic stiffness (k_N) on the low, medium, and high performing bats.

Changing e_{0N} affected the low performing bat the most and the high performing bat the least as seen in figure 3.29. Changing the k_N had relatively no effect on the low performing bat and a large effect on the high performing bat as seen in figure 3.30. The larger the trampoline effect the larger correction in BBS the normalizing procedure had on the bats with dynamic stiffness.

3.4.3. The Range Of Normalizing

To consider the effect of large differences in CCOR and dynamic stiffness on bat performance, 3 bats of differing performance (table 3.3) were tested with balls ranging in CCOR and dynamic stiffness.

Table 3.3: Manufacturer and model of bats used in the study with the specifications of each bat.

Code	Manufacturer	Model	Material	Length (in)	Weight (oz)	BP (in)	MOI (oz-in^2)	BBS (mph)
BW01	Brett Bros	Pro-Model 110	Wood (Ash)	33.0	29.2	21.6	9649	85.87
BS48	Worth	M7598	Composite	33.9	27.8	20.7	8860	95.00
ASA25	Louisville	Catalyst	Composite	34.0	26.5	21.6	8821	99.96

3.4.3.1 Normalizing On A Low Performance Bat

The low performance wood bat (BW01) was tested with 14 ball models and normalized as seen in table 3.4 and figure 3.31.

Table 3.4: The bat performance results of wood bat BW01 and the non-standard test balls with varying CCOR and dynamic stiffness.

Test Number	Model	e_{0T}	k_T (lb/in)	e_T	r_N	e_N	BBS (mph)	NBBS (mph)
1*	A9044 ASA WR	0.370	5861	**0.368**	**-500**	**0.367**	**86.1**	**86.0**
2*	SX44RLA3	0.372	5929	**0.369**	**-599**	**0.368**	**86.2**	**86.1**
3	12RSC40	0.312	5696	**0.317**	**335**	**0.374**	**82.0**	**86.6**
4	WS12RF40Y	0.331	6646	**0.338**	**-3572**	**0.375**	**83.7**	**86.7**
5	12RSC44	0.360	5315	**0.361**	**-331**	**0.371**	**85.5**	**86.4**
6	WT-12 RF80	0.356	6935	**0.363**	**217**	**0.376**	**85.7**	**86.8**
7	SBA12W44L	0.371	5902	**0.371**	**288**	**0.369**	**86.3**	**86.2**
8	12R44	0.373	6547	**0.369**	**-386**	**0.367**	**86.2**	**86.0**
9	CSB10	0.387	6500	**0.385**	**-107**	**0.368**	**87.5**	**86.2**
10	VR-6000S	0.372	6981	**0.368**	**760**	**0.367**	**86.1**	**86.0**
11	DRS12SGL	0.385	6799	**0.385**	**1410**	**0.371**	**87.5**	**86.4**
12	MP-RP-Y	0.442	4313	**0.434**	**354**	**0.357**	**91.5**	**85.2**
13	AK-EZ-USSSA-Y	0.332	8543	**0.332**	**162**	**0.370**	**83.2**	**86.3**
14	UC12S (USSSA)	0.324	7123	**0.324**	**197**	**0.370**	**82.6**	**86.3**

*** Standard Ball**

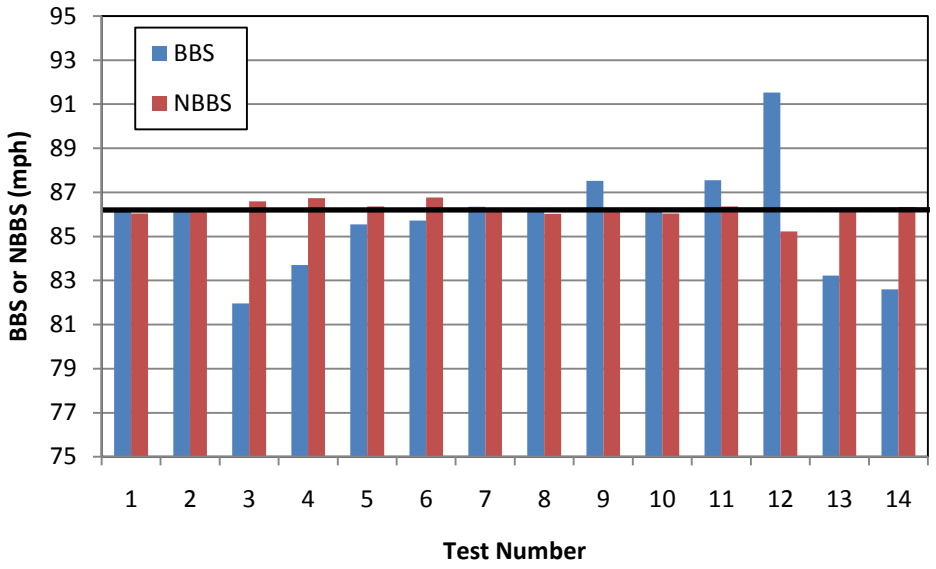

Figure 3.31: The BBS and NBBS values for the wood bat BW01 with the balls of varying CCOR and dynamic stiffness.

As seen in figure 3.31 normalizing on a wood bat works very well. The range of BBS was 9.6 mph, after normalizing the range in NBBS was to 1.5 mph. For test numbers 1, 2, 8, 9, 10, 11 and 12, $r_N < 0$. According to equation 2.23, when $e_T \approx e_{0T}$, $r_N \rightarrow \infty$. Due to experimental accuracy we sometimes had $e_{0T} > e_T$ which resulted in $r_N < 0$. While $r_N < 0$ has no physical meaning, it has only a negligible effect on normalizing since by equation 2.25 $e_N \approx e_{0N}$ when $r_N \rightarrow \infty$.

Figure 3.32 shows the normalizing on the low performing wood bat as a function of CCOR with balls that had constant dynamic stiffness (test numbers 4, 6, 8, 9,10, and 11 from table 3.4).

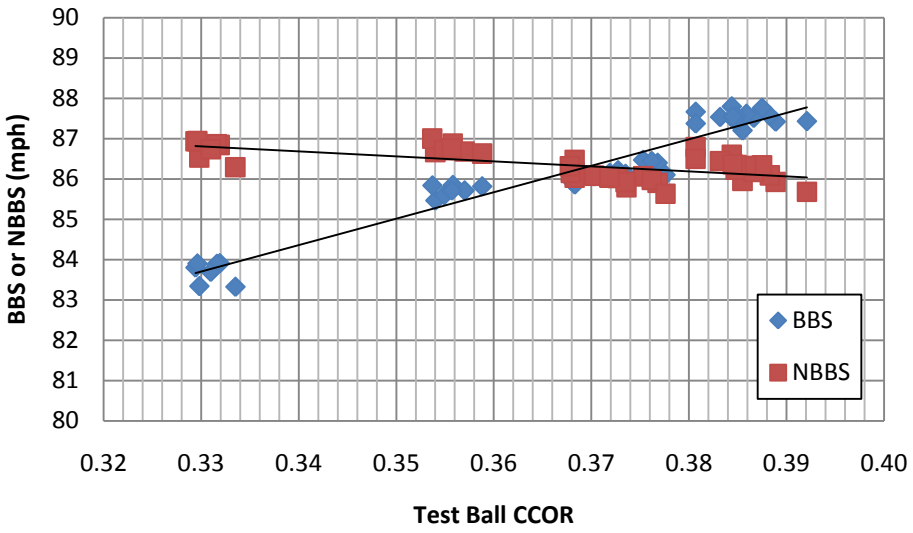

Figure 3.32: The BBS and NBBS with ball CCOR on a wood bat BW01 with balls of varying CCOR and constant dynamic stiffness.

Normalizing for CCOR had a slight over correction. The slope for the balls of constant dynamic stiffness was 65.6 (mph/CCOR) and when normalized was -12.5 (mph/CCOR), an 81% improvement. The range in BBS was 3.8 mph and the range in NBBS was 0.8 mph.

Figure 3.33 shows the normalizing on the low performing wood bat as a function of dynamic stiffness with balls that had constant CCOR (test numbers 1, 2, 7, 8 and 10 from table 3.4).

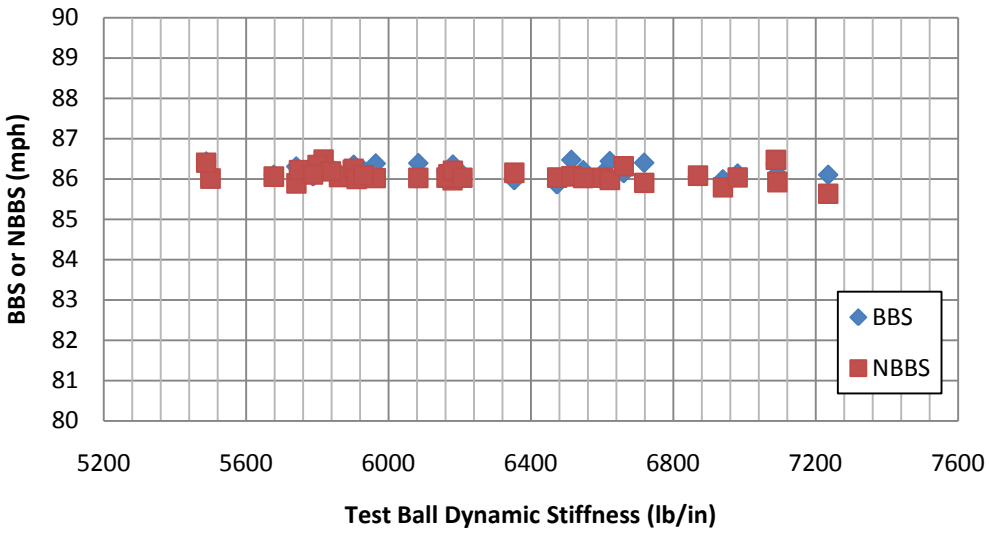

Figure 3.33: The BBS and NBBS with ball dynamic stiffness on a wood bat BW01 with balls of varying dynamic stiffness and constant CCOR.

Varying the test ball dynamic stiffness had no effect on BBS and normalizing for dynamic stiffness also had no effect. The range in BBS was 0.2 mph and the range in NBBS was 0.2 mph. These results were consistent with results shown in figure 3.30.

3.4.3.2 Normalizing On A Medium Performance Bat

The normalizing procedure was performed on a medium performance bat (BS48) with seventeen ball models as summarized in table 3.5. The results from BS48 can be seen in table 3.5 and figure 3.34.

Table 3.5: Data from performance testing of a Worth M7598 bat (BS48)

Test Number	Model	e_{0T}	k_T (lb/in)	e_T	r_N	e_N	BBS (mph)	NBBS (mph)
1*	A9044ASAWR*	0.375	5643	**0.502**	**6.5**	**0.501**	**96.6**	**96.6**
2	MP-RP-Y	0.442	4313	**0.491**	**12.5**	**0.449**	**95.8**	**92.4**
3	AK-EZ-USSSA-Y	0.332	8543	**0.522**	**6.6**	**0.500**	**98.2**	**96.5**
4*	YS44RLA3*	0.385	6261	**0.520**	**6.4**	**0.503**	**98.1**	**96.8**
5	UC12SY	0.324	7123	**0.514**	**5.7**	**0.516**	**97.6**	**97.8**
6	OA1247CL	0.400	5361	**0.478**	**10.9**	**0.461**	**94.7**	**93.3**
7	SY-12 RFFP	0.391	6049	**0.510**	**7.2**	**0.492**	**97.3**	**95.8**
8	1A312	0.372	6894	**0.514**	**6.9**	**0.496**	**97.6**	**96.2**
9	NFHS	0.391	5026	**0.463**	**11.4**	**0.456**	**93.5**	**92.9**
10	MLT 12 RF80	0.364	10819	**0.591**	**5.6**	**0.518**	**103.9**	**97.9**
11	290XLRA3	0.382	7772	**0.553**	**5.8**	**0.514**	**100.8**	**97.6**
12	A1244PS	0.371	7023	**0.521**	**6.6**	**0.500**	**98.2**	**96.5**
13	M12SUY	0.338	6630	**0.504**	**6.1**	**0.509**	**96.9**	**97.2**
14	MS-ASA44-1	0.369	9293	**0.566**	**5.9**	**0.512**	**101.8**	**97.4**
15	T12ASY	0.363	7368	**0.535**	**5.9**	**0.512**	**99.3**	**97.5**
16	12RSC40	0.325	7002	**0.516**	**5.5**	**0.519**	**97.8**	**98.0**
17*	A9044ASAWR*	0.375	5643	**0.499**	**6.7**	**0.499**	**96.4**	**96.4**

*** Standard ball**

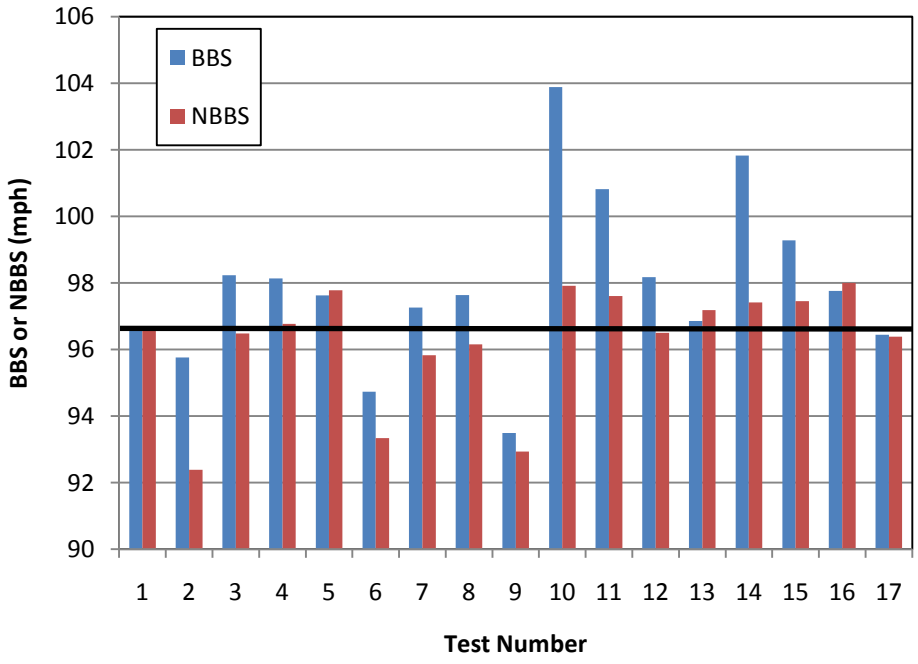

Figure 3.34: BBS and BBBS values for the Worth M7598 bat (BS48) where test 1, 4 and 17 were performed with the standard ball.

To test that the performance of the bat did not change during the tests, the bat was tested twice with the standard test balls (Test #1 and #17, table 3.5). The change in BBS from the first test to the last was 0.2 mph, within the repeatability of the test. Overall, the range of BBS was 10.4 mph. After normalizing the range in NBBS was 5.6 mph. Normalizing appears to improve the comparison in all cases except test numbers, 2, 6 and 9. These balls all have high CCOR, low dynamic stiffness and $e_T \approx e_{0T}$. Removing test #2, 6 and 9 the range in NBBS improved to 2.2 mph. The effect of high CCOR, low stiffness will be investigated further in section 3.3.7. and chapter 4.

The BBS and NBBS was plotted against the ball CCOR (e_{0T}) and dynamic stiffness as seen in figure 3.35 and figure 3.36 respectively. Test numbers 4, 7, 8 and 13 for constant dynamic stiffness. Ball models 1, 8, 10, 12, 14, 15 and 17 for constant CCOR.

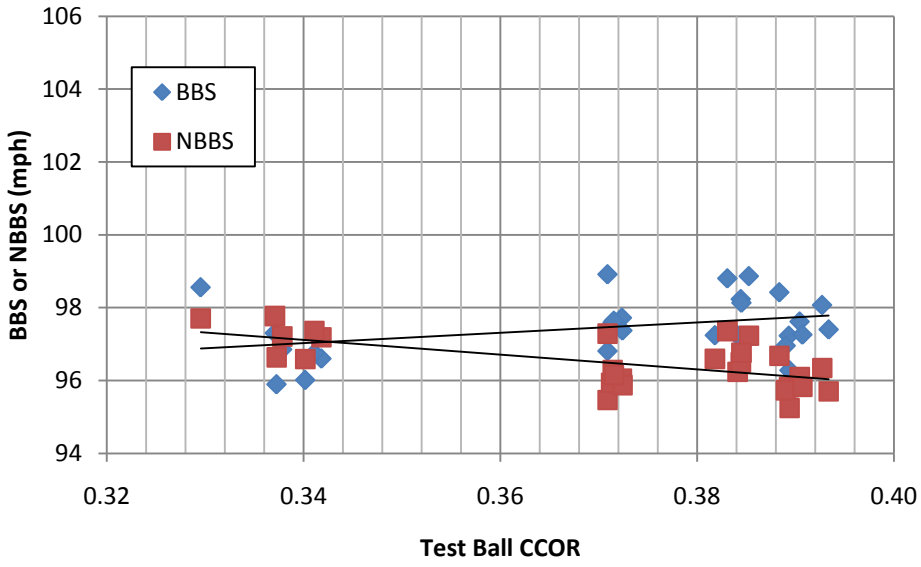

Figure 3.35: The BBS and NBBS with ball CCOR on a composite bat model Worth M7598 (BS48) with balls of constant dynamic stiffness.

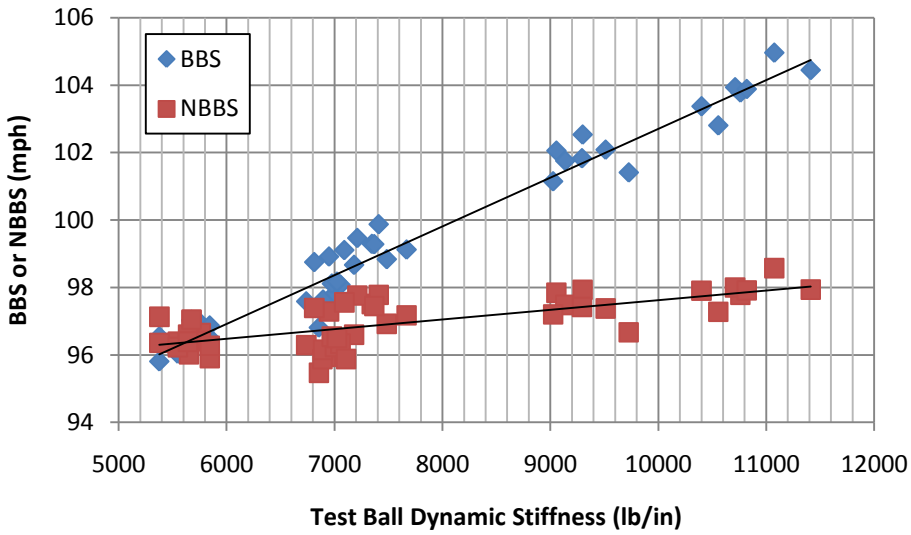

Figure 3.36: The BBS and NBBS with ball dynamic stiffness on a composite bat model Worth M7598 (BS48) with balls of constant CCOR.

The BBS slope for the balls of constant dynamic stiffness was 14.1 (mph/CCOR) and NBBS was -20.1 (mph/CCOR), an increase of 44%. Normalizing for CCOR over corrected for the balls of constant dynamic stiffness and did not improve the slope. The range for BBS was 1.3 mph and the range for NBBS was 1.4 mph. While it was unfortunate that normalizing did not improve the effect of CCOR, the range in BBS was relatively small, so the over correction was deceiving. It these cases experimental error in CCOR and BBS play a larger role in normalizing. The BBS slope for the balls of constant CCOR was 0.0014 (mph/DS) and NBBS (mph/DS) was 0.0003, a 79% improvement. The range in BBS was 7.4 mph and the range in NBBS was 1.8 mph.

3.4.3.3 Normalizing On A High Performance Bat

The normalizing procedure was performed on a high performing (ASA25) bat with seventeen ball models. The results from ASA25 can be seen in table 3.6 and figure 3.37.

Table 3.6: Data from performance testing and normalizing of the high performing Louisville Catalyst bat (ASA25).

Test Number	Model	e_{0T}	k_T (lb/in)	e_T	r_N	e_N	BBS (mph)	NBBS (mph)
1*	A9044 ASA WR*	0.370	5861	**0.538**	**4.7**	**0.536**	**100.0**	**99.8**
2*	SX44RLA3*	0.372	5929	**0.540**	**4.7**	**0.537**	**100.1**	**99.9**
3	12RSC40	0.312	5696	**0.511**	**4.4**	**0.544**	**97.7**	**100.4**
4	WS12RF40Y	0.331	6646	**0.543**	**4.4**	**0.546**	**100.3**	**100.6**
5	12RSC44	0.360	5315	**0.507**	**5.4**	**0.522**	**97.4**	**98.7**
6	WT-12 RF80	0.356	6935	**0.561**	**4.4**	**0.546**	**101.8**	**100.6**
7	SBA12W44L	0.371	5902	**0.540**	**4.7**	**0.537**	**100.1**	**99.9**
8	12R44	0.373	6547	**0.566**	**4.2**	**0.550**	**102.2**	**100.9**
9	CSB10	0.387	6500	**0.569**	**4.4**	**0.546**	**102.4**	**100.6**
10	VR-6000S	0.372	6981	**0.577**	**4.1**	**0.553**	**103.1**	**101.1**
11	DRS12SGL	0.385	6799	**0.579**	**4.2**	**0.552**	**103.3**	**101.1**
12	MLT12RF80(ASA)	0.365	9677	**0.632**	**3.8**	**0.564**	**107.6**	**102.1**
13	MLT12RF80USSSA	0.363	9097	**0.625**	**3.7**	**0.566**	**107.0**	**102.2**
14*	A9044 ASA WR*	0.370	5861	**0.538**	**4.7**	**0.537**	**100.0**	**99.9**
15	MP-RP-Y	0.442	4313	**0.501**	**10.2**	**0.464**	**96.6**	**93.6**
16	AK-EZ-USSSA-Y	0.332	8543	**0.553**	**5.2**	**0.525**	**100.8**	**98.5**
17	UC12SY	0.324	7123	**0.546**	**4.5**	**0.543**	**100.3**	**100.0**

*** Standard ball**

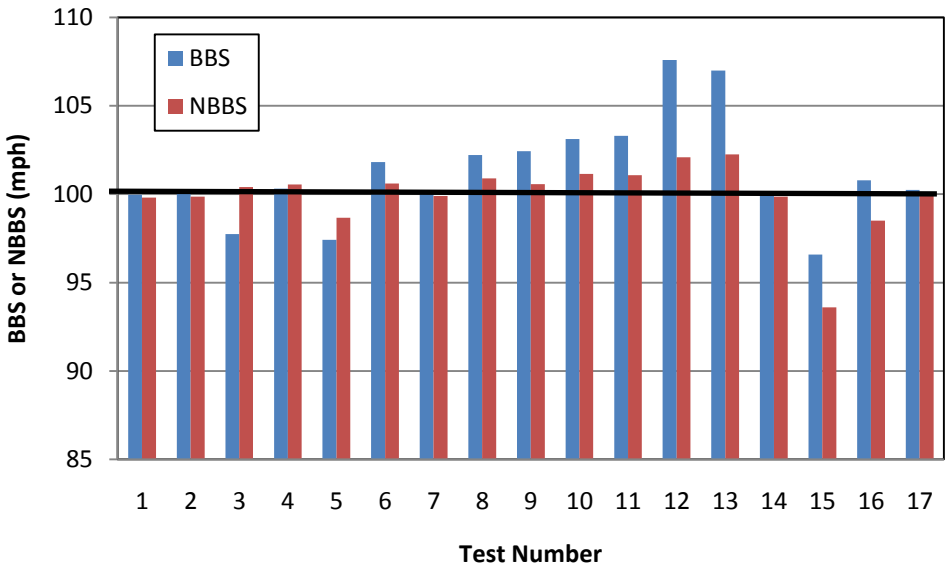

Figure 3.37: The BBS and NBBS values for the Louisville Catalyst bat (ASA25) where test 1, 2 and 14 were performed with the standard ball.

The bat was also tested twice with the control ball (test #1 and #14) where the performance remained within 0.1 mph. The range of BBS was 11.0 mph but after normalizing the range in NBBS was 8.7 mph. The outlier was test number 15 which was another high CCOR, low dynamic stiffness ball and again $e_T \approx e_{0N}$. Without test number 15, the range in NBBS improved to 3.7 mph. The normalizing procedure does not correct enough for the high and low dynamic stiffness balls as seen in table 3.6. The NBBS was plotted against the ball CCOR (e_{0T}) and dynamic stiffness, as seen in figure 3.38 and figure 3.39 respectively. Test numbers 4, 5, 8, 9, 10, 11 and 17 were used for constant dynamic stiffness. Test numbers 1, 2, 5, 7, 8, 10, 12, 13 and 14 were used for constant CCOR.

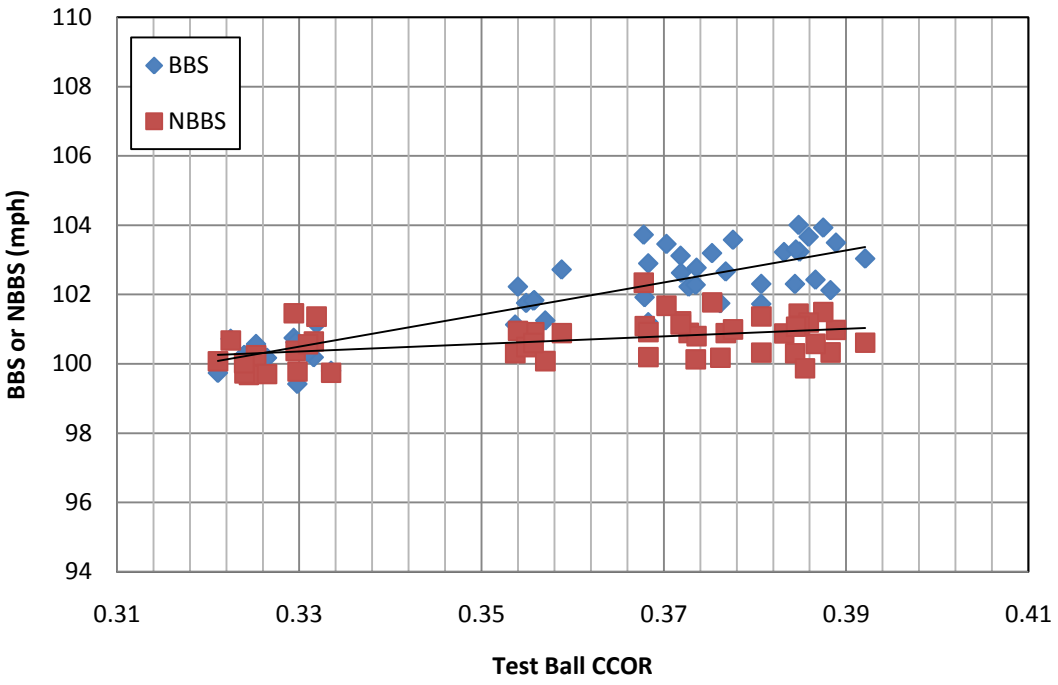

Figure 3.38: The BBS and NBBS with ball CCOR on a composite bat, model Louisville Catalyst (ASA25) with balls of constant dynamic stiffness.

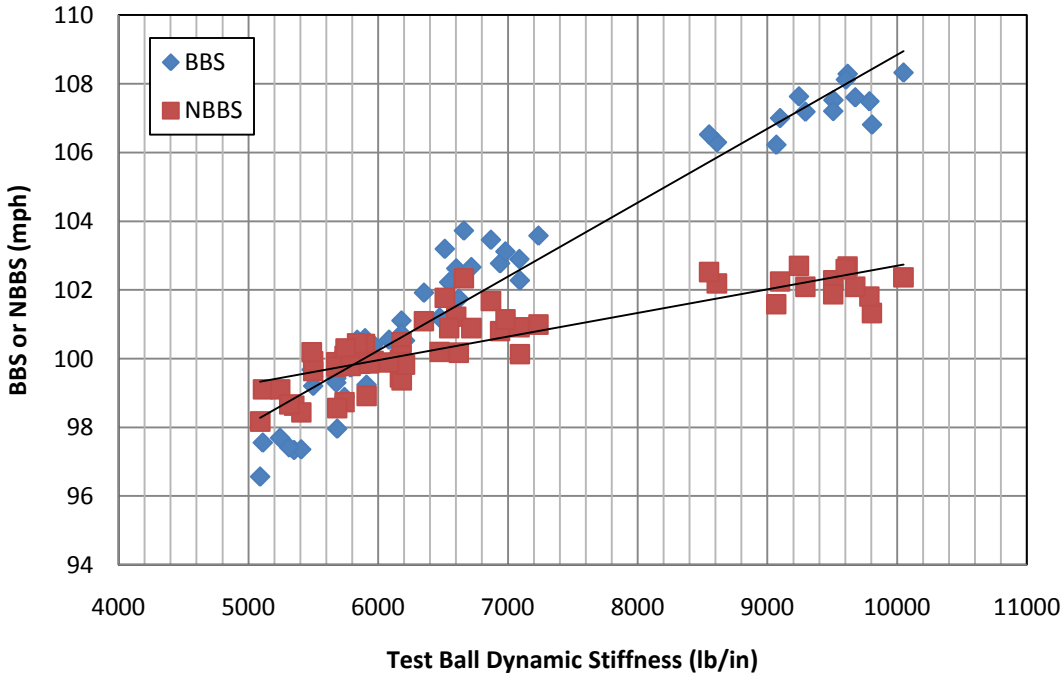

Figure 3.39: The BBS and NBBS with ball dynamic stiffness on a composite bat, model Louisville Catalyst (ASA25) with balls of constant CCOR.

The slope for the balls of constant dynamic stiffness was 46.2 (mph/CCOR) and when normalized was 10.9 (mph/CCOR), a 76% improvement. The range in BBS was 3.0 mph and the range in NBBS was 1.1 mph. The slope for the balls of constant CCOR was 0.0022 (mph/DS) and when normalized was 0.0007 (mph/DS) a 68% improvement. The range in BBS was 10.2 mph and the range in NBBS was 3.6 mph. Normalizing for CCOR worked better than for stiffness. Note that NBBS was relatively constant with CCOR for all three bats, while NBBS showed an increasing dependence on dynamic stiffness as bat performance increased. This will be explored further in chapter 4.

Overall, for balls with a range of $0.332 < e_T < 0.385$ and 5643 lb/in $< k_T <$ 7123 lb/in the range of BBS with the low performing bat was 3.8 mph, the range of BBS with the medium performing bat was 1.8 mph and the range of BBS with the high performing bat was 2.5 mph. All three bats normalized to -0.5 mph < NBBS-BBS* < 0.6 mph.

3.4.4 Other Factors Affecting Bat Performance

The anomalous results of the high CCOR low dynamic stiffness balls (model MP-RP-Y) on NBBS observed in the hollow bats were not apparent in the wood bat (compare test # 12, 2 and 15 in tables 3.4, 3.5 and 3.6 respectively). The unique response of this ball was, therefore, related to its dynamic stiffness. The deformation of MP-RP-Y was compared to the control ball in figures 3.40 and 3.41. MP-RP-Y appeared to deform more and restore faster; responses which were consistent with its low stiffness and high COR.

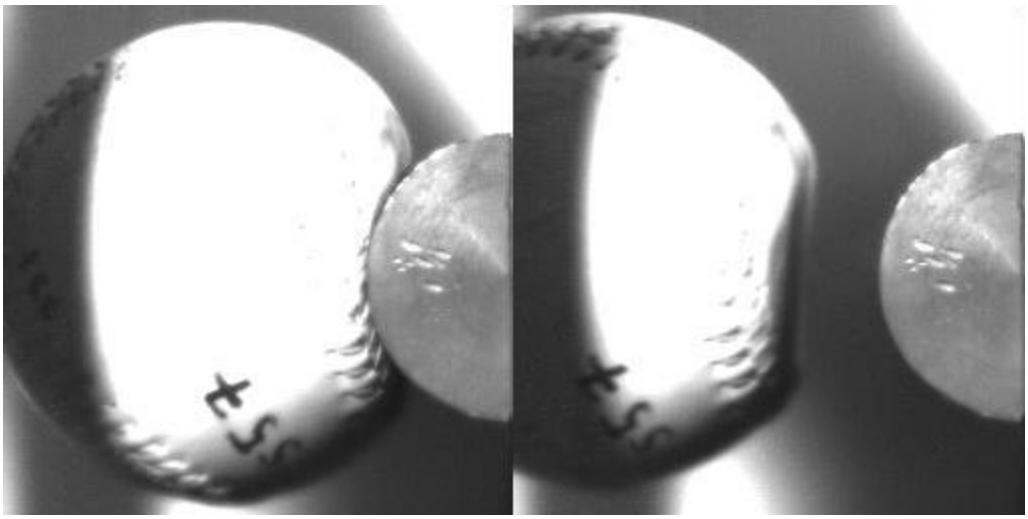

Figure 3.40: The standard ball model during and after impact with the dynamic stiffness cylinder.

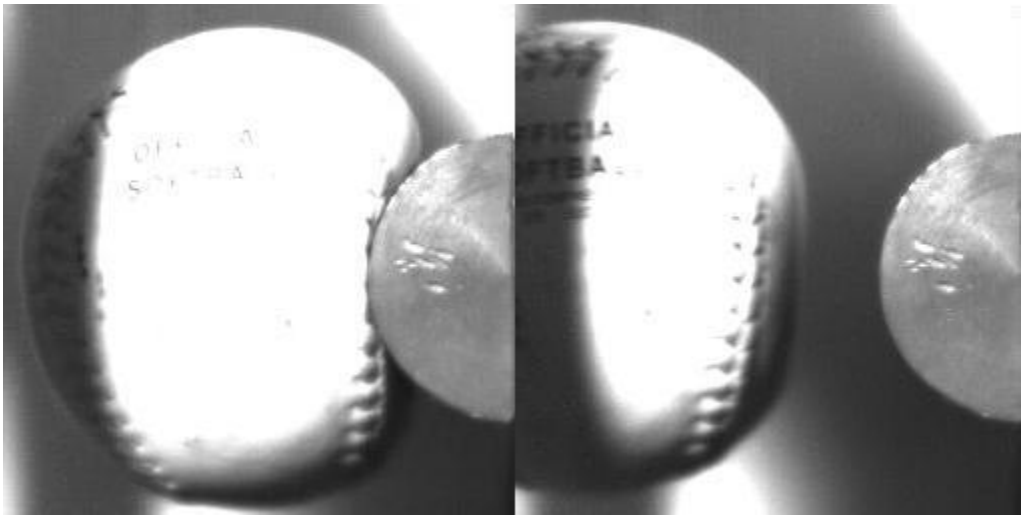

Figure 3.41: The MP-RP-Y ball model during and after impact with the dynamic stiffness cylinder.

The force-displacement response of MP-RP-Y was compared to the control ball in figure 3.42.

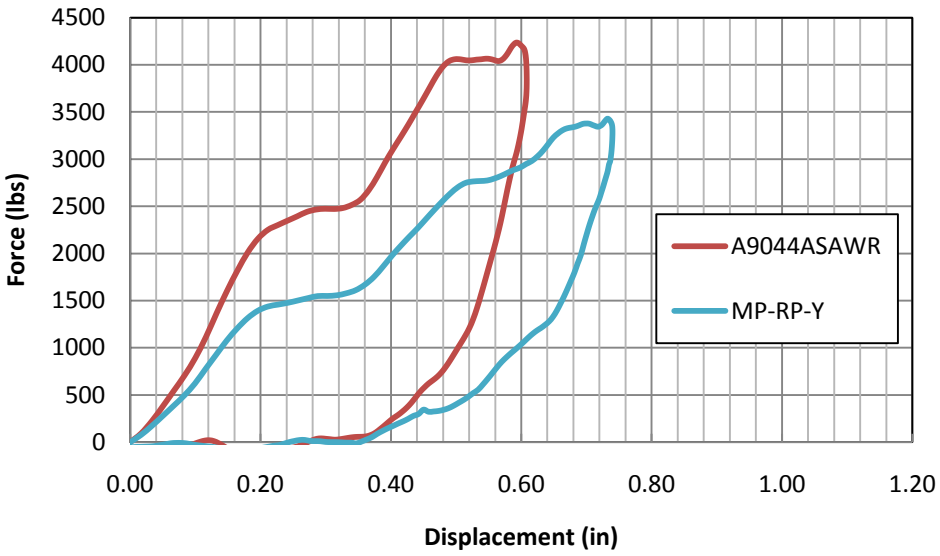

Figure 3.42: The force-displacement curves for the A9044ASAWR and MP-RP-Y ball models.

The figure describes MP-RP-Y as the softer ball, but provides no evidence of unusual response to explain why it does not normalize correctly. The response of this ball will be examined further in the next chapter.

3.5. Summary

In order to normalize bat performance the CCOR and dynamic stiffness of the test ball were found. Four different approaches to find the dynamic stiffness of a softball were considered. While the results varied, the relative differences between the approaches were relatively constant. Given the simplicity and consistency of the results, k_F (peak force) was chosen to find the dynamic stiffness. The standard test ball had values of 0.37 and 5800 lb/in for the CCOR and dynamic stiffness respectively.

Ball properties affect low and high performing bats differently. The CCOR of the ball was important for low performing bats, while the stiffness of the ball was important for high

performing bats. These trends were consistent with our understanding of the trampoline effect in the barrel.

It was found that the normalizing procedure generally worked well for CCOR and for dynamic stiffness. The wood bat had a BBS range of 9.6 mph and a NBBS range of 1.5 mph. The medium performance bat had a BBS range of 10.4 mph and a NBBS range of 5.6 mph. The high performance bat had a BBS range of 11.0 mph and a NBBS range of 8.7 mph.

While the range in performance decreased for all bats, normalizing did not work well for balls that had high CCOR and low stiffness. The correction for these balls was supposed to be positive however, for the medium and high performing bats the correction was negative. Removing these outliers, the range in NBBS was 2.2 mph and 3.7 mph for the medium and high performing bats respectively. The response of this ball will be considered further in chapter 4.

When the test ball had a range of $0.332 < e_T < 0.385$ and 5643 lb/in $< k_T <$ 7123 lb/in the range of BBS with the low performing bat was 3.8 mph, the range of BBS with the medium performing bat was 1.8 mph and the range of BBS with the high performing bat was 2.5 mph. When normalized using these balls the performance had a range of -0.5 mph < NBBS-BBS* < 0.6 mph for the low, medium and high performance bats. Using this data it was recommended that a range of $0.33 < e_T < 0.38$ and 5600 lb/in $< k_T <$ 7000 lb/in be used in bat performance testing.

REFERENCES

[3.1] **F1887-02, ASTM.** Standard test method for measuring the coefficient of restitution of baseballs and softballs. West Conshohocken, Pa : s.n., 2003.

[3.2] **F2219-07, ASTM.** Standard Test Methods for Measuring High-Speed Bat Performance. West Conshohocken, PA : s.n., November 2007.

[3.3] **F1888-02, ASTM.** Test Method for Compression-Displacement of Baseballs and Softballs. West Conshohocken, PA : s.n., January 2003.

[3.4] **Smith, L. V.** *Measuring the Hardness of Softballs.* Orlando, FL : s.n., 2008. IMAC-XXVI.

[3.5] **F2845, ASTM.** Measuring the Dynamic Stiffness (DS) and Cylinderical Coefficient of Restitution (CCOR) of Baseballs and Softballs.

[3.6] **F2398, ASTM.** Standard Test Method for Measuring Moment of Inertia and Center of Percussion of a Baseball or Softball Bat. *ASTM International.*

[3.7] **Russell, Dan.** *Swing Weights of Baseball and Softball Bats.* Flint : The Physics Teacher, 2009 Submitted.

[3.8] **F2219-07, ASTM.** Standard Test Methods for Measuring High-Speed Bat Performance. West Conshohocken, PA : s.n., November 2007.

Chapter Four

Computer Modeling

4.1. Introduction

Normalizing had some problems that could not be addressed experimentally. A numerical model was developed using LS-DYNA. The purpose of the model was to investigate the assumptions and mechanisms affecting normalization.

4.2. Finite Element Analysis

The ball models were tuned to desired values of CCOR and stiffness. This study used the power law visco-elastic material model (equation 2.26). The dynamic stiffness test was modeled numerically shown in figure 4.1.

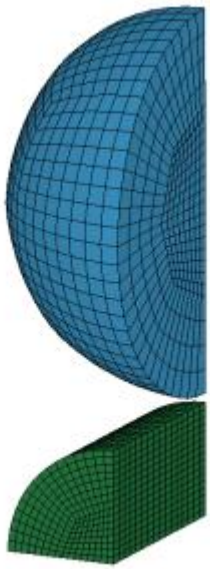

Figure 4.1: FEA model of the dynamic stiffness test.

A quarter of the ball and cylinder was modeled to reduce computation time. The ball was modeled with 2,560 8-node solid elements and the cylinder was modeled with 3,072 8-node solid elements.

The bat model used in this study was a single wall aluminum bat. The performance of the bat was changed by modifying the elastic modulus to simulate different wall thickness without affecting the MOI, weight or length of the bat. The bat was modeled using thick shell (8 node), linear, elastic elements.

A picture of the bat model with the ball can be seen in figure 4.2.

Figure 4.2: FEA model of the performance test.

The bat was pinned at 6 inches from the end of the knob to simulate the performance test. The bat, knob, and endcap were modeled separately because they have different material properties. The bat was modeled with 8,784 elements, the knob was modeled with 900 elements, the endcap was modeled with 540 elements and the ball was modeled with 10,240 elements.

4.3. CCOR and Dynamic Stiffness Results

To determine if the ball model represented experimental data, the force-time curve and force-displacement of the FEA model and experiment were plotted together as seen in figure 4.3

and figure 4.4 (For this comparison the FEA model has the same CCOR and dynamic stiffness as the experiment with k = 0.10 Msi, G_0 = 20 ksi, G_∞ = 1.0 ksi and $\beta = 6.8 \times 10^4$).

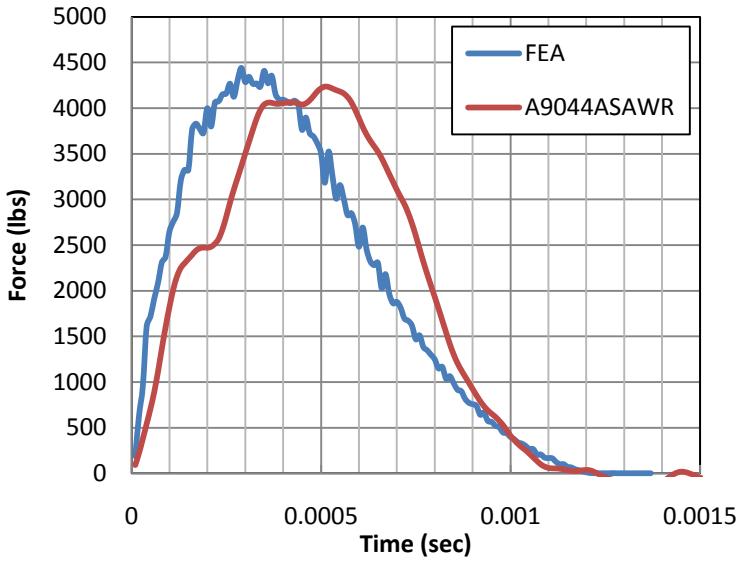

Figure 4.3: Representative force-time curve for the experimental and FEA analysis for a softball at 95 mph.

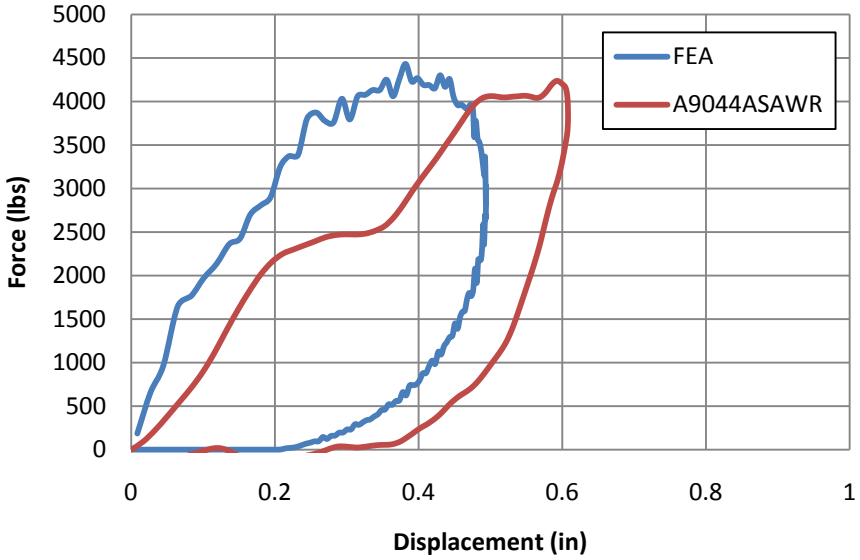

Figure 4.4: Representative force-displacement curve for the experimental and FEA analysis for a softball at 95 mph.

The FEA model matched the contact time of the experimental data but the FEA model reached max force sooner (~0.2 ms sooner) and the maximum displacement was not the same (~0.1 in. less). The results closely matched Smith and Duris's model [4.1].

By carefully choosing k, G_0, G_∞, and β the CCOR and dynamic stiffness was controlled [4.2]. The dynamic stiffness was found four ways (equations 3.3, 3.5, 3.7, 3.10) as done with the experimental data. The properties of the balls can be seen in table 4.1 and the values of the different ways to find dynamic stiffness can be seen in table 4.2.

Table 4.1: Balls used in the FEA model showing the physical properties used in the Power Law.

Model Number	ρ (lb/in^3)	k (Msi)	G_0 (ksi)	G_∞ (ksi)	β
1	3.97E-05	0.10	25.0	0.90	6.80E+04
2	3.97E-05	0.10	21.0	0.92	6.80E+04
3	3.97E-05	0.10	21.0	0.97	6.80E+04
4	3.97E-05	0.10	20.2	0.98	6.80E+04
5*	3.97E-05	0.10	20.0	1.00	6.80E+04
6	3.97E-05	0.10	19.0	1.00	6.80E+04
7	3.97E-05	0.10	18.2	1.00	6.80E+04
8	3.97E-05	0.10	17.0	1.04	6.80E+04
9	3.97E-05	0.10	15.0	1.07	6.80E+04
10	3.97E-05	0.10	15.0	0.68	6.80E+04
11*	3.97E-05	0.10	20.0	1.00	6.80E+04
12	3.97E-05	0.10	30.0	1.80	6.80E+04
13	3.97E-05	0.10	35.0	2.20	6.80E+04
14	3.97E-05	0.10	11.5	0.69	6.80E+04
15	3.97E-05	0.10	35.0	1.60	6.80E+04

*** Standard ball**

Table 4.2: FEA model balls showing the different ways to find dynamic stiffness (Eqns. 3.3, 3.5, 3.7, 3.10).

		Dynamic Stiffness (lb/in)			
Model Number	**CCOR**	k_F	k_V	k_x	k_t
1	0.298	6721	14178	5339	22609
2	0.343	6195	12990	5800	20380
3	0.352	6397	13239	6221	20410
4	0.363	6244	13032	6366	19966
5*	0.369	6227	13065	6626	19839
6	0.382	6333	12747	6531	19447
7	0.393	6336	12493	6592	19072
8	0.417	6297	12282	6829	18394
9	0.454	6267	11822	7165	17273
10	0.371	4689	9952	4763	17041
11*	0.369	6227	13065	6626	19839
12	0.373	9857	19809	10004	24602
13	0.371	11339	23371	11399	26407
14	0.439	4583	8934	5048	15719
15	0.314	9752	20788	9117	25979

*** Standard ball**

The model numbers 1-9 correspond to balls with constant dynamic stiffness and varying CCOR. Model numbers 10-13 correspond to balls with constant CCOR and varying dynamic stiffness. Model numbers 14 and 15 correspond to balls with high CCOR with low dynamic stiffness and low CCOR with high dynamic stiffness respectively.

The values for the four different ways to determine the dynamic stiffness can be seen in figure 4.5.

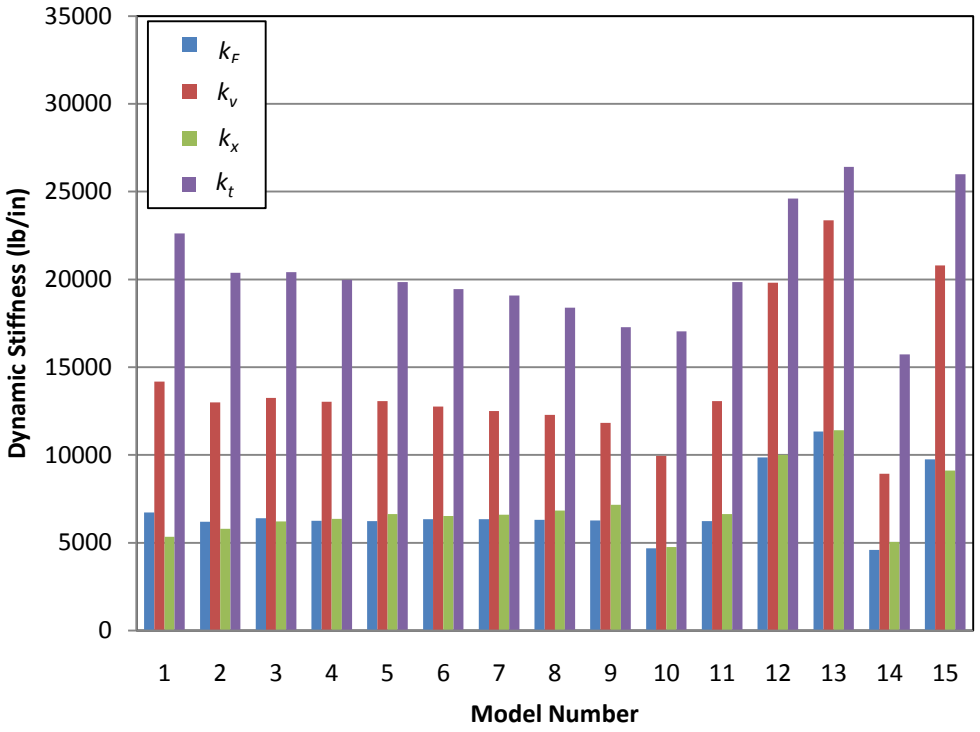

Figure 4.5: The FEA model balls and the four different ways to find dynamic stiffness.

The four ways to find dynamic stiffness gave four different results similar to the experimental data. The FEA model did have larger percent difference then the experimental data. Between k_F and k_v the percent difference ranged from 89% to 113%, between k_F and k_x the range was -21% to 14%, and between k_F and k_t the range was 133% to 263%. Once again however, k_F and k_x were the closest together and the largest percent difference was with the balls that were on the ends of the spectrum with balls of constant dynamic stiffness and varying CCOR. Overall the trends match the experimental data, so k_F was used to find dynamic stiffness.

The FEA force-time results were fit to a sine curve as done for the experimental data, as shown in figure 4.6. The sine fit induced more error because in the FEA model the maximum force was reached quickly and then dissipated slowly as seen in figure 4.6.

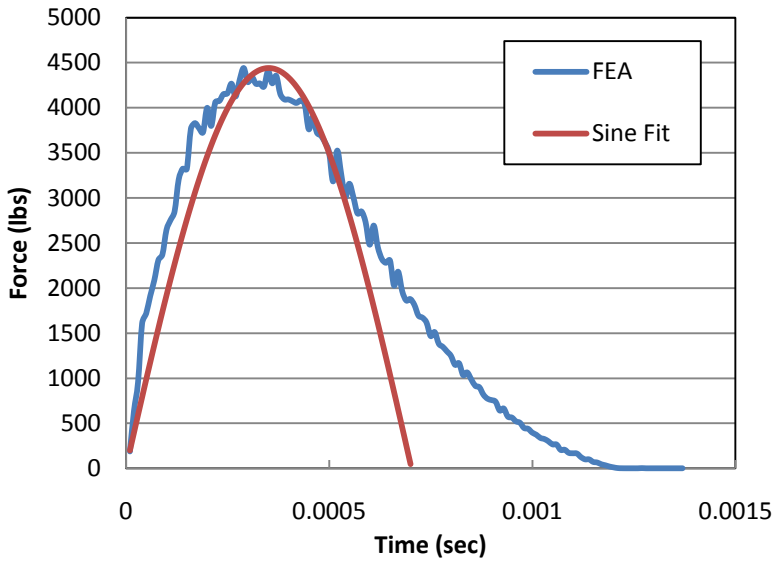

Figure 4.6: Force-time curve and sine fit for the FEA model standard ball (number 5).

The balls with constant dynamic stiffness and varying CCOR had very similar force-time curves and force-displacement curves as seen in figures 4.7 and 4.8 respectively.

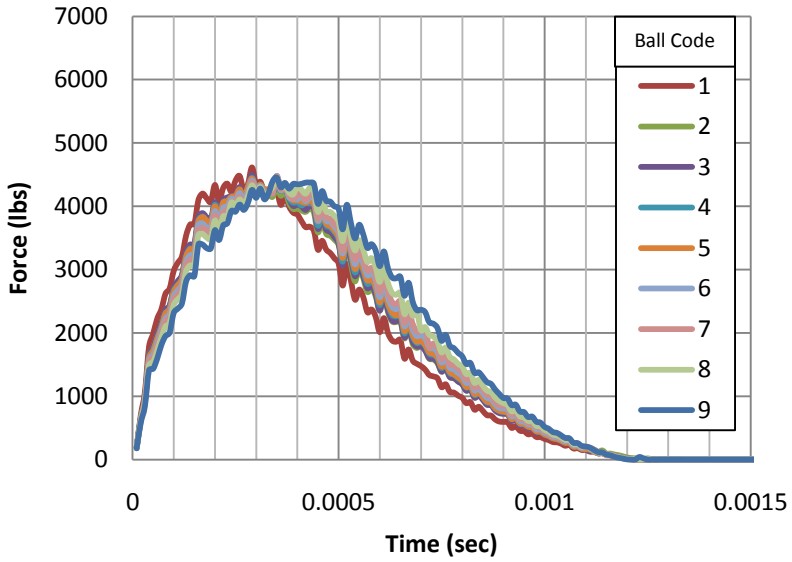

Figure 4.7: The force-time curves for the balls with constant dynamic stiffness and varying CCOR in the FEA model.

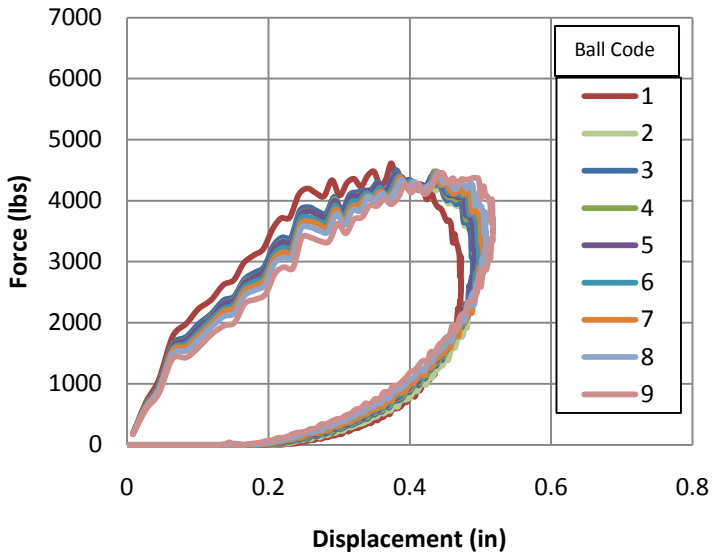

Figure 4.8: The force-displacement curves for the balls with constant dynamic stiffness and varying CCOR in the FEA model

Hysteresis was the same with balls of constant dynamic stiffness and varying CCOR.

The balls with constant CCOR and varying dynamic stiffness had different force-time curves and force-displacement curves as seen in figures 4.9 and 4.10 respectively. The differences were consistent with changes in dynamic stiffness.

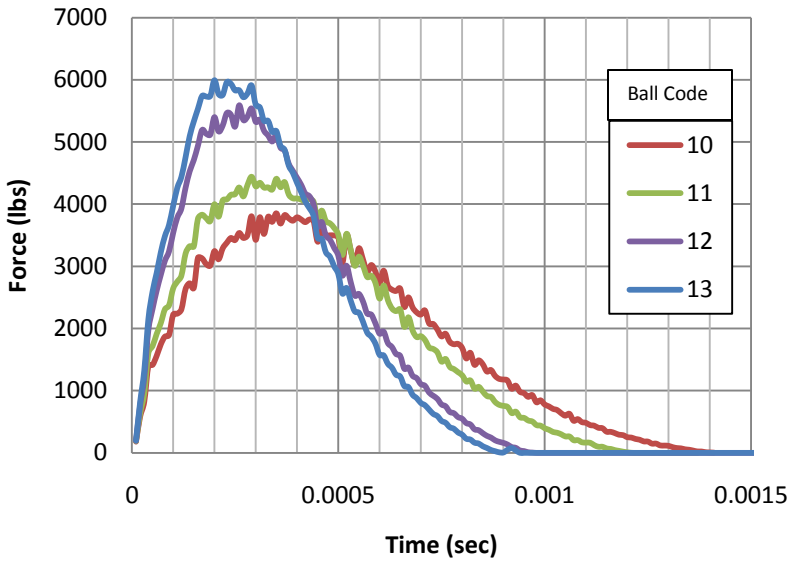

Figure 4.9: The force- time curves for the balls with constant CCOR and varying dynamic stiffness in the FEA model.

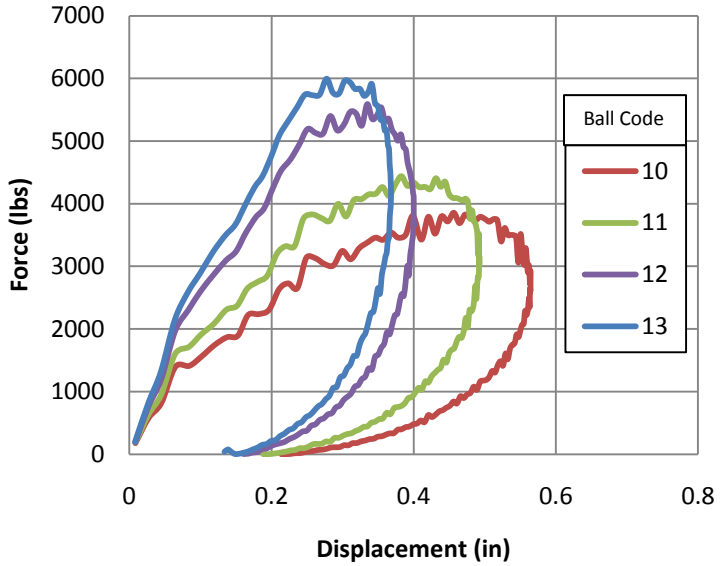

Figure 4.10: The force-displacement curves for the balls with constant CCOR and varying dynamic stiffness in the FEA model

The hysteresis was not constant with changing dynamic stiffness. Comparing figure 4.7 and 4.9 showed that dynamic stiffness was dependent on contact duration.

4.4. Bat-Ball Collision Simulation and Normalizing Results

The FEA model simulated the BBS performance test with bats in table 4.3 and the balls in table 4.1. The bat had a length of 34 inches, barrel diameter of 2.25 inches, barrel wall thickness of 0.076 inches and MOI of 9784 in-oz^2.

Table 4.3: FEA model bat specifications

	Barrel and Handle			Knob			Endcap		
Bat	Density, ρ (lb/in^3)	Elastic Modulus (Msi)	Possion's Ratio, v	Density, ρ (lb/in^3)	Elastic Modulus (Msi)	Possion's Ratio, v	Density, ρ (lb/in^3)	Elastic Modulus (Msi)	Possion's Ratio, v
Low	2.50E-04	20	0.3	2.50E-04	10	0.3	1.79E-03	0.5	0.28
Medium	2.50E-04	10	0.3	2.50E-04	10	0.3	1.79E-03	0.5	0.28
High	2.50E-04	7.5	0.3	2.50E-04	10	0.3	1.79E-03	0.5	0.28

The sweet spot of the bat was determined by impacting the bat at different locations along the barrel. The sweet spot was found to be 22.5 inches from the pivot as seen in figure 4.11. The sweet spot was found using the medium performance bat with the standard ball.

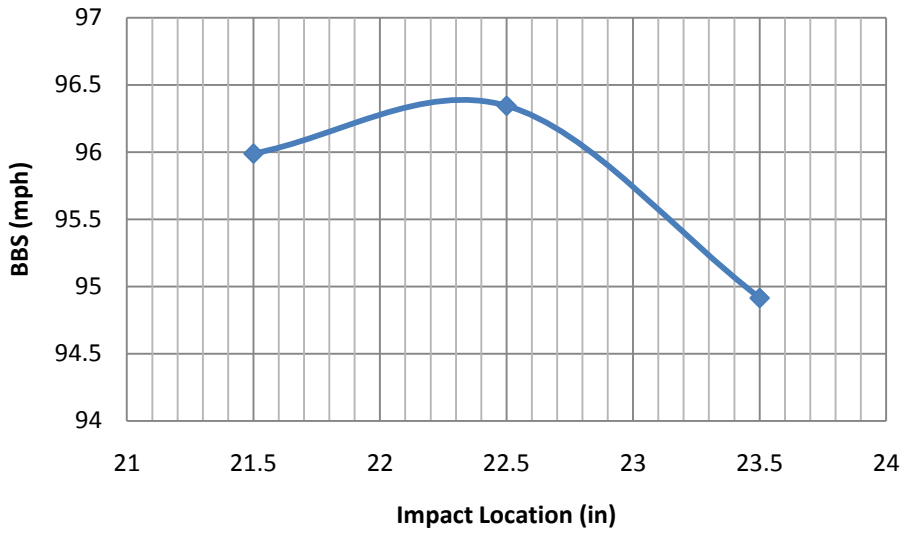

Figure 4.11: The FEA model finding the sweet spot on the medium performance bat with the standard ball.

Normalizing for CCOR and dynamic stiffness using NBBS through equation 3.17 was performed at 22.5 inches from the pivot.

4.4.1. FEA Normalizing For A Low Performance Bat

The results for the low performing bat can be seen in table 4.4 and figure 4.12.

Table 4.4: FEA performance results for the low performing bat.

Ball Model Number	e_{0T}	k_T (lb/in)	e_T	r_N	e_N	BBS (mph)	NBBS (mph)
1	0.298	6721	0.342	33.3	0.402	**84.0**	**88.9**
2	0.343	6195	0.378	33.3	0.402	**87.0**	**88.9**
3	0.352	6397	0.391	30.1	0.406	**88.0**	**89.2**
4	0.363	6244	0.400	29.6	0.406	**88.8**	**89.2**
5*	0.369	6227	0.408	28.0	0.408	**89.4**	**89.4**
6	0.382	6333	0.418	29.3	0.407	**90.2**	**89.3**
7	0.393	6336	0.427	30.0	0.406	**90.9**	**89.2**
8	0.417	6297	0.450	28.1	0.408	**92.8**	**89.4**
9	0.454	6267	0.485	26.6	0.410	**95.6**	**89.5**
10	0.371	4689	0.376	190.7	0.376	**86.8**	**86.8**
11*	0.369	6227	0.408	28.0	0.408	**89.4**	**89.4**
12	0.373	9857	0.468	15.4	0.435	**94.3**	**91.6**
13	0.371	11339	0.486	14.0	0.440	**95.7**	**92.0**
14	0.439	4583	0.439	-3317.4	0.370	**91.9**	**86.3**
15	0.314	9752	0.412	18.2	0.426	**89.7**	**90.9**

*** Standard ball**

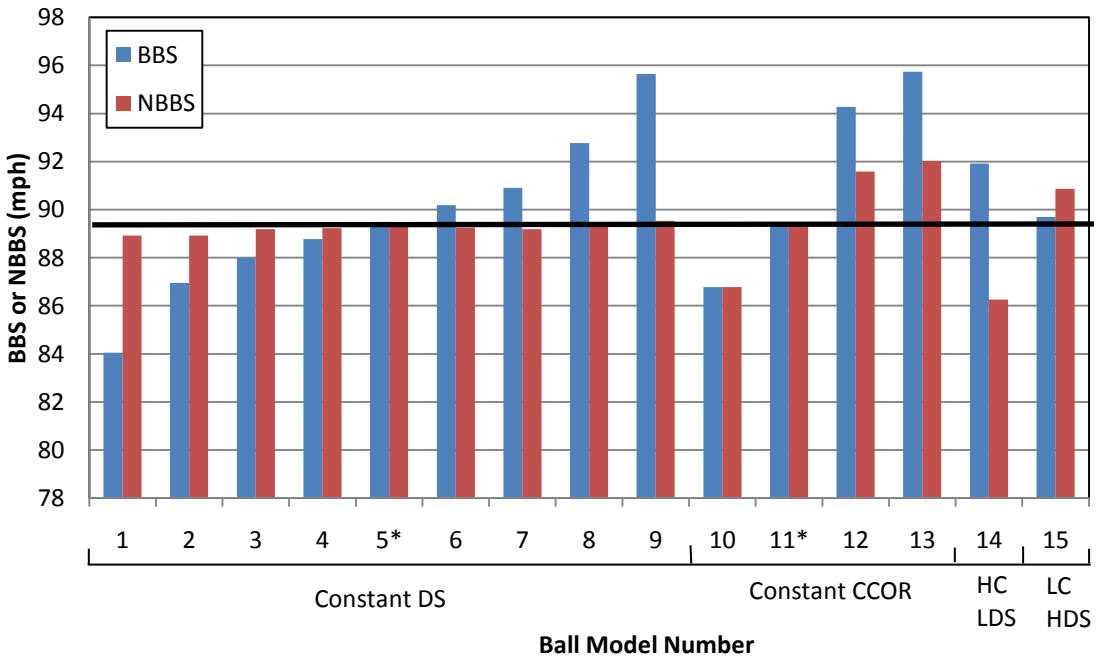

Figure 4.12: The FEA model BBS and NBBS for the low performing bat.

The range of BBS was 11.7 mph and after normalizing the range in NBBS was 5.8 mph a 51% improvement. There were some outliers that did not normalize, namely ball models 10, 14, and 15. For ball model 10 and 14 $e_T \approx e_{0T}$, so again $r_N \rightarrow \infty$ and $e_N \approx e_{0N}$. For ball model 15, equation 2.25 appeared to slightly over correct for its unusually low CCOR.

Normalizing appeared to have a different effect on CCOR than dynamic stiffness. Figure 4.13 shows the normalizing results on the low performance bat as a function of CCOR with the balls of constant stiffness. Figure 4.14 shows the normalizing results on the low performance bat as a function of dynamic stiffness with the balls of constant CCOR.

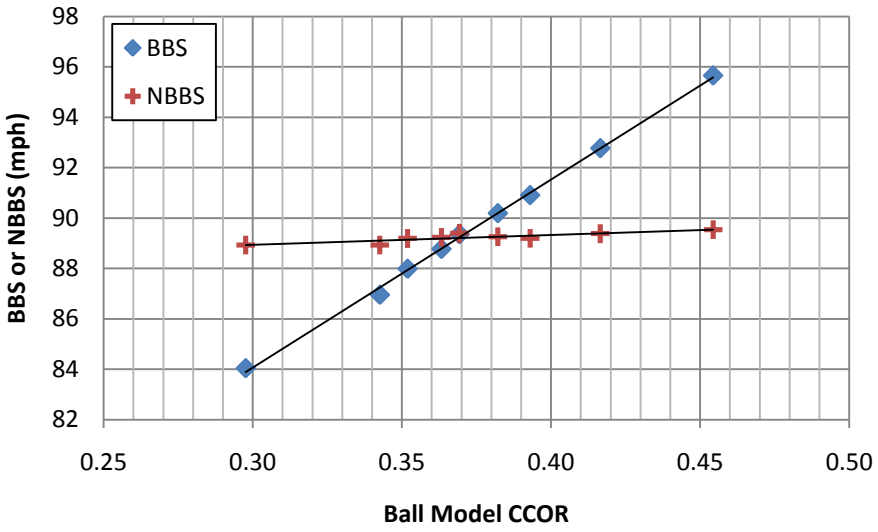

Figure 4.13: The FEA model BBS and NBBS with ball CCOR on the low performance bat with balls that have constant dynamic stiffness.

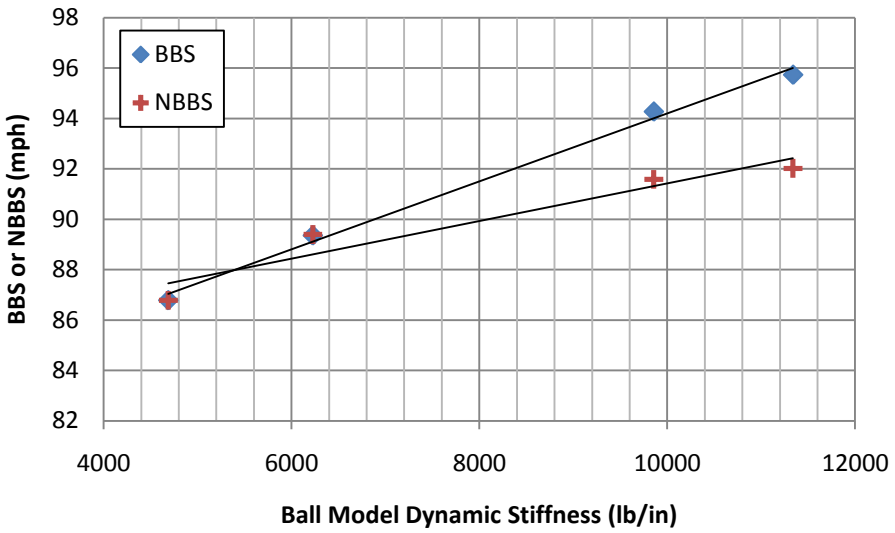

Figure 4.14: The FEA model BBS and NBBS with ball dynamic stiffness on the low performance bat with balls that have constant CCOR.

Figures 4.13 and 4.14 shows that the normalizing procedure worked well for CCOR but did not work as well for dynamic stiffness. The range in correction for balls of constant dynamic stiffness and varying CCOR went from 11.6 mph to 0.6 mph a 95% improvement. The outlier of figure 4.14 was the low dynamic stiffness ball (ball model #10), this was the ball that $e_T \approx e_{0T}$. Still normalizing for balls of constant CCOR and varying dynamic stiffness reduced the range from 9.0 mph to 5.8 mph a 35% improvement. For the low performing bat the BBS went up linearly for both increasing CCOR and increasing dynamic stiffness.

4.4.2. FEA Normalizing For A Medium Performance Bat

The normalizing method was performed on the medium performance bat and the results can be seen in table 4.5 and figure 4.15.

Table 4.5: The FEA performance results for the medium performing bat.

Ball Model Number	e_{0T}	k_T (lb/in)	e_T	r_N	e_N	BBS (mph)	NBBS (mph)
1	0.298	6721	0.436	8.6	0.476	**91.7**	**94.9**
2	0.343	6195	0.465	7.9	0.484	**94.0**	**95.6**
3	0.352	6397	0.478	7.5	0.488	**95.1**	**95.9**
4	0.363	6244	0.487	7.3	0.491	**95.8**	**96.1**
5*	0.369	6227	0.494	7.0	0.494	**96.3**	**96.4**
6	0.382	6333	0.502	7.2	0.493	**97.0**	**96.2**
7	0.393	6336	0.510	7.2	0.493	**97.6**	**96.3**
8	0.417	6297	0.530	6.8	0.498	**99.3**	**96.7**
9	0.454	6267	0.561	6.4	0.504	**101.8**	**97.2**
10	0.371	4689	0.450	9.3	0.469	**92.8**	**94.4**
11*	0.369	6227	0.494	7.0	0.494	**96.3**	**96.4**
12	0.373	9857	0.578	5.4	0.521	**103.2**	**98.6**
13	0.371	11339	0.604	5.1	0.528	**105.3**	**99.2**
14	0.439	4583	0.506	8.7	0.475	**97.4**	**94.9**
15	0.314	9752	0.533	6.1	0.509	**99.5**	**97.6**

*** Standard ball**

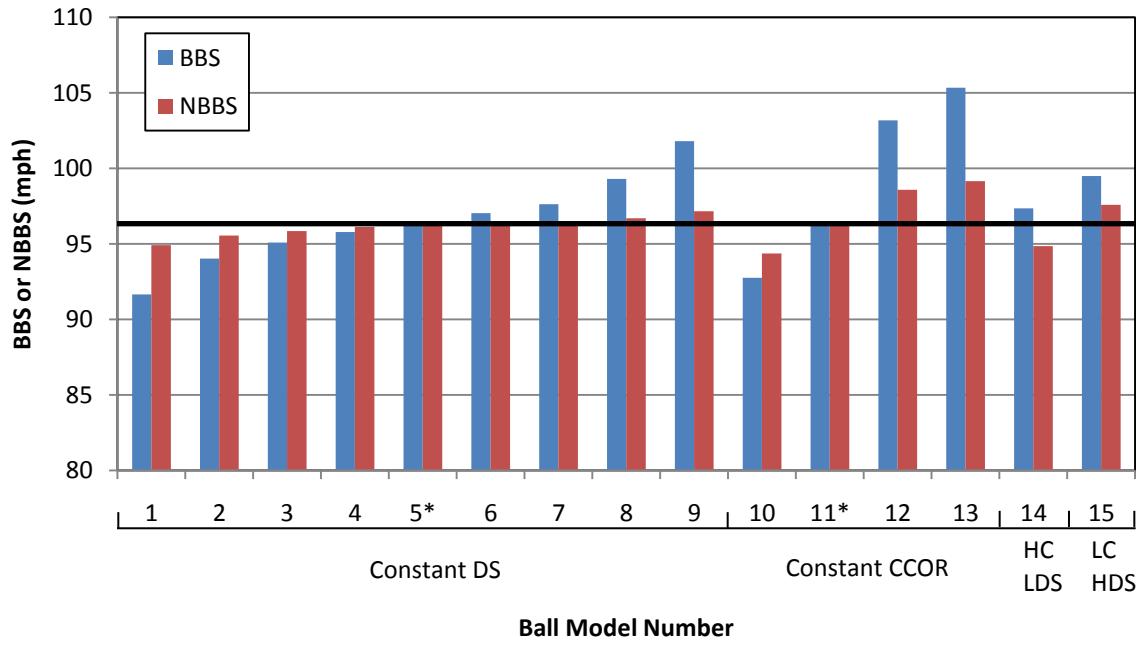

Figure 4.15: The FEA model BBS and NBBS for the medium performing bat.

The range of BBS was 13.7 mph and after normalizing the range was reduced to 4.8 mph a 65% improvement. All of the balls show improvement however, for some balls normalizing did not go far enough. This was most evident in the balls with constant CCOR, and ball models 14 and 15. Figure 4.16 shows the normalizing results on the medium performance bat as a function of CCOR with the balls of constant stiffness. Figure 4.17 shows the normalizing results on the medium performance bat as a function of dynamic stiffness with the balls of constant CCOR.

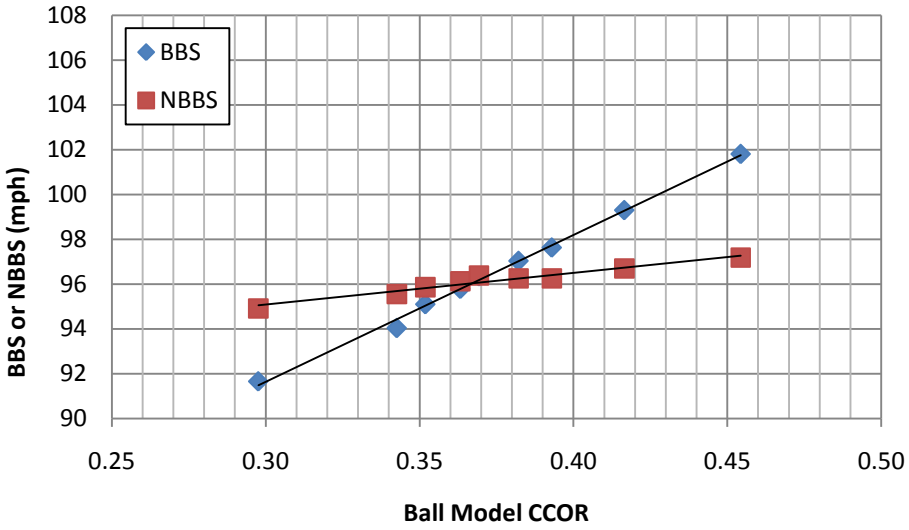

Figure 4.16: The FEA model BBS and NBBS with ball CCOR on the medium performance bat with balls that have constant dynamic stiffness.

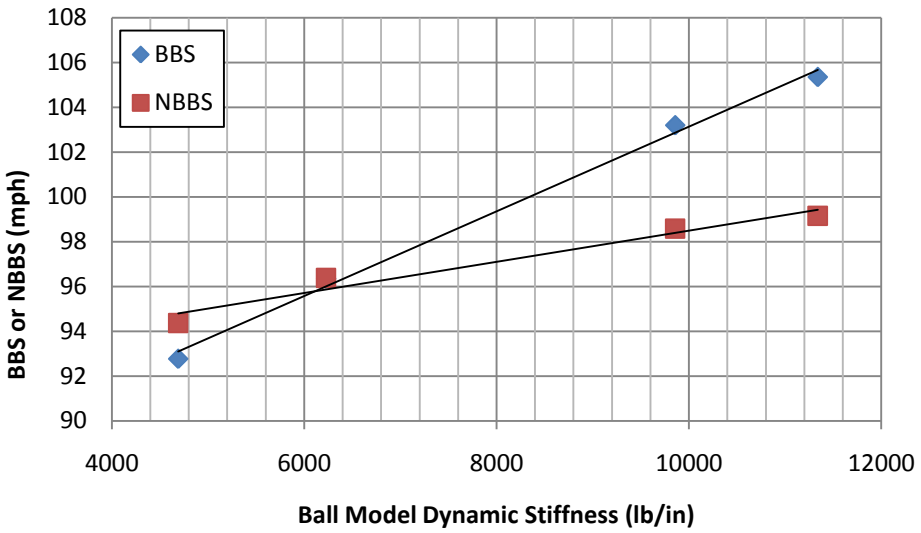

Figure 4.17: The FEA model BBS and NBBS with ball dynamic stiffness on the medium performance bat with balls that have constant CCOR.

Figures 4.16 and 4.17 show that the normalizing procedure improved the correction for both CCOR and dynamic stiffness, however it did not fully correct the BBS. For balls of constant dynamic stiffness and varying CCOR normalizing decreased the range from 10.2 mph to 2.3 mph a 78% improvement. For balls of constant dynamic stiffness and varying CCOR normalizing decreased the range from 12.6 mph to 4.8 mph a 62% improvement. It was also noteworthy that for a medium performing bat the BBS went up linearly with increasing CCOR and increasing dynamic stiffness.

4.4.3. FEA Normalizing For A High Performance Bat

The normalizing method was performed on the high performance bat and the results can be seen in table 4.6 and figure 4.18.

Table 4.6: The FEA performance results for the high performing bat.

Ball Model Number	e_{0T}	k_T (lb/in)	e_T	r_N	e_N	BBS (mph)	NBBS (mph)
1	0.298	6721	0.500	5.0	0.529	**96.9**	**99.2**
2	0.343	6195	0.523	4.7	0.538	**98.7**	**99.9**
3	0.352	6397	0.536	4.5	0.542	**99.8**	**100.2**
4	0.363	6244	0.543	4.4	0.546	**100.3**	**100.6**
5*	0.369	6227	0.549	4.2	0.549	**100.9**	**100.8**
6	0.382	6333	0.556	4.3	0.547	**101.4**	**100.6**
7	0.393	6336	0.562	4.3	0.546	**101.9**	**100.6**
8	0.417	6297	0.580	4.1	0.552	**103.4**	**101.1**
9	0.454	6267	0.607	3.9	0.558	**105.5**	**101.6**
10	0.371	4689	0.492	5.5	0.520	**96.2**	**98.5**
11*	0.369	6227	0.549	4.2	0.549	**100.9**	**100.8**
12	0.373	9857	0.637	3.5	0.572	**108.0**	**102.7**
13	0.371	11339	0.659	3.5	0.574	**109.8**	**102.9**
14	0.439	4583	0.541	5.2	0.525	**100.2**	**98.9**
15	0.314	9752	0.600	3.8	0.561	**104.9**	**101.8**

*** Standard ball**

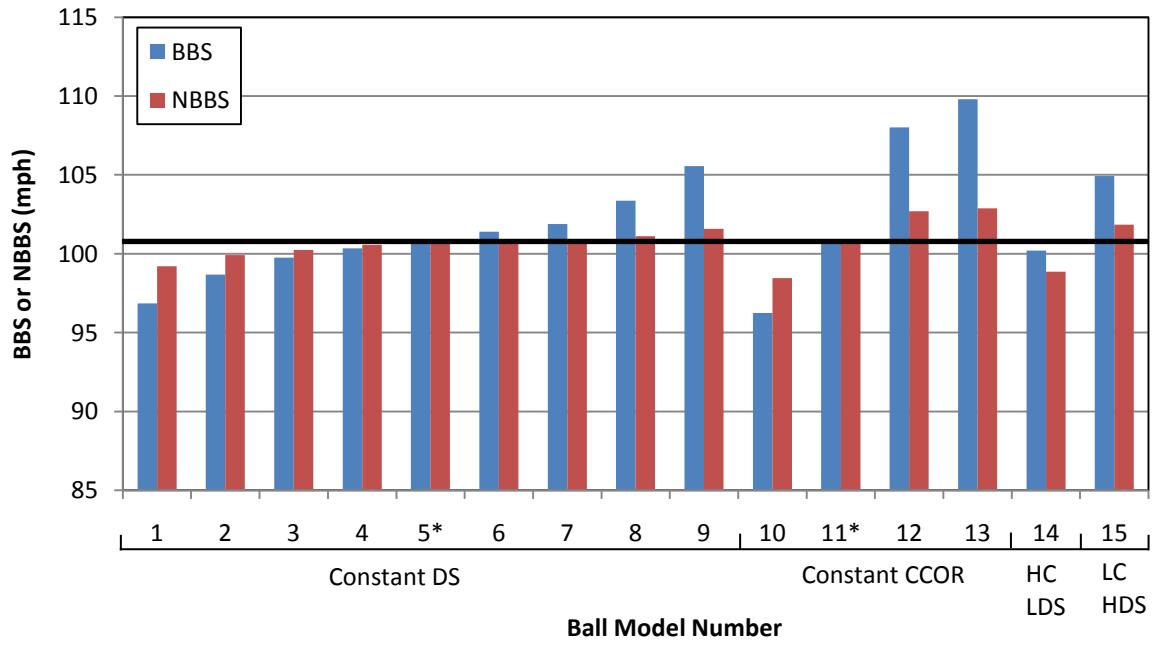

Figure 4.18: The FEA model BBS and NBBS for the high performing bat.

The range of BBS was 13.6 mph and after normalizing the range was reduced to 4.4 mph a 67% improvement. Again all of the balls show improvement in normalizing, but to varying degrees. Figure 4.19 shows the normalizing results on the high performance bat as a function of CCOR with the balls of constant stiffness. Figure 4.20 shows the normalizing results on the high performance bat as a function of dynamic stiffness with the balls of constant CCOR.

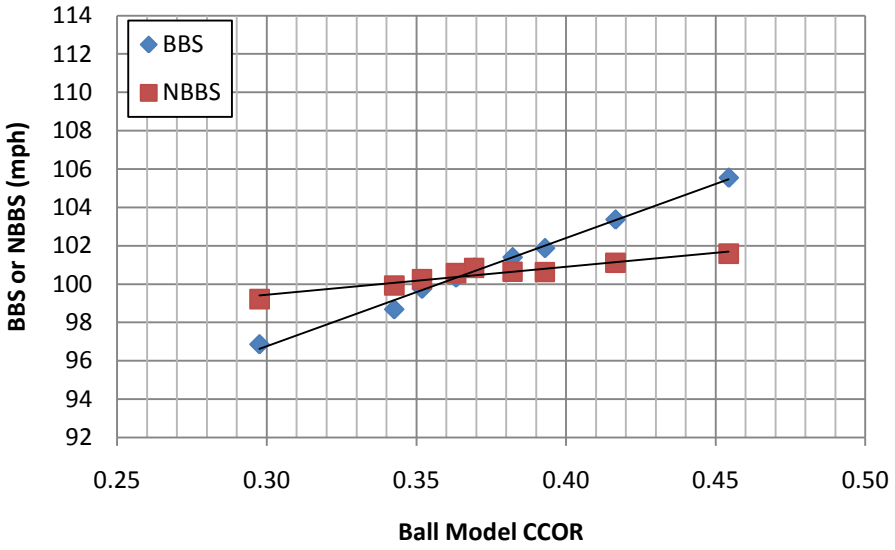

Figure 4.19: The FEA model BBS and NBBS with ball CCOR on the high performance bat with balls that have constant dynamic stiffness.

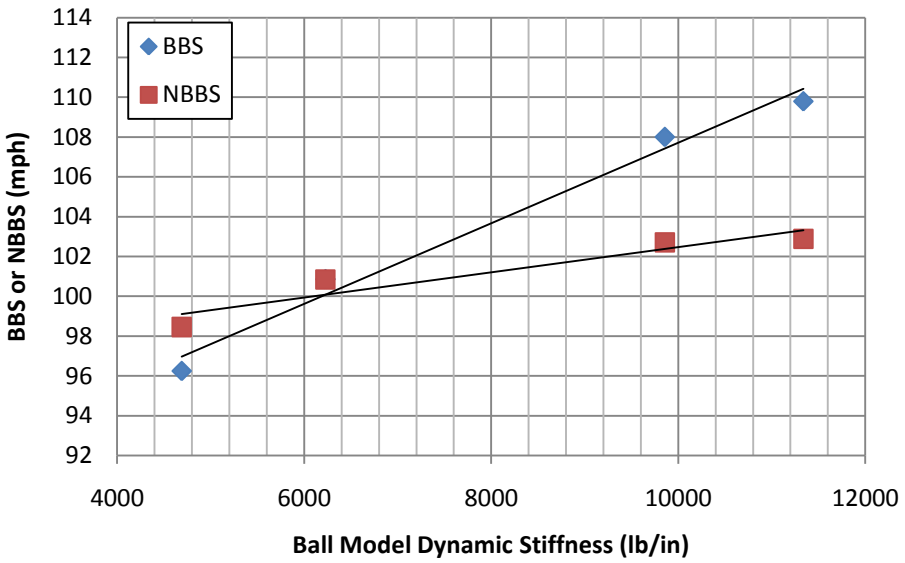

Figure 4.20: The FEA model BBS and NBBS with ball dynamic stiffness on the high performance bat with balls that have constant CCOR.

Figures 4.19 and 4.20 show that the normalizing procedure improved the correction for both CCOR and dynamic stiffness, however it did not fully correct the BBS. For balls of constant dynamic stiffness and varying CCOR normalizing decreased the range from 8.7 mph to 2.4 mph a 73% improvement. For balls of constant dynamic stiffness and varying CCOR normalizing decreased the range from 13.6 mph to 4.4 mph a 67% improvement. It was also noteworthy that for a high performing bat the BBS went up linearly with increasing CCOR and increasing dynamic stiffness.

Overall, for balls with a range of $0.352 < e_T < 0.417$ and 6227 lb/in $< k_T <$ 6397 lb/in resulted in a range of -0.6 mph < NBBS-BBS* < 0.7 mph for the low, medium and high performance bats.

4.4.4. Trends of Normalizing

Normalizing for ball CCOR and stiffness has a predictable pattern. By looking at the slopes of the BBS and NBBS it was possible to tell if normalizing degraded as bat performance changed. Figure 4.21 compares the BBS and NBBS slopes for balls of constant dynamic stiffness and varying CCOR (ball models 1-9). Figure 4.22 compared the BBS and BBBS slopes for balls of constant CCOR and varying dynamic stiffness (ball models 10-13).

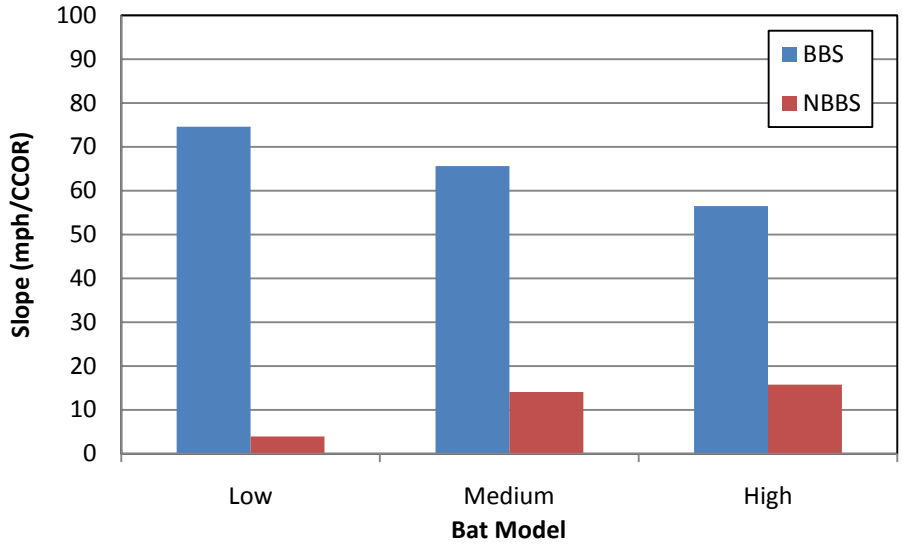

Figure 4.21: The slopes of BBS and NBBS for the bat models tested with balls of varying CCOR.

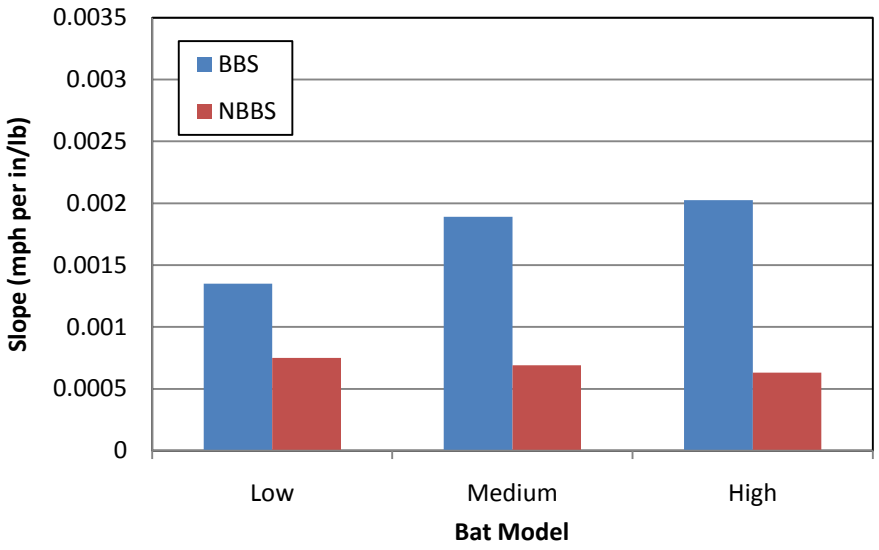

Figure 4.22: The slopes of BBS and NBBS for the bat models tested with balls of varying dynamic stiffness.

For balls of varying CCOR the effect of normalizing degraded as bat performance increased however, the medium and high performing bats had nearly the same slope (0.0019 and 0.002 mph per in/lb), suggesting a possible limit. The limit was caused by the increase of the trampoline effect in high performance bats. For balls of varying dynamic stiffness the effect of normalizing increases as bat performance increases if only slightly. Overall, normalizing for CCOR worked better than normalizing for dynamic stiffness.

4.5. Uncertainty in Ball Stiffness

Although the dynamic stiffness found with equations 3.3 and 3.7 were close compared to the other methods, there were slight differences. The different trends in dynamic stiffness with balls 1-9 found from equation 3.3 (k_x) and 3.7 (k_F) can be seen in figure 4.23

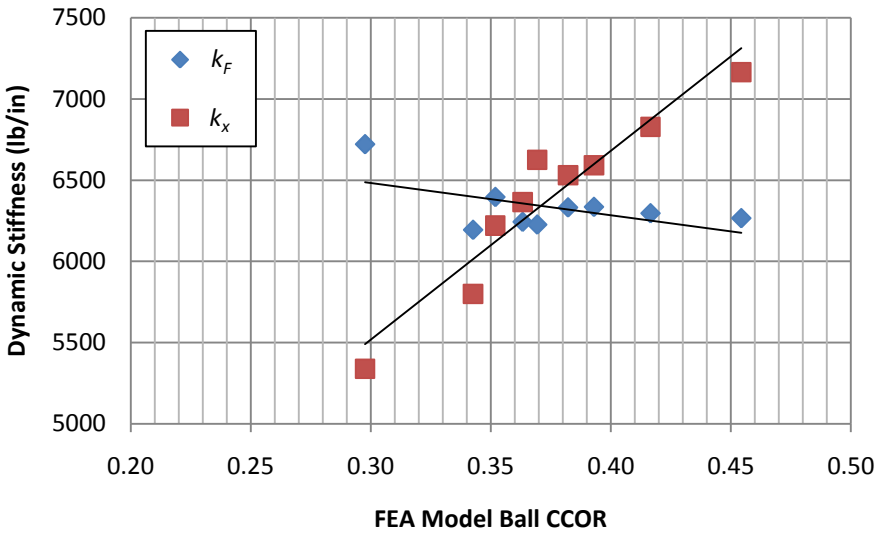

Figure 4.23: FEA model showing the difference in dynamic stiffness if found by the peak force method (k_F) and by the slope method (k_x).

In figure 4.23 the dynamic stiffness found with equation 3.3 (k_x) increased with ball CCOR while with equation 3.7 (k_F) the dynamic stiffness was relatively constant and actually decreased. This trend was not observed with balls of varying dynamic stiffness (balls 10-13).

Using k_x the bats were normalized again. Figures 4.24 – 4.26 compare BBS to NBBS with k_F and k_x for ball of varying CCOR with the low, medium and high performing bats.

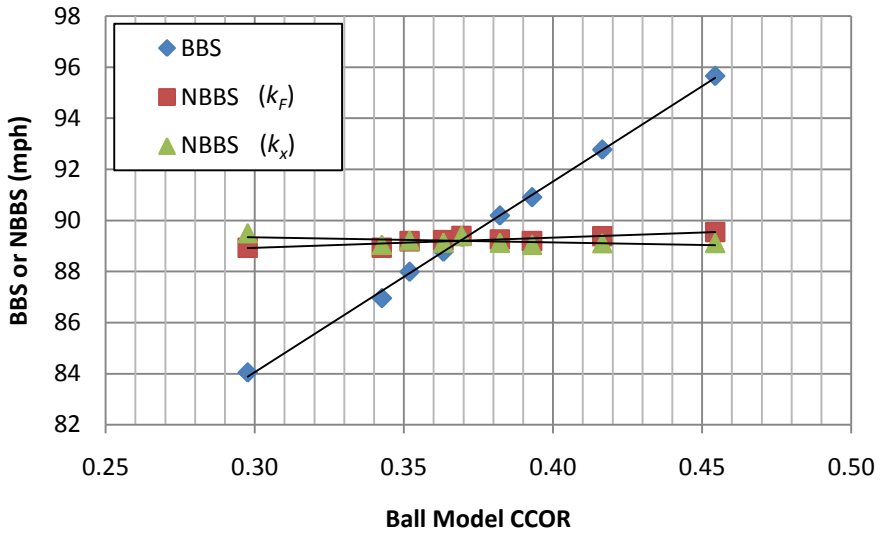

Figure 4.24: The FEA model BBS and NBBS with ball CCOR on the low performance bat with dynamic stiffness found from the peak force method and the slope method.

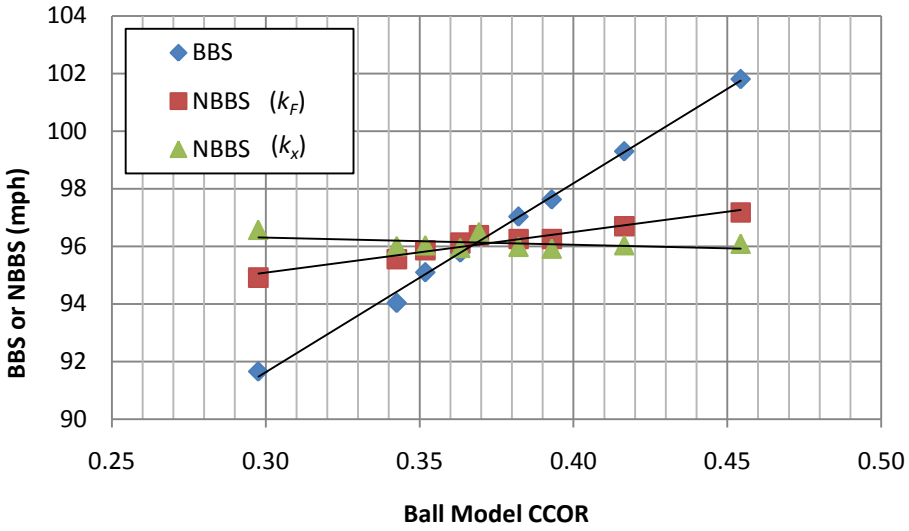

Figure 4.25: The FEA model BBS and NBBS with ball CCOR on the medium performance bat with dynamic stiffness found from the peak force method and the slope method.

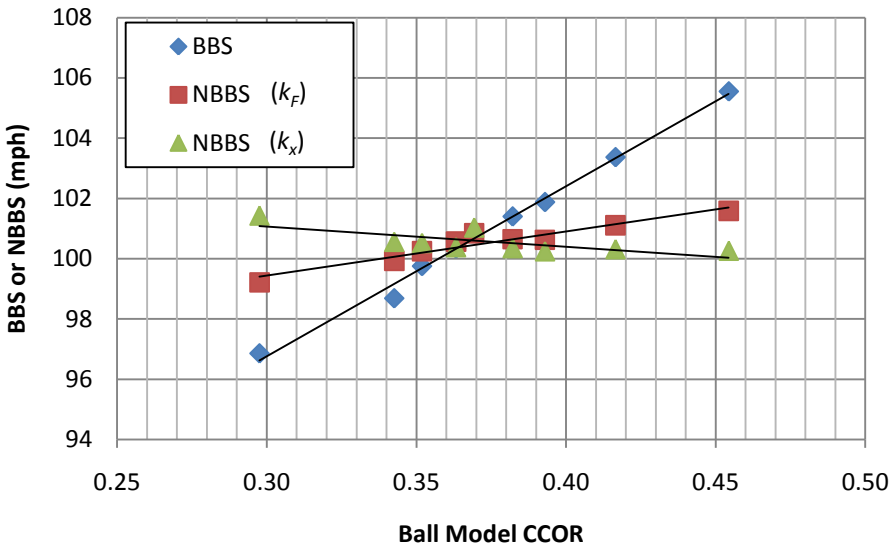

Figure 4.26: The FEA model BBS and NBBS with ball CCOR on the high performance bat with dynamic stiffness found from the peak force method and the slope method.

By normalizing with k_x, the normalized range for the balls with varying CCOR (1-9) decreased from 0.6 mph to 0.5 mph for the low performance bat, from 2.3 mph to 0.7 mph for the medium performance bat and 2.4 mph to 1.2 mph for the high performance bat. The low performance bat had the least correction, because dynamic stiffness has a small effect on low performing bats. The foregoing illustrates the challenges in characterizing the dynamic response of ball and it's implication on bat performance. The numeric results may overestimate the effect of differences between k_F and k_x since the difference between them was smaller in the experimental data (2%-8%) than the numerical model (-21%-14%).

4.6. Changes in Bat Stiffness

In section 2.3.2 it was assumed that the bat stiffness was independent of the ball. Bat effective stiffness can be found from the numerical results by tracking the force and the displacement of the bat at the impact location and dividing the force by the displacement.

The force-displacement curves for the medium performance bat when impacted with the low stiffness ball (model 10) and high stiffness ball (model 13) can be seen in figure 4.27, showing evidence of geometric non-linearity.

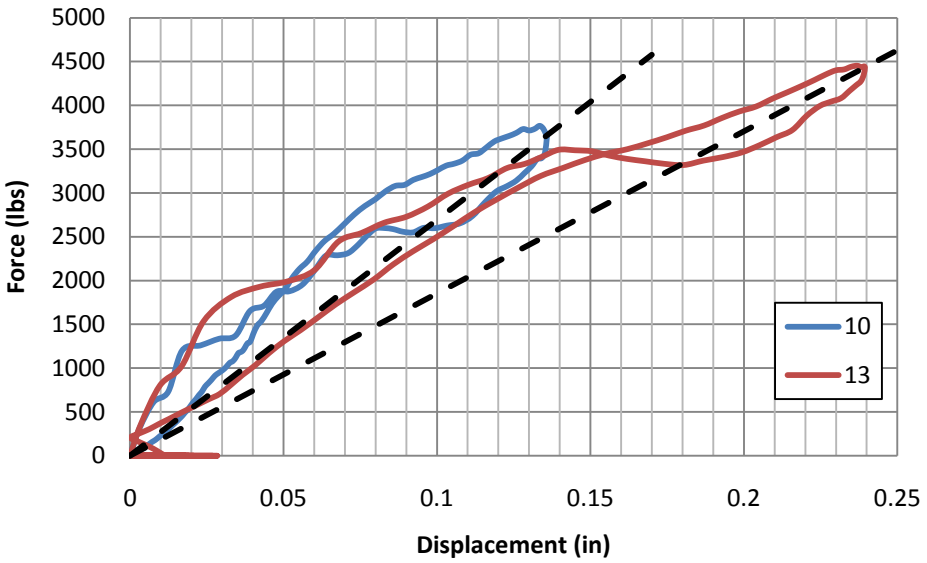

Figure 4.27: Force-displacement curve of the bat for the low stiffness ball (10) and the high stiffness ball (13).

The force-displacement curve of the bat showed how the barrel stiffness changed when impacted with a low or high stiffness ball. The bat was modeled with elastic properties so any non-linear response in the force-displacement curve was from geometric effects. The hysteresis in figure 4.27 was likely due to numerical accuracy. However, the slopes were different and gave different bat stiffnesses (the lines on figure 4.27 illustrate the different bat stiffnesses). Bat stiffness was found from the maximum force and dividing by the corresponding displacement.

Figure 4.28 shows that the bat stiffness decreased linearly with increased ball stiffness on all three bats. For the balls with constant dynamic stiffness and varying CCOR the bat stiffness was nearly constant as seen in figure 4.29.

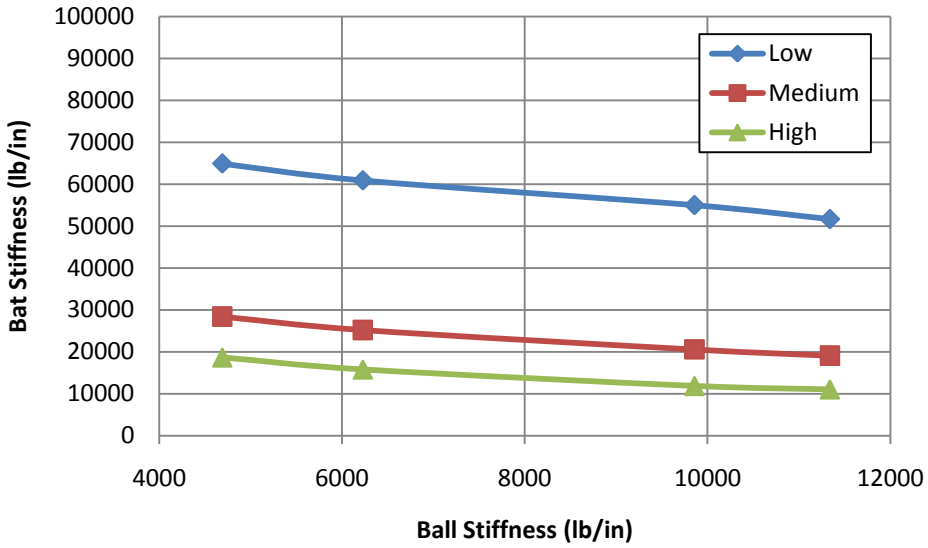

Figure 4.28: Bat stiffness on balls with changing dynamic stiffness and constant CCOR.

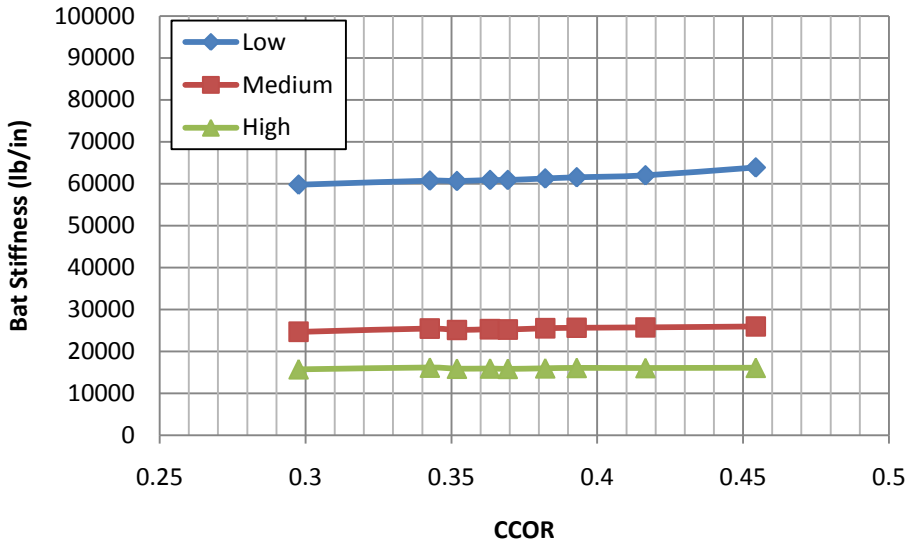

Figure 4.29: Bat stiffness with balls of constant dynamic stiffness and varying CCOR.

Previous studies following ASTM F 2884 showed typical experimental barrel stiffness range from 6000 lb/in to 10000 lb/in [4.3]. The results presented in figures 4.28 and 4.29 showed larger barrel stiffness and a much larger range. The differences were not surprising since F2884 was a quasi-static test involving steel cylindrical plates. A ball will give a more uniform pressure distribution, resulting in higher stiffness.

Figures 4.30 and 4.31 compare the cross-section of a bat-ball impact at maximum displacement for stiff and compliant ball, respectively. A possible explanation of the dependence of bat stiffness on the ball concerns the bat's deformed shape. The stiffer ball was observed to retain its shape better, causing a flatter deformed bat shape in comparison to the softer ball (figure 4.31). The softer ball had more of a uniform pressure distribution, than the stiffer ball, resulting in a larger effective contact area and stiffer bat response.

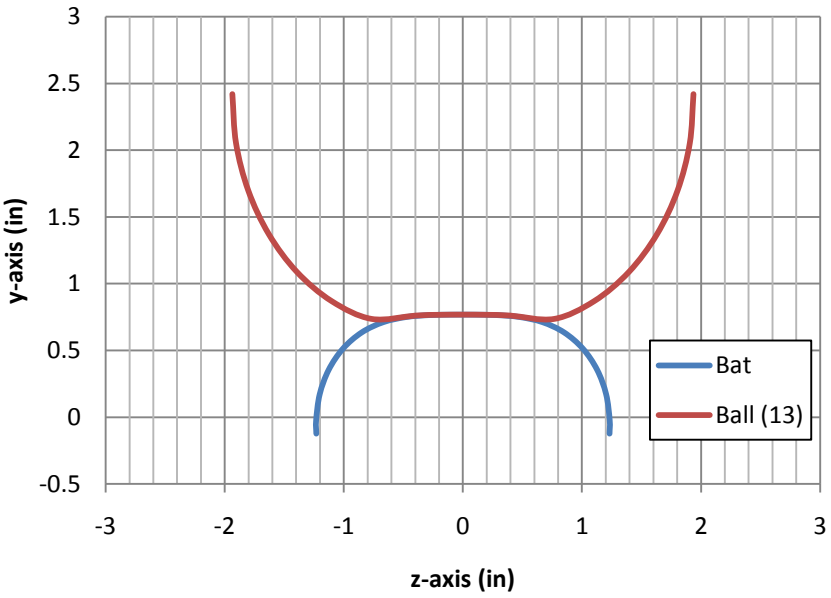

Figure 4.30: Profile of the FEA model medium performance bat with the high stiffness ball.

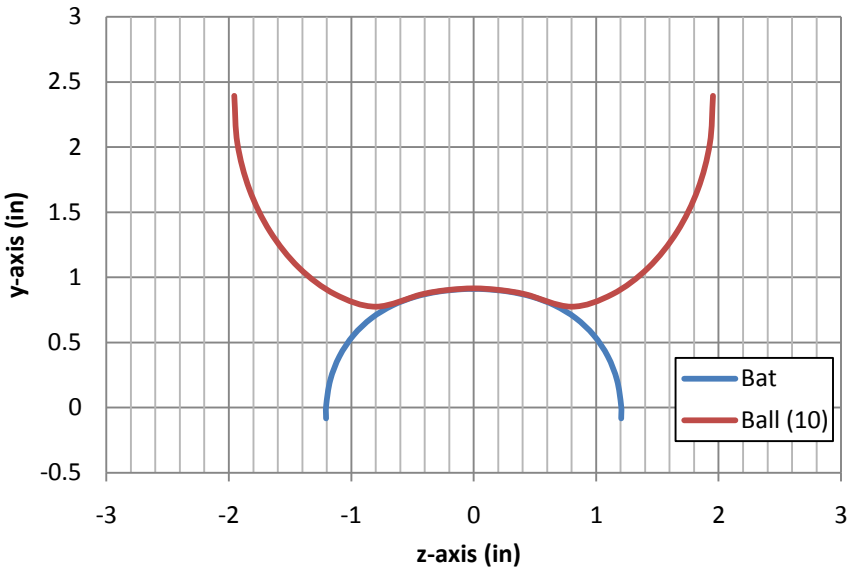

Figure 4.31: Profile of the FEA model medium performance bat with the low stiffness ball.

The contact pressure was found the along the radial axis at the initial contact point. A representation of the contact pressure from the bat-ball impact (ball model 10) can be seen in figure 4.32.

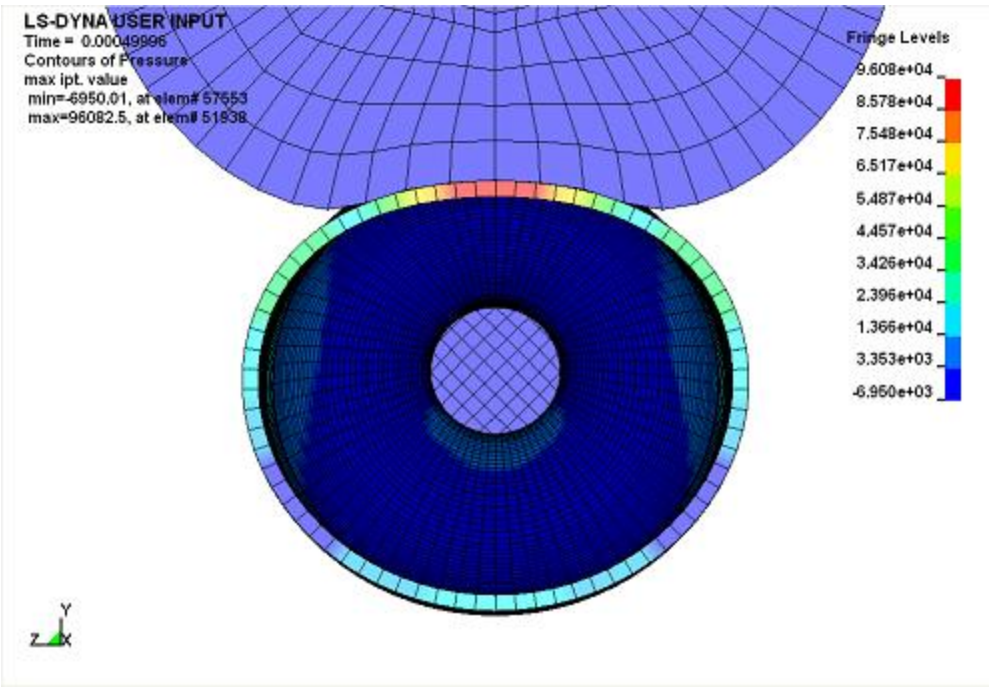

Figure 4.32: A representation of the contact pressure from a bat-ball impact.

The contact pressure profile of the two ball models (10 and 13) on the medium performing bat can be seen in figure 4.33.

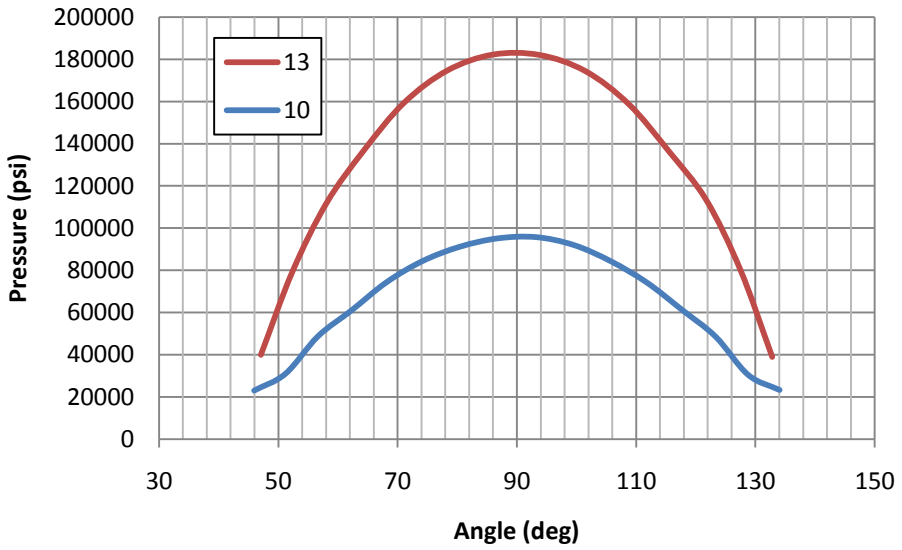

Figure 4.33: Contact pressure profile for the low and high stiffness balls (10 and 13 respectively).

Figure 4.33 shows the pressure of where the ball was in contact with the bat. The variability in contact pressure contributes to the non-linear response of the ball and the increase in bat stiffness.

If bat stiffness was independent of CCOR than it will be predictable given a ball stiffness. It was observed that bat stiffness changed the same amount as the ball stiffness. Figure 4.34 shows that the quantity ($k_0 + k_1$) did not change for each bat and was independent of e_0.

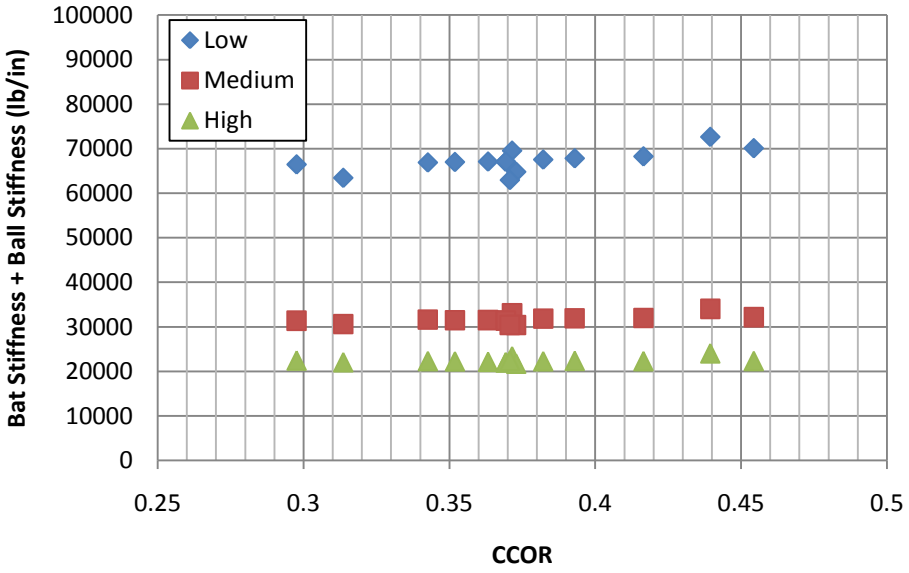

Figure 4.34: The correlation of bat stiffness and ball stiffness.

Figure 4.34 also shows that stiffer bats were harder to predict, for example, this relationship would not be consistent for a wood bat that has constant barrel stiffness.

4.6.1. Normalizing For Bat Stiffness

It was possible that the apparent shortcomings of normalizing were not due to the simplified model, but to changing bat stiffness. A solution would be to normalize for changing

bat stiffness. The effective bat stiffness was found from the force-displacement curve as described in section 4.6. A nominal bat stiffness for each bat was found from an impact with a standard ball (test ball #11). The effective bat stiffness for balls of varying dynamic stiffness were reported in table 4.7.

Table 4.7: Effective bat stiffness for balls with varying dynamic stiffness.

			Bat Perfromance		
			Low	Medium	High
Ball Model	DS (lb/in)	Ball CCOR (e_{0T})	Bat Stiffness (lb/in)	Bat Stiffness (lb/in)	Bat Stiffness (lb/in)
10	4689	0.371	64882	28398	18695
11*	6227	0.369	60870	25209	15820
12	9857	0.373	54962	20564	11887
13	11339	0.371	51627	19083	11071

The bat stiffness was normalized by using the Faber correction coefficient, F_c, defined as the ratio of the nominal bat stiffness, k_{Nbat} (from ball #11), and the actual bat stiffness, k_{Tbat}, so that,

$$\boldsymbol{F_c = \frac{k_{Nbat}}{k_{Tbat}}} \tag{4.1}$$

In the context of normalizing through the two-spring model and with some algebraic manipulation we arrived at the normalized stiffness ratio r_N,

$$\boldsymbol{r_{Fc} = \frac{k_T}{k_N}\frac{k_{Nbat}}{k_{Tbat}}\frac{1-e_T{}^2}{e_T{}^2-e_{0T}{}^2}} \tag{4.2}$$

The normalizing data for the low performance, medium performance, and high performance bats can be seen in figure 4.35, figure 4.36, and figure 4.37 respectfully.

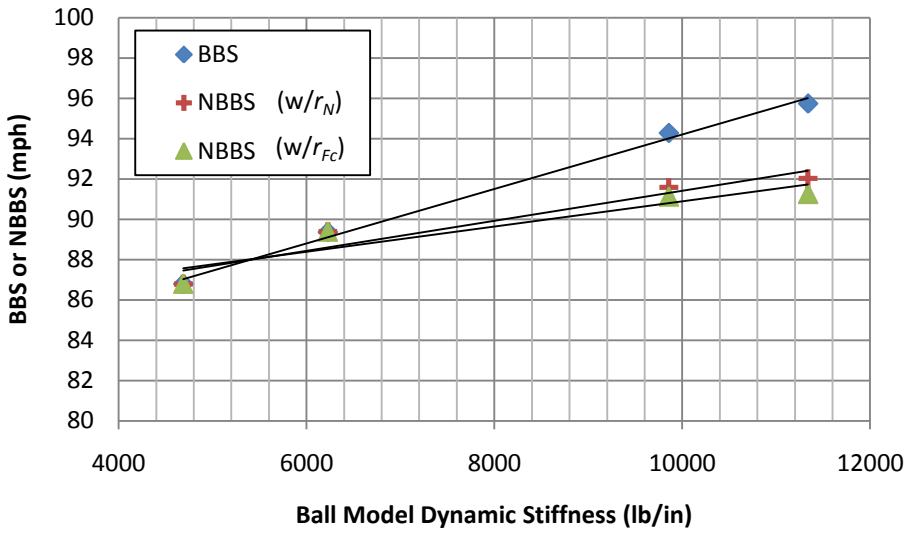

Figure 4.35: The FEA model BBS and NBBS with and without bat stiffness for ball dynamic stiffness on the low performance bat with balls that have constant CCOR.

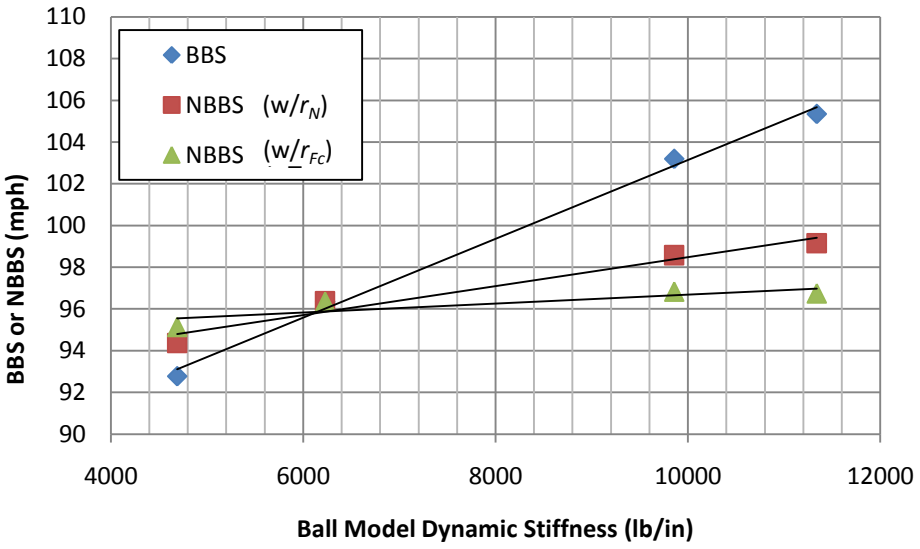

Figure 4.36: The FEA model BBS and NBBS with and without bat stiffness for ball dynamic stiffness on the medium performance bat with balls that have constant CCOR.

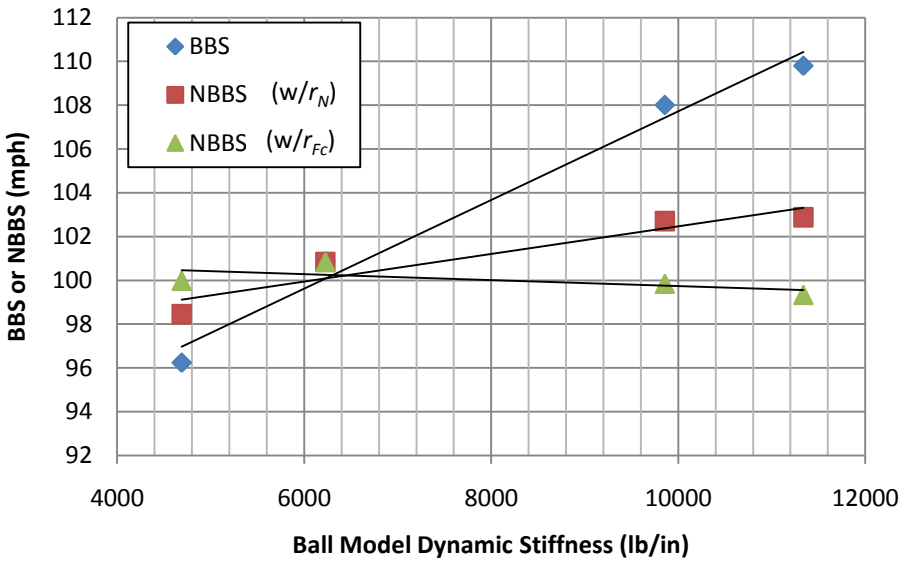

Figure 4.37: The FEA model BBS and NBBS with and without bat stiffness for ball dynamic stiffness on the high performance bat with balls that have constant CCOR.

By normalizing for bat stiffness the range in NBBS was substantially reduced. Normalizing with bat stiffness appears to work better as bat performance increases. Comparing normalizing with r_N to r_{Fc}, the normalized range for the balls with varying dynamic stiffness (test # 10-13) decreased from 5.3 mph to 4.4 mph for the low performance bat, from 4.8 mph to 1.7 mph for the medium performance bat and 4.4 mph to 1.5 mph for the high performance bat. Normalizing for changing bat stiffness improved the range in NBBS. From a practical point of view implementing normalizing for changing bat stiffness in BBS measurements was unrealistic because currently accurate bat stiffness cannot be found experimentally.

4.7. Bat Coefficient of Restitution

In the development of equation 2.24 it was assumed that at impacts near the sweet spot the bat experiences no energy loss or that the bat coefficient of restitution is one ($e_1 = 1$). This

assumption was made in part because e_1 cannot be found experimentally. The FEA model found e_1 using the bat stiffness calculated from performance test. Starting with the fundamental equation for the energy dissipated in the collision (equation 2.16).

$$\mathbf{1} - \boldsymbol{e^2} = (\mathbf{1} - \boldsymbol{e_0}^2)\boldsymbol{f_0} + (\mathbf{1} - \boldsymbol{e_1}^2)\boldsymbol{f_1} \tag{4.3}$$

Solving for e_1 in terms of the bat and ball stiffnesses equation 4.3 becomes,

$$\boldsymbol{e_1} = \sqrt{\frac{\boldsymbol{k_1}}{\boldsymbol{k_0}}(\boldsymbol{e^2} - \boldsymbol{e_0}^2) + \boldsymbol{e^2}} \tag{4.4}$$

Bat stiffness was found as described in section 4.6. Table 4.8 shows e_1 for each bat-ball combination, where it ranged from 0.434 to 0.885. Figures 4.38 and 4.39 show e_1 for each bat-ball combination for constant CCOR ball models (10-13) and constant dynamic stiffness ball models (1-9) respectfully.

Table 4.8: FEA results for the bat coefficient of restitution (e_1) on the bats of different performances.

			Low Performance Bat		Medium Performance Bat		High Performance Bat	
Ball Model	DS (lb/in)	Ball CCOR (e_0)	Bat Stiffness (lb/in)	BCOR (e_1)	Bat Stiffness (lb/in)	BCOR (e_1)	Bat Stiffness (lb/in)	BCOR (e_1)
1	6721	0.298	59753	0.609	24660	0.750	15723	0.792
2	6195	0.343	60719	0.628	25436	0.790	16117	0.823
3	6397	0.352	60624	0.653	25103	0.801	15858	0.831
4	6244	0.363	60872	0.662	25282	0.814	15907	0.842
5*	6227	0.369	60870	0.677	25209	0.824	15820	0.850
6	6333	0.382	61234	0.672	25500	0.824	15947	0.848
7	6336	0.393	61518	0.672	25603	0.827	16039	0.851
8	6297	0.417	61987	0.696	25697	0.848	16009	0.867
9	6267	0.454	63861	0.728	25904	0.873	16068	0.885
10	4689	0.371	64882	0.434	28398	0.769	18695	0.812
11*	6227	0.369	60870	0.677	25209	0.824	15820	0.850
12	9857	0.373	54962	0.816	20564	0.861	11887	0.853
13	11339	0.371	51627	0.829	19083	0.865	11071	0.851
14	4583	0.439	68089	0.436	29444	0.813	19465	0.847
15	9752	0.314	53703	0.750	20883	0.825	12312	0.830

*** Standard ball**

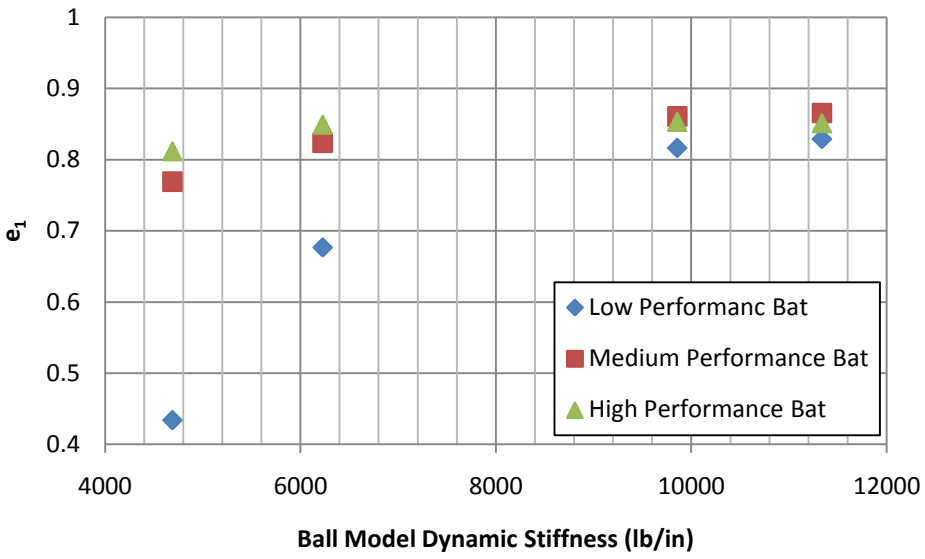

Figure 4.38: The FEA model bat coefficient of restitution (e_1) of three bats with differing dynamic stiffness.

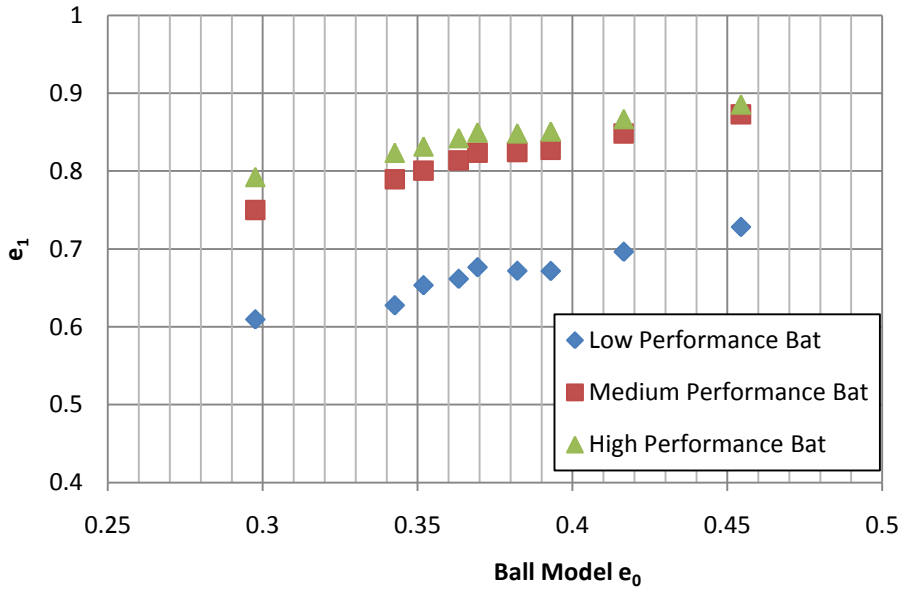

Figure 4.39: The FEA model bat coefficient of restitution (e_1) of three bats with differing CCOR (e_0).

The low performing bat had the lowest e_1 of all the bats and progressed higher with increasing bat performance. The highest e_1 was 0.885 on the high performing bat. The assumption that e_1 =

1 appears partially responsible for the poor normalized performance, particularly for the low performing bat.

4.7.1. Normalizing With Bat Coefficient of Restitution

Recognizing that $e_1 \neq 1$ equation 2.23 becomes,

$$r_S = \frac{k_T}{k_N}\frac{{e_1}^2-{e_T}^2}{{e_T}^2-{e_{0T}}^2} \tag{4.5}$$

The low, medium and high performance bats were normalized using equation 4.5. The normalizing results for the low performance bat can be seen in figure 4.40. Figures 4.41 and 4.42 compare the results for the balls of constant dynamic stiffness and constant CCOR respectively.

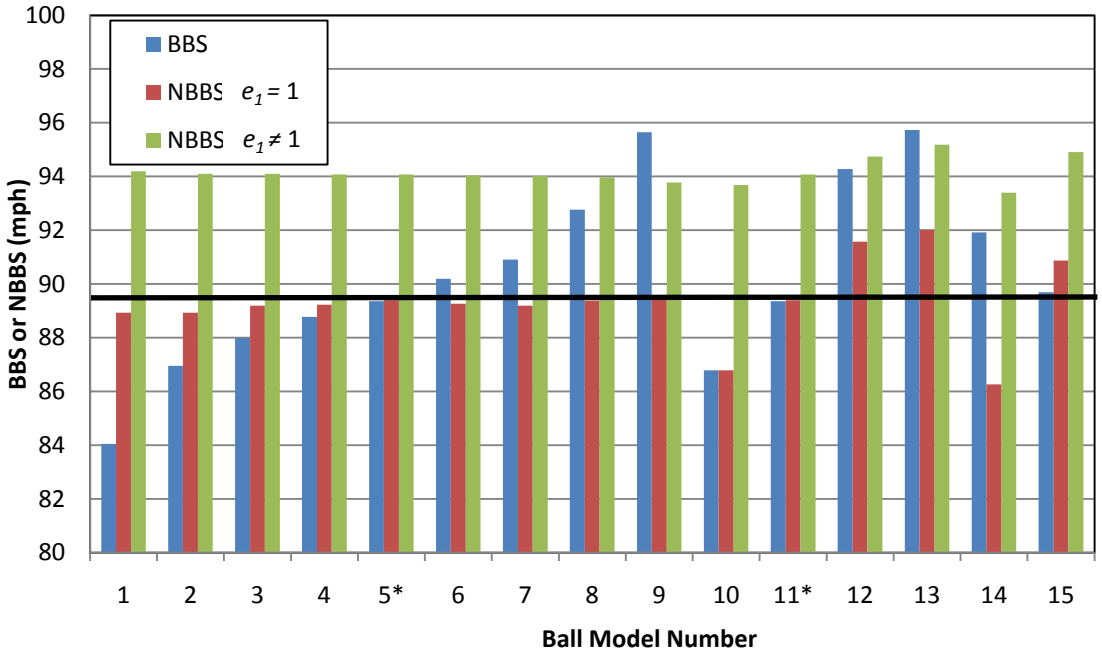

Figure 4.40: The results for the low performance bat with normalizing for e_1.

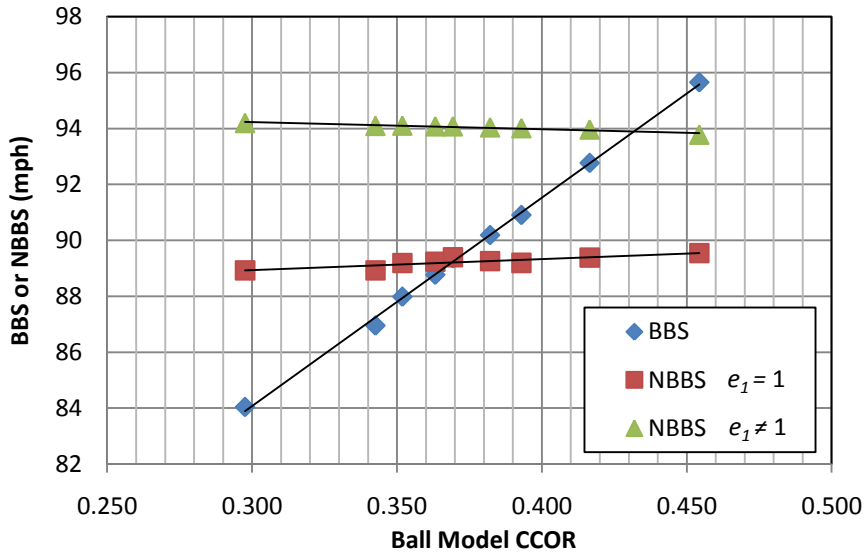

Figure 4.41: The results for the low performance bat with normalizing for e_1 with balls of constant dynamic stiffness.

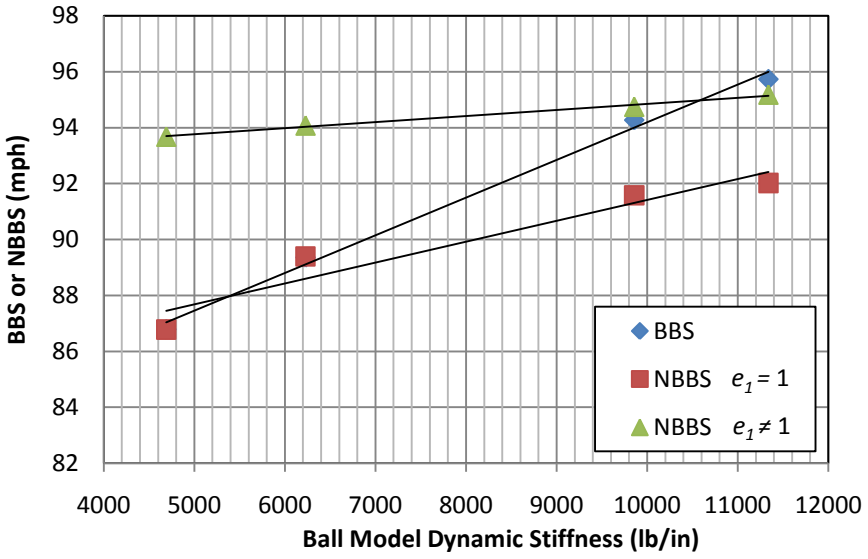

Figure 4.42: The results for the low performance bat with normalizing for e_1 with balls of constant CCOR.

Using e_1 in the normalizing equations the performance with the standard ball increased by 4.7 mph. This was because now we normalized to a bat with $e_1 = 1$. The range in normalizing improved from 11.7 mph to 1.8 mph compared to just 5.8 mph when normalized with $e_1 = 1$.

There was a small improvement when normalizing for CCOR and a large improvement normalizing for dynamic stiffness.

The normalizing results for the medium performance bat can be seen in figure 4.43. Figures 4.44 and 4.45 compare the results for the balls of constant dynamic stiffness and constant CCOR respectively.

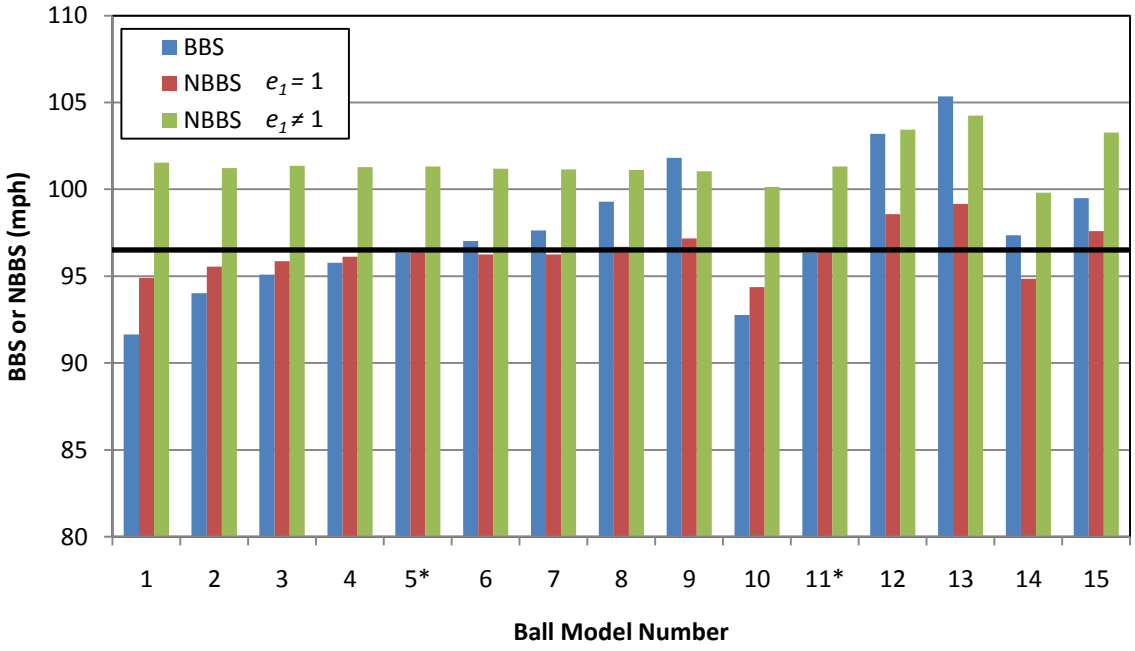

Figure 4.43: The results for the medium performance bat with normalizing with and without e_1.

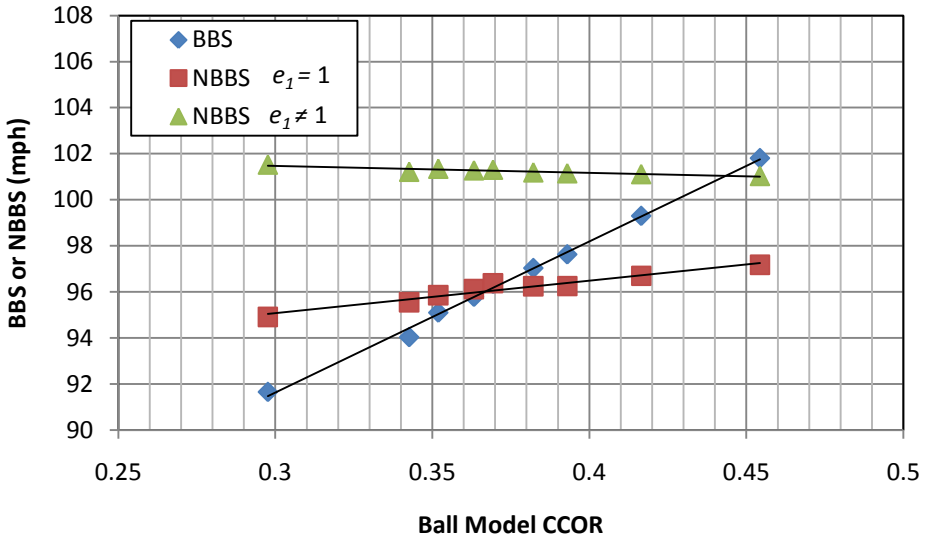

Figure 4.44: The results for the medium performance bat with normalizing using e_1 with balls of constant dynamic stiffness.

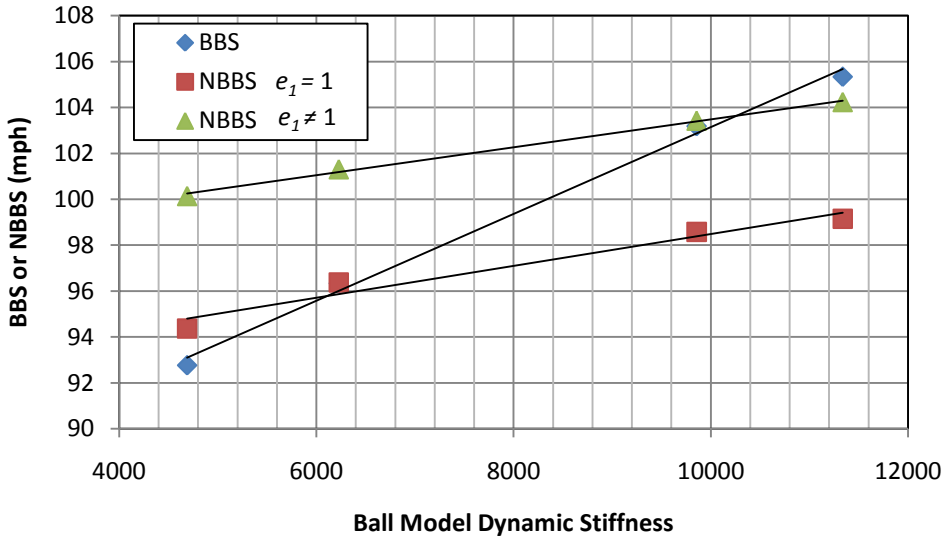

Figure 4.45: The results for the medium performance bat with normalizing using e_1 with balls of constant CCOR.

Using e_1 in the normalizing equations the performance with for the standard ball increased by 5.0 mph, the range in normalizing improved from 13.7 mph to 4.4 mph compared to 4.8 mph when

normalized with $e_1 = 1$. The procedure showed improvement when normalized for CCOR but no improvement when normalized for dynamic stiffness when using e_1.

The normalizing results for the high performance bat can be seen in figure 4.46. Figures 4.47 and 4.48 compare the results for the balls of constant dynamic stiffness and constant CCOR respectively.

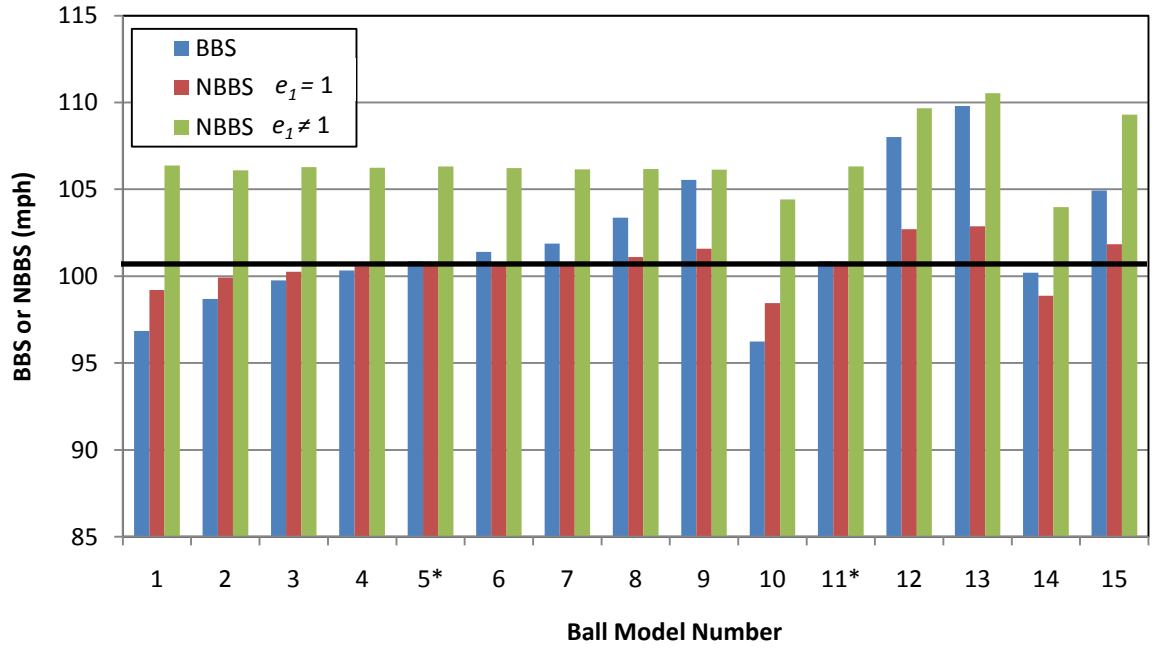

Figure 4.46: The results for the high performance bat when normalizing for e_1.

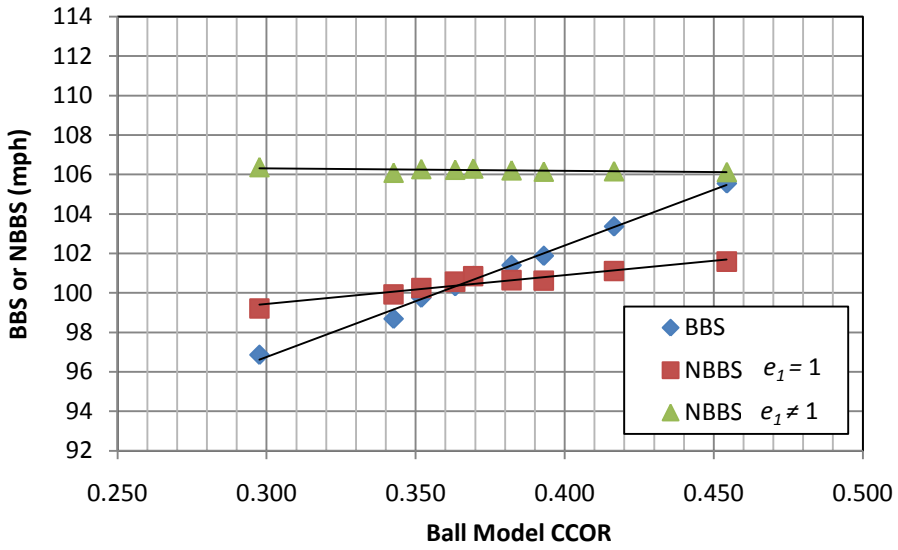

Figure 4.47: The results for the high performance bat with normalizing using e_1 with balls of constant dynamic stiffness.

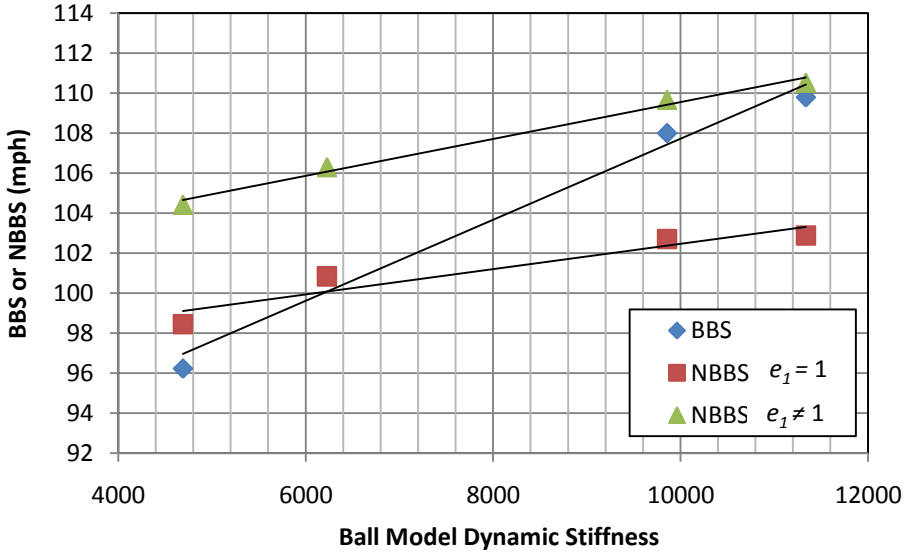

Figure 4.48: The results for the high performance bat with normalizing using e_1 with balls of constant CCOR.

Using e_1 in the normalizing equations the performance with the standard ball increased by 5.5 mph, the range in normalizing decreased from 11.7 mph to 6.6 mph, however when normalized

with e_1 = 1 the range was 4.4 mph. Again, normalizing improved for CCOR but not for dynamic stiffness.

Normalizing with bat COR increased the overall performance on all the bats and did not reduce the range in normalized performance on the medium and high bats. Most impacts had e_1 ≈ 0.80 so normalizing for this effect did not change the range much. Normalizing for the bat stiffness on the other hand did significantly reduce the range in normalized performance. It was desired to normalize for bat stiffness and bat COR at the same time, however due to calculating e_1 using k_1 the effect of normalizing for both eliminated bat performance altogether.

4.7.2. Alternative Bat Coefficient of Restitution

The bat COR can be found without bat stiffness, by finding the kinetic energy of the bat after collision. The bat COR was found by,

$$e_1 = \sqrt{1 - \frac{KE_{bat}}{KE_{in}}} \tag{4.6}$$

where, KE_{bat} was the kinetic energy of the bat after collision and KE_{in} was the total initial kinetic energy. KE_{bat} was found by calculating the kinetic energy of the ball after collision and subtracting that from the total kinetic energy after collision. Table 4.9 shows e_1 for each bat-ball combination, where it ranged from 0.636 to 0.799. Figures 4.49 and 4.50 show e_1 for each bat-ball combination for constant CCOR ball models (10-13) and constant dynamic stiffness ball models (1-9) respectfully.

Table 4.9: FEA results for the bat coefficient of restitution (e_1) on the bats of different performances using kinetic energy.

			Low Performance Bat	Medium Performance Bat	High Performance Bat
Ball Model	DS (lb/in)	Ball CCOR (e_0)	BCOR (e_1)	BCOR (e_1)	BCOR (e_1)
1	6721	0.298	0.799	0.755	0.722
2	6195	0.343	0.788	0.746	0.715
3	6397	0.352	0.784	0.741	0.709
4	6244	0.363	0.781	0.737	0.706
5*	6227	0.369	0.778	0.735	0.704
6	6333	0.382	0.775	0.733	0.702
7	6336	0.393	0.772	0.730	0.700
8	6297	0.417	0.764	0.722	0.692
9	6267	0.454	0.751	0.710	0.681
10	4689	0.371	0.791	0.758	0.734
11*	6227	0.369	0.778	0.735	0.704
12	9857	0.373	0.750	0.690	0.652
13	11339	0.371	0.740	0.674	0.636
14	4583	0.439	0.770	0.739	0.717
15	9752	0.314	0.769	0.709	0.669

*** Standard Ball**

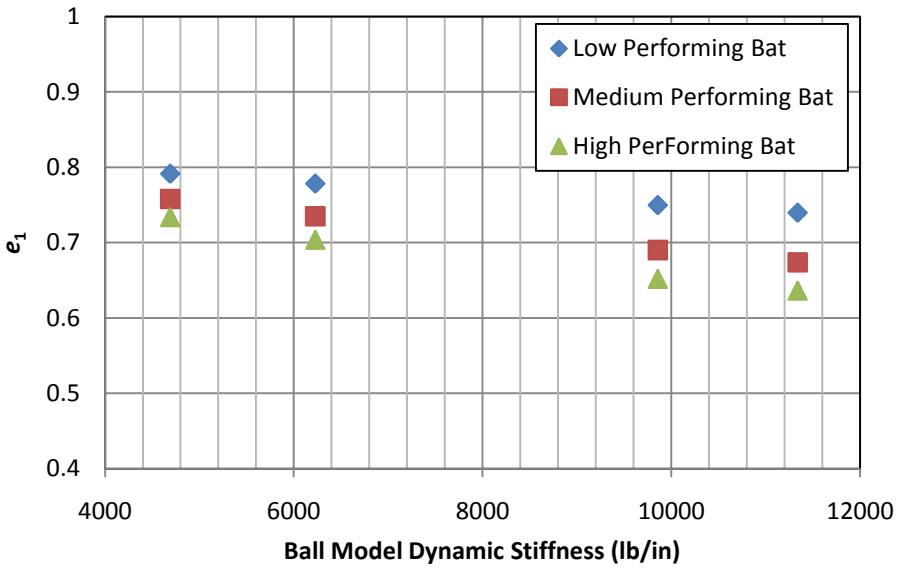

Figure 4.49: The FEA model bat coefficient of restitution (e_1) found from kinetic energy of three bats with differing dynamic stiffness.

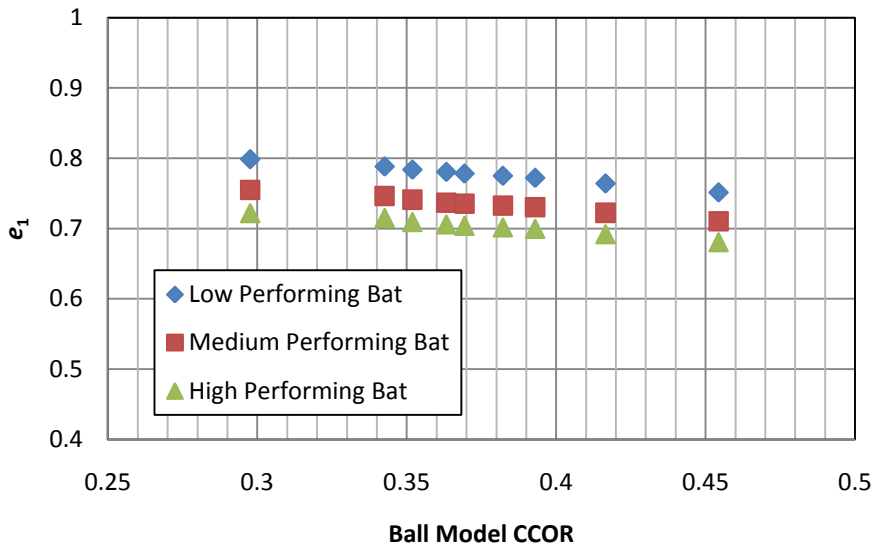

Figure 4.50: The FEA model bat coefficient of restitution (e_1) found from kinetic energy of three bats with differing CCOR.

Tracking kinetic energy in the model to find e_1 resulted in opposite trends from the technique detailed in section 4.7. The low performing bat had a larger e_1 decreased as bat performance increased and decreased lineally as dynamic stiffness and CCOR increased. The range in e_1 was 0.636 to 0.799, smaller than before. Using e_1 found with kinetic energy did not improve the range in normalizing and in fact made it substantially worse; therefore it was not included in this work.

4.8. Normalizing With An Elastic Ball

The competing effect of ball CCOR and stiffness may be separated by considering elastic balls. To verify if this was a valid assumption an elastic ball was modeled in LS-DYNA with dynamic stiffness in the same range as in the previous sections and tested on a medium performing bat.

4.8.1. Modeling The Elastic Ball

In LS-DYNA when the elastic modulus was low there was nodal penetration and hour glassing in the dynamic stiffness simulation. To circumvent this obstacle the visco-elastic model was used with $G_0 \approx G_\infty$. The properties of the balls can be seen in table 4.10. Ball model 17 was chosen as the standard ball.

Table 4.10: Properties of the elastic balls.

Code	ρ (lb/in^3)	k (Msi)	G_0 (ksi)	G_∞ (ksi)	β
16	3.97E-05	0.10	0.500	0.501	6.8E+10
17*	3.97E-05	0.10	0.850	0.851	6.8E+10
18	3.97E-05	0.10	1.200	1.201	6.8E+10
19	3.97E-05	0.10	1.650	1.651	6.8E+10

*** Standard ball**

The force-displacement curves of each ball can be seen in figure 4.51.

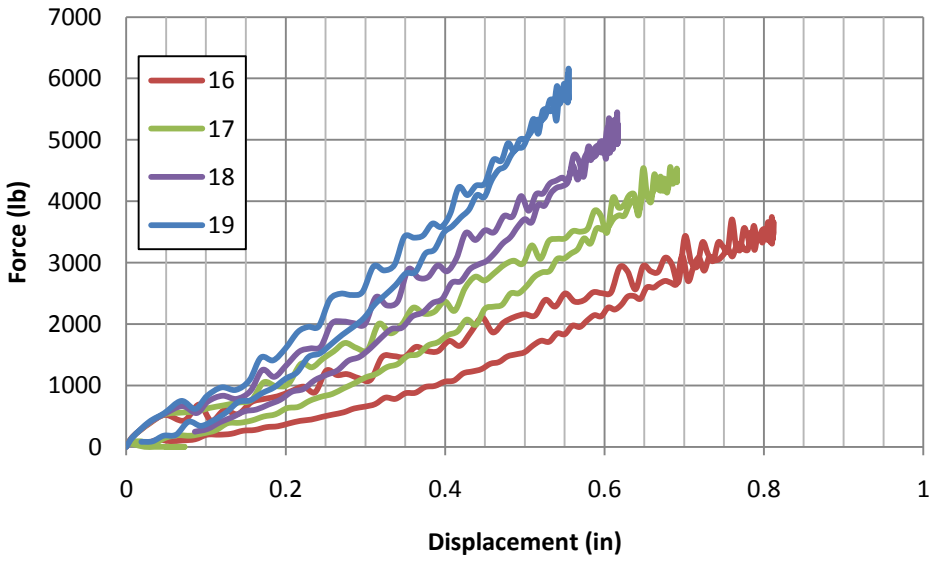

Figure 4.51: The force-displacement curves for the elastic balls.

The elastic models response was slightly non-linear. The hysteresis seen in figure 4.43 was likely due to computational accuracy.

As expected the different methods of obtaining the dynamic stiffness were numerically closer for elastic balls. The performance of the dynamic stiffness simulations can be seen in table 4.11.

Table 4.11: Performance of the dynamic stiffness simulations for the elastic balls.

		Dynamic Stiffness (lb/in)			
Code	**CCOR**	k_F	k_x	k_v	k_t
16	0.858	4422	4622	4832	4699
17*	0.877	6486	6563	6642	6860
18	0.890	9369	8843	8346	8809
19	0.901	11977	11104	10295	10534

*** Standard ball**

The CCOR of the elastic balls were higher than the visco-elastic model with relatively the same stiffness. For the elastic balls the percent difference range between k_F and k_x was -7% to 5%, between k_F and k_v the range was -14% to 9%, and between k_F and k_t the range was -12% to 6%. The sine fit method (equation 3.10, k_t) matched the other methods better with the elastic model. A representative force-time curve and sine fit curve can be seen in figure 4.52.

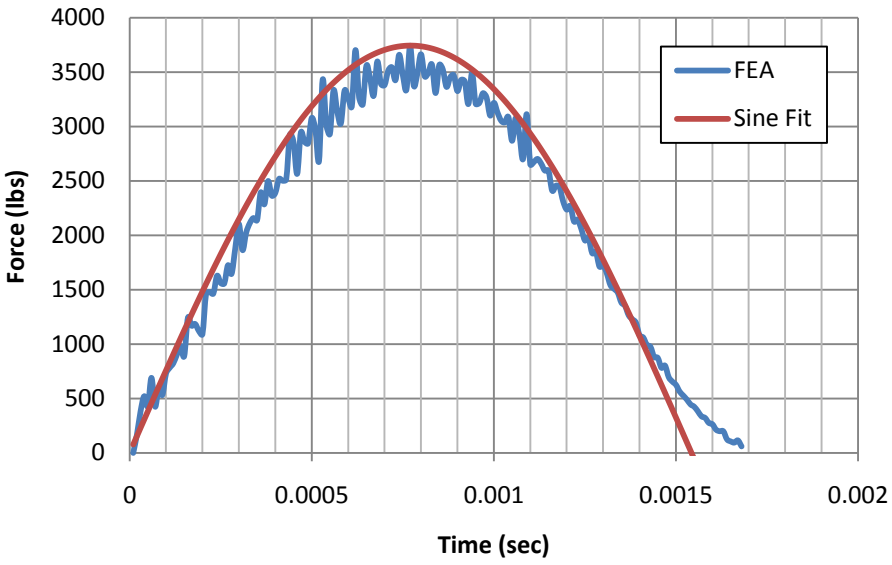

Figure 4.52: The representative force-displacement curve and the sine fit for an elastic ball.

4.8.2. Bat Performance and Normalizing With The Elastic Ball

In elastic balls the trampoline effect was minimized so the stiffness was the dominating factor in bat performance. The rebound velocity of the bat ball collision can be seen in figure 4.53.

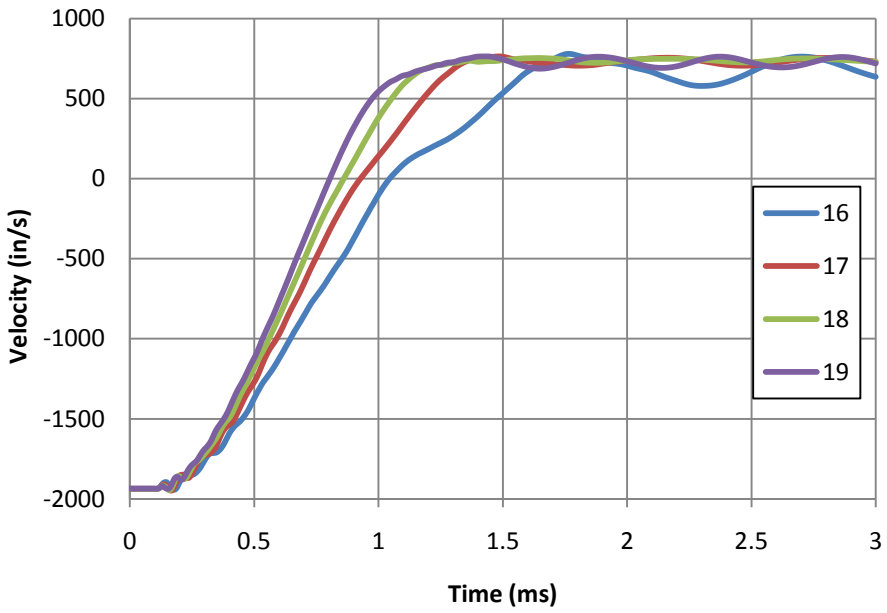

Figure 4.53: Velocity profiles of the elastic balls.

The rebound speed was taken from the center of mass of the ball and on balls 16 and 19 the bat impact excited a nodal frequency causing the center of mass of the ball to oscillate. The oscillations absorbed energy lowering the average rebound velocity (figure 4.45) and the performance.

The normalizing method (equation 2.25) was performed with the elastic balls on the medium performance bat. The normalizing results can be seen in table 4.12 and figure 4.54.

Table 4.12: Results of normalizing with the medium performance bat and the elastic balls.

Ball Model Number	e_0	k_T (lb/in)	Bat Stiffness (lb/in)	e_T	e_N	BBS (mph)	NBBS (mph)
16	0.858	4422	41040	0.847	0.862	**125.0**	**126.3**
17*	0.877	6486	33166	0.876	0.876	**127.4**	**127.4**
18	0.890	9369	28039	0.883	0.871	**128.0**	**127.0**
19	0.901	11977	22977	0.873	0.861	**127.2**	**126.1**

*** Standard ball**

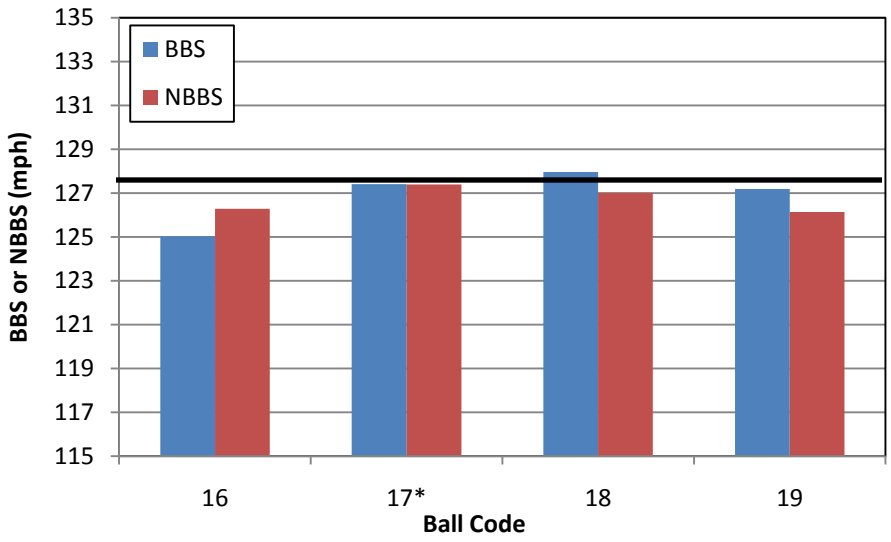

Figure 4.54: Normalizing results of the elastic balls on the medium performance bat.

The range of BBS was 2.9 mph and after normalizing the range was reduced to 1.3 mph a 57% improvement. The range was small and model 19 had a lower BBS than model 17 despite having a high CCOR and stiffness causing the NBBS to be even lower. The range was small because an elastic ball minimizes the trampoline effect in a hollow bat and where or little energy was dissipated in the collision. Thus, elastic balls were not ideal candidates to study the trampoline effect.

4.9. Energy Dissipation In The Dynamic Stiffness Simulation of The Numeric Model

The CCOR is a measure of the total energy loss during impact. The total energy loss (E_{TL}) during the dynamic stiffness simulation was found by,

$$\boldsymbol{E_{TL} = \left(\frac{1}{2} m v_i^2\right)(1 - e^2)} \qquad (4.7)$$

Energy was dissipated during deformation and restoration. If x_m was the maximum displacement, the dissipated energy from the deformation phase, E_L, is,

$$\boldsymbol{E_L = \frac{1}{2}(mv_i^2 - Fx_m)} \tag{4.8}$$

The energy loss during the dynamic stiffness simulation for the visco-elastic balls can be seen in table 4.13.

Table 4.13: Energy loss during the dynamic stiffness simulation.

Model Number	E_{TL} (lb-in)	E_L (lb-in)	% Loss During Deformation	CCOR	Dynamic Stiffness (lb/in)
1	1444	988	68%	0.298	6721
2	1398	877	63%	0.343	6195
3	1388	840	61%	0.352	6397
4	1375	810	59%	0.363	6244
5*	1368	781	57%	0.369	6227
6	1353	773	57%	0.382	6333
7	1340	748	56%	0.393	6336
8	1309	703	54%	0.417	6297
9	1257	624	50%	0.454	6267
10	1366	826	60%	0.371	4689
11*	1368	781	57%	0.369	6227
12	1364	784	57%	0.373	9857
13	1367	812	59%	0.371	11339
14	1278	689	54%	0.439	4583
15	1428	889	62%	0.314	9752

*** Standard ball**

The results showed that most of the energy loss occurs during deformation. The percent loss during deformation ranged from 50% to 68%. There was a linear correlation with energy loss during deformation and CCOR as seen in figure 4.55.

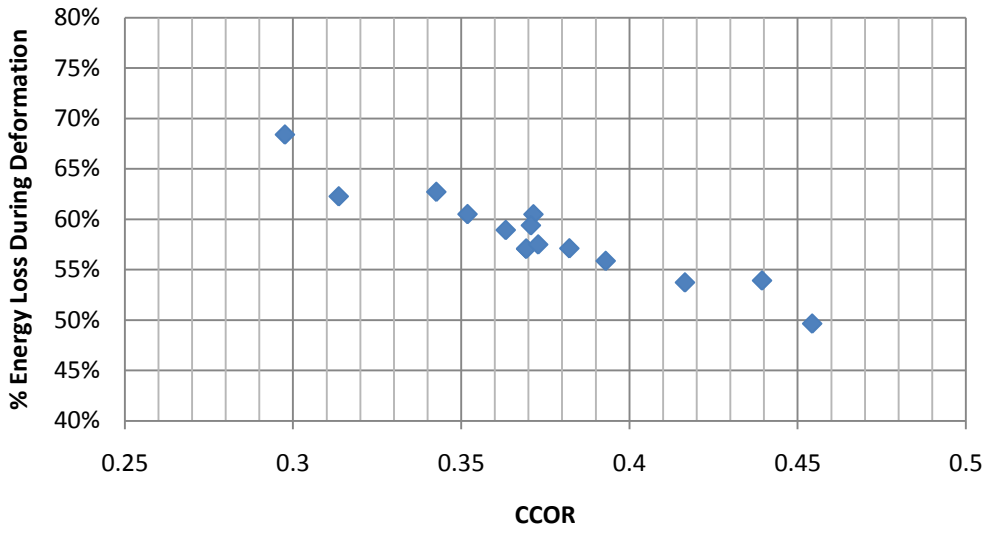

Figure 4.55: The correlation between energy loss during deformation and CCOR.

The simple spring model used for developing the normalizing equations assumes no dissipation during the compression stage and all of it occurring in the restoration stage through equations 2.18 and 2.19. The fact that most of the energy was dissipated in the compression stage could be a factor in the short comings of the normalizing model.

4.9.1. Energy Dissipation In the Experimental Data

To check if the large energy dissipation during deformation in the dynamic stiffness simulation was a product of the numeric model, the energy dissipation was found for the experimental balls from table 3.1 as seen in table 4.14.

Table 4.14: Energy dissipation in the experimental data.

Ball model	E_{LT} (lb-in)	E_L (lb-in)	% Loss during deformation	CCOR	Dynamic Stiffness (lb/in)
A9044ASAWR*	1348	370	27%	0.373	5716
SX44RLA3*	1339	358	27%	0.371	5687
UC12S	1346	355	26%	0.322	7187
MP-RP-Y	1186	232	20%	0.442	4003
AK-EZ-USSSA-Y	1310	313	24%	0.327	8497

*** Standard Ball.**

The experimental results show that most of the energy loss occurs on restoration not deformation this in contrast to the numeric model despite having relatively the same range in CCOR and dynamic stiffness. The percent loss during deformation ranged from 20% to 27%. There was also no linear correlation with energy loss during deformation and CCOR that was seen with the numeric model. The results showed that large energy dissipation during deformation was a product of the numeric model. While ongoing work seeks to improve the numeric ball model, a substantial portion of the dissipated energy (1/4) occurs during deformation.

4.10. Normalized Bat Performance Dependence on r_N

Normalizing through equation 2.24 has been shown to be effective, except when $e_T \approx e_{0T}$, suggesting a high dependence on r_N. Table 4.15 shows r_N for all the bats. Figure 4.56 shows the low, medium and high performance bats' dependence on r_N. The quantity NBBS – BBS* was the amount that NBBS differs from the bat performance with a standard ball.

Table 4.15: Bat models dependence on r_N in the FEA model.

			Bat Performance					
			Low		Medium		High	
Ball Model	CCOR	DS (lb/in)	r_N	NBBS-BBS*	r_N	NBBS-BBS*	r_N	NBBS-BBS*
1	0.298	6721	33.3	-0.4	8.6	-1.4	5.0	-1.6
2	0.343	6195	33.3	-0.4	7.9	-0.8	4.7	-0.9
3	0.352	6397	30.1	-0.2	7.5	-0.5	4.5	-0.6
4	0.363	6244	29.6	-0.1	7.3	-0.2	4.4	-0.3
5*	0.369	6227	28.0	0.0	7.0	0.0	4.2	0.0
6	0.382	6333	29.3	-0.1	7.2	-0.1	4.3	-0.2
7	0.393	6336	30.0	-0.2	7.2	-0.1	4.3	-0.2
8	0.417	6297	28.1	0.0	6.8	0.4	4.1	0.3
9	0.454	6267	26.6	0.2	6.4	0.8	3.9	0.7
10	0.371	4689	190.7	-2.6	9.3	-2.0	5.5	-2.4
11*	0.369	6227	28.0	0.0	7.0	0.0	4.2	0.0
12	0.373	9857	15.4	2.2	5.4	2.2	3.5	1.8
13	0.371	11339	14.0	2.7	5.1	2.8	3.5	2.0
14	0.439	4583	-3317.4	-3.1	8.7	-1.5	5.2	-2.0
15	0.314	9752	18.2	1.5	6.1	1.3	3.8	1.0

*** Standard ball**

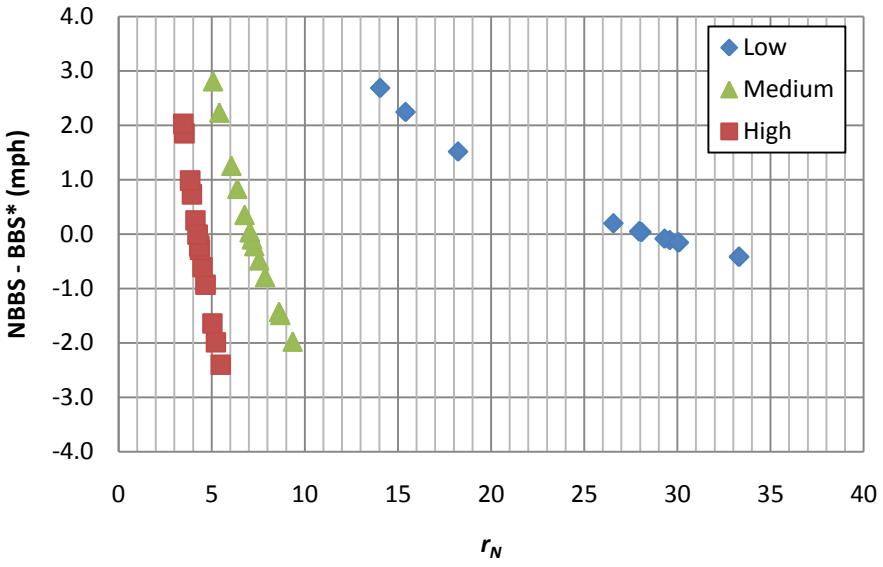

Figure 4.56: The normalized bat performance dependence on r_N.

Data points with large r_n (i.e. $e_{0T} \approx e_T$) were omitted from figure 4.48 (ball model 10 and 14 with the low performing bat). Figure 4.48 shows strong correlation with r_N and the amount that

NBBS was off of BBS. Form the work in previous sections it was observed that normalizing for CCOR was better than normalizing for dynamic stiffness. Figures 4.57 and 4.58 confirm that NBBS's dependence on r_N was due to the balls dynamic stiffness and not on CCOR.

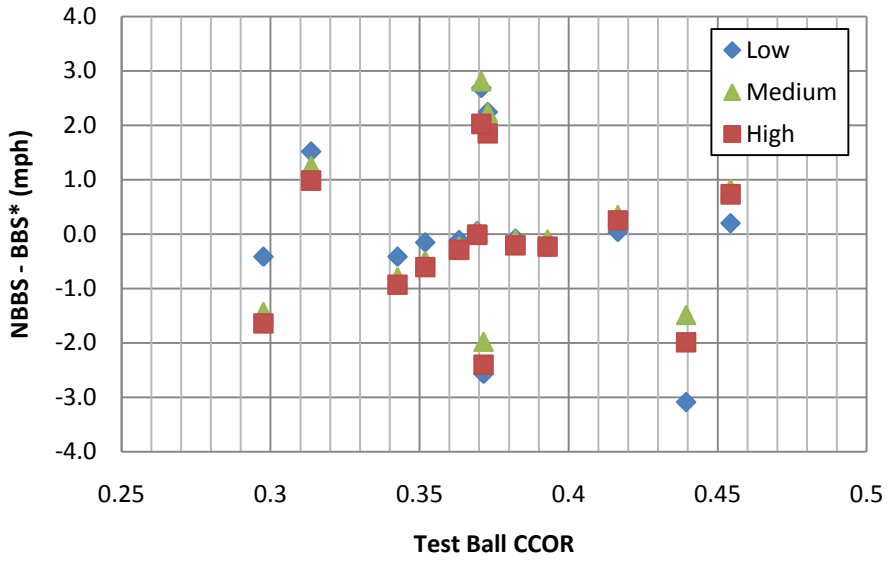

Figure 4.57: Correlation between CCOR and how far normalizing was under or over correcting.

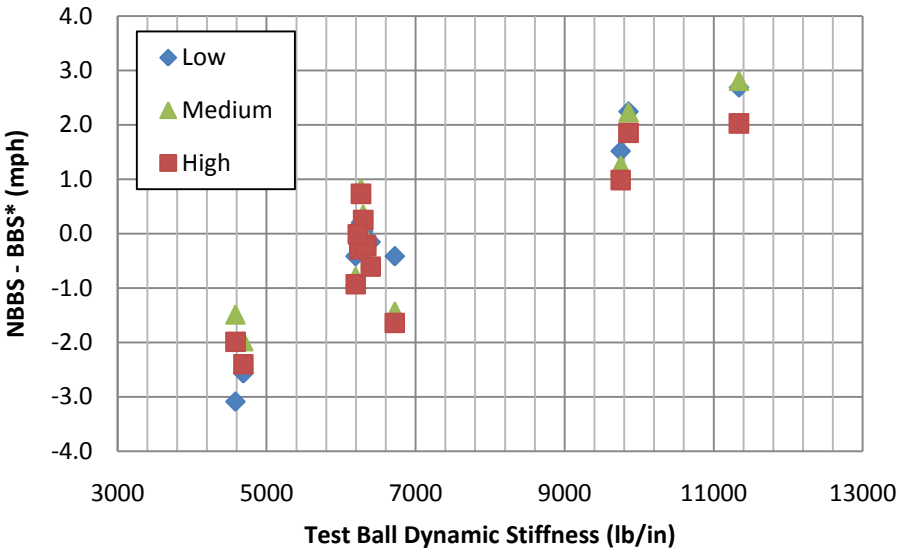

Figure 4.58: Correlation between dynamic stiffness and how far normalizing was under or over correcting.

How far normalizing was under or over correcting was highly dependent on dynamic stiffness and there was no such correlation with CCOR. The highly linear correlation between NBBS – BBS* and dynamic stiffness shown in figure 4.50 illustrates that normalizing with dynamic stiffness leaves the NBBS short by the same amount for all bats. Since normalizing for dynamic stiffness has the same linear effect on any bat an equation of the line in figure 4.50 can be used to correct for any bat. With this conclusion we arrive at Faber's First Empirical Law of Normalizing in the Numerical Model:

Faber's First Empirical Law of Normalizing in the Numerical Model

All corrections on a hollow bat in the numeric model is governed by,

$$\boldsymbol{NBBS_F = NBBS - F_n} \quad (4.9)$$

$$\boldsymbol{F_n = -4.4 + 0.0006 * k_T} \quad (4.10)$$

This correction improved the range of performance in all three cases. The normalizing data for the low performance, medium performance, and high performance bats can be seen in figure 4.59, figure 4.60, and figure 4.61 respectfully.

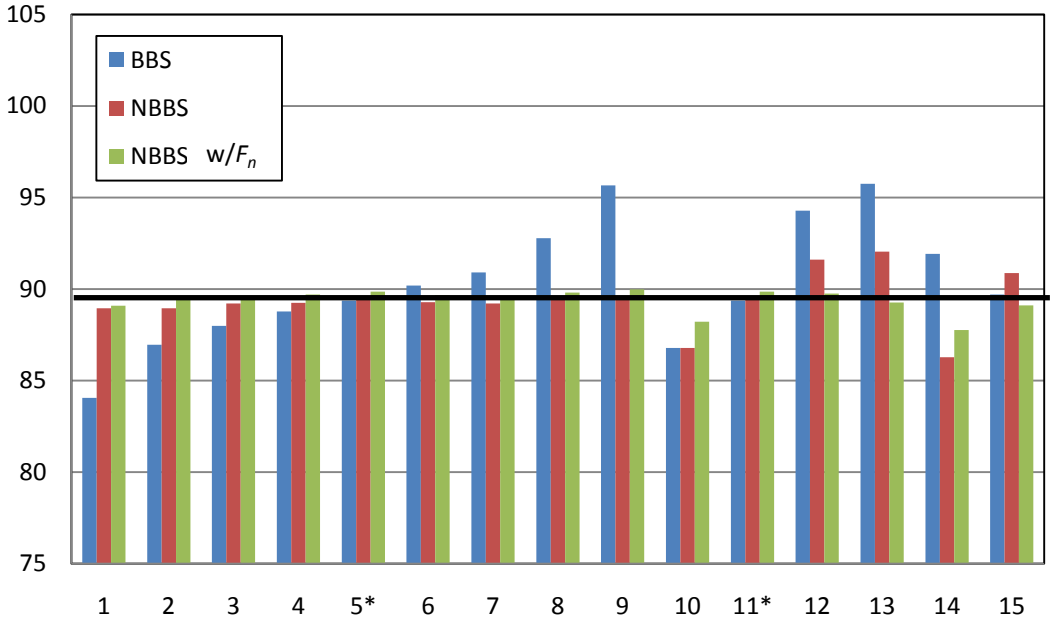

Figure 4.59: Comparing normalizing using F_n on the low performance bat.

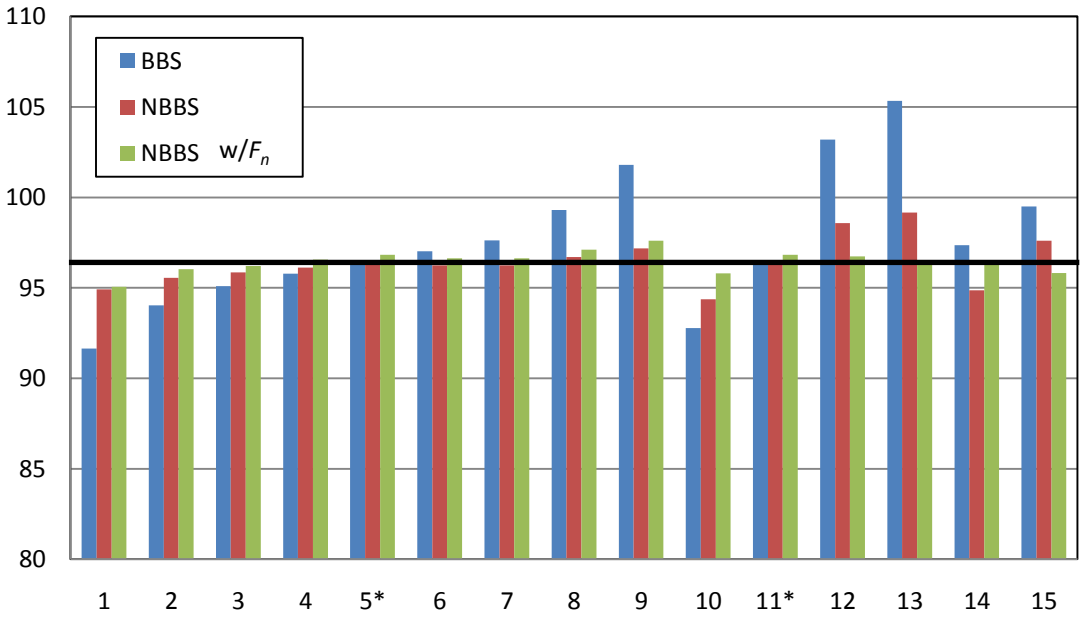

Figure 4.60: Comparing normalizing using F_n on the medium performance bat.

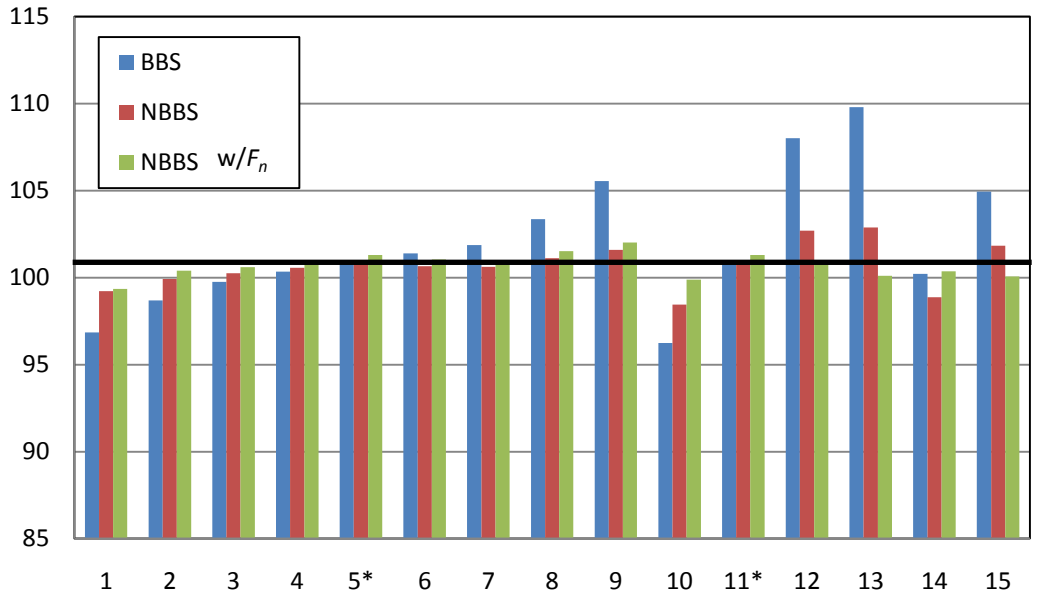

Figure 4.61: Comparing normalizing using F_n on the high performance bat.

By using F_n, the normalized range decreased from 5.8 mph to 2.2 mph for the low performance bat, from 4.8 mph to 2.6 mph for the medium performance bat and from 4.4 mph to 2.7 mph for the high performance bat.

4.10.1. Experimental Data's Dependence on r_N.

To determine if normalized bat performance's dependence on r_N was a product of the numeric model or if it transcends to experimental data, r_N was found for the data presented in chapter 3. Figure 4.62 shows the wood bat's (BW01) dependence on r_N with the balls found in table 3.4. Figure 4.63 shows the medium (MC90) and high (ASA25) performance bat's dependence on r_N with the balls found in table 3.5 and 3.6 respectively.

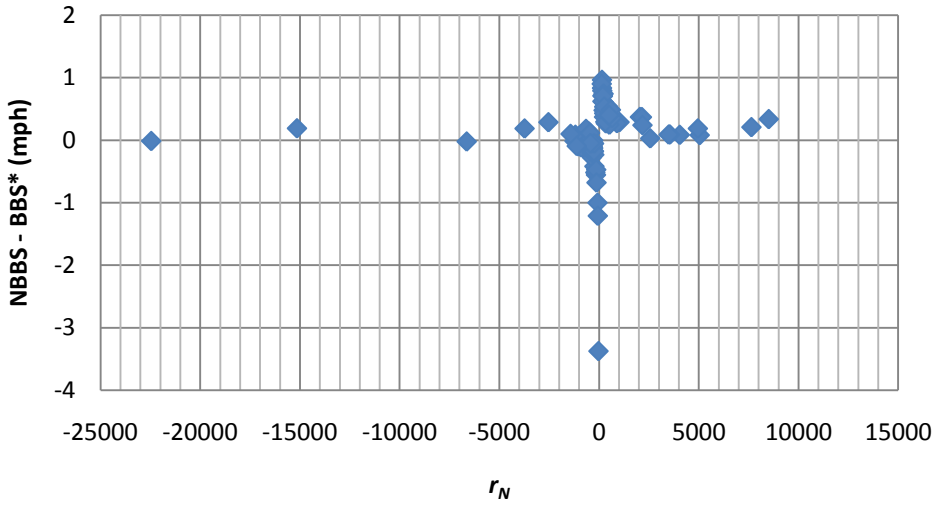

Figure 4.62: The normalized bat performance's dependence on r_N with the wood bat (BW01).

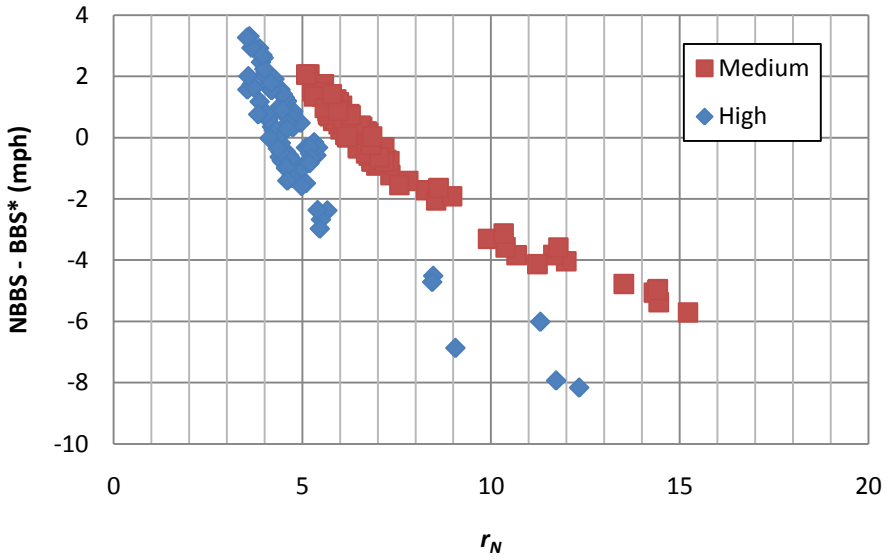

Figure 4.63: The normalized bat performance's dependence on r_N with the medium (MC90) and high (ASA25) performance bats.

The wood bat had a different trend than the medium and high performing bats due to $e_T \approx e_{0T}$ causing negative and large values. The medium and high performing bats had the same trend

seen in the numeric data (figure 4.48). Figures 4.64 and 4.65 show the dependence of NBBS on r_N with CCOR and dynamic stiffness respectively.

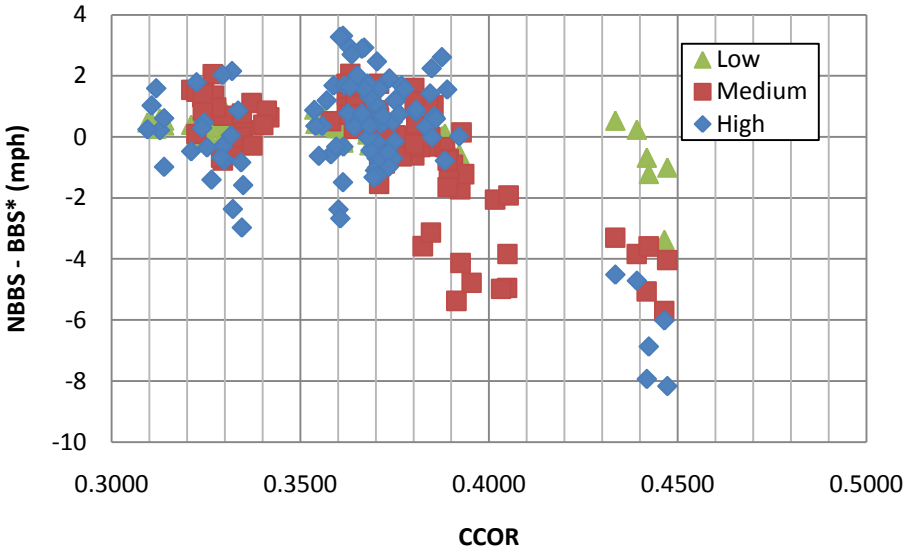

Figure 4.64: Correlation between CCOR and how far normalizing was under or over correcting.

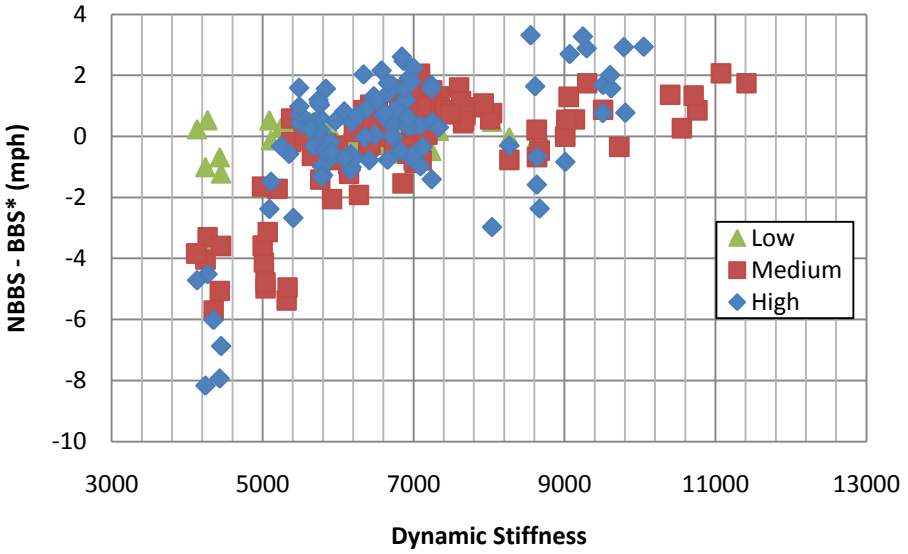

Figure 4.65: Correlation between dynamic stiffness and how far normalizing was under or over correcting.

There was a lot of scatter in figures 4.56 and 4.57 but it did appear to correlate linearly with dynamic stiffness with the hollow bats, and the largest discrepancy was with balls that were low in dynamic stiffness. Fitting the data in figure 4.57 resulted in,

$$F_e = -5.6 + 0.0008 * k_T \tag{4.11}$$

Using this correction on the medium and high performance bats along with equation 4.9 improved the range in normalizing. The normalizing data for the medium and high performance bats can be seen in figure 4.66 and figure 4.67 respectfully.

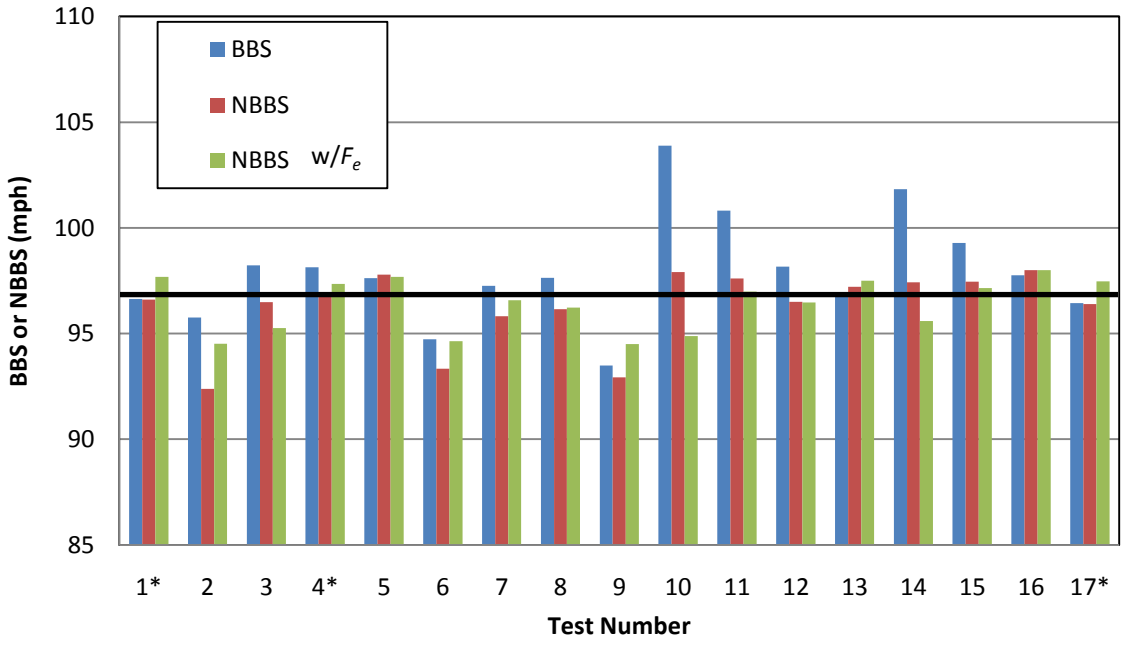

Figure 4.66: Comparing normalizing using F_e on the medium performance bat.

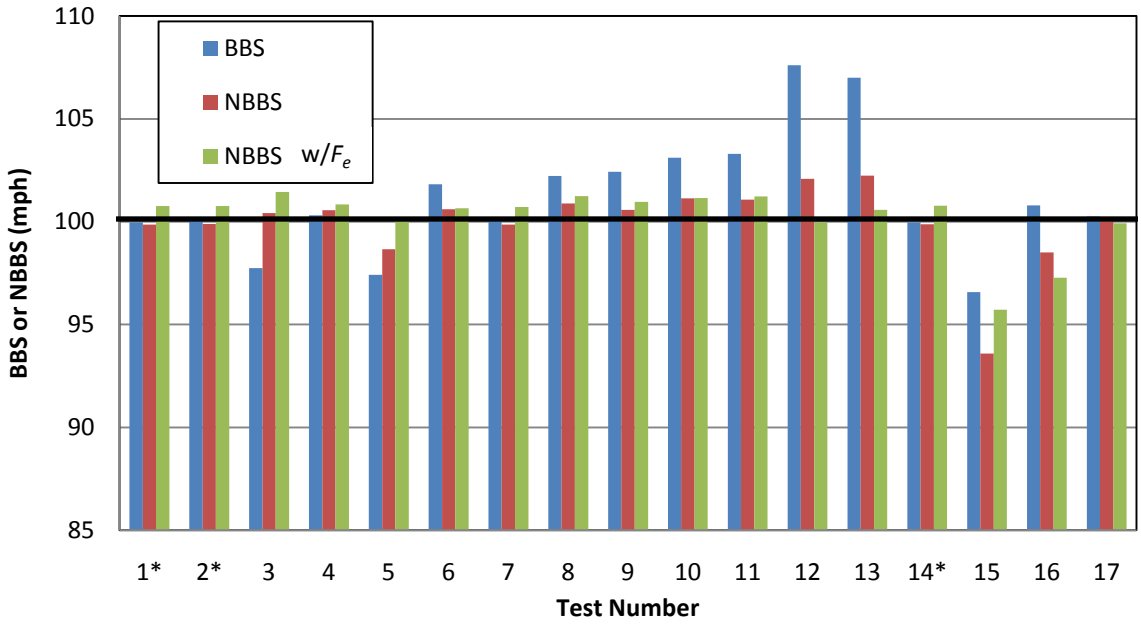

Figure 4.67: Comparing normalizing using F_e on the high performance bat.

By using with F_e, the normalized range decreased from 5.6 mph to 3.5 mph for the medium performance bat and from 8.7 mph to 5.7 mph for the medium performance bat.

This was an empirical solution found on three particular bats. If a smaller range of test ball dynamic stiffness and was confirmed to be consistent it would not be unforeseeable to have an empirical correction in normalizing.

4.11. Summary

The dynamic stiffness test was modeled numerically to find the stiffness and CCOR of balls with different properties. Dynamic stiffness was found with the four equations developed in chapter 3. The trends for all four experimental dynamic stiffness solutions were similar numerically.

The bat test was modeled after a single wall aluminum bat. The performance of the bat was varied by changing the elastic modulus of the aluminum simulating a changing the wall thickness. This allowed the performance of the bat to change without changing the length, weight or MOI. The normalizing procedure was completed on three bats. Normalizing for CCOR worked well. Normalizing for dynamic stiffness did not work as well. It was found that bat stiffness decreased with increasing ball stiffness and stayed constant with CCOR. The varying bat stiffness was a contributing factor why normalizing for dynamic stiffness had a large range in normalizing. The changing bat stiffness was normalized and it improved the range in NBBS.

It was observed in the numerical model that the short coming of normalizing with e_N was through r_N when $e_T \approx e_{0T}$. This occurs with balls of low stiffness and with balls of low CCOR and high dynamic stiffness. This can be avoided if the range in dynamic stiffness and CCOR was limited.

It was observed that bat COR (e_1) was not one and not constant as the normalizing procedure assumed and it was particularly low for the low performance bat. It was found that low stiffness balls result in a low e_1 and was amplified with a low performing bat. Including e_1 in normalizing did not reduce the range in performance. The assumption that $e_1 = 1$ appeared partially responsible for the poor normalized performance.

A range of $0.352 < e_T < 0.417$ and 6227 lb/in $< k_T <$ 6397 lb/in resulted in a range of -0.6 mph < NBBS-BBS* < 0.7 mph for the low, medium and high performance bats. The range in e_T was similar to experimental data, however the range in k_T was not. The range for k_T was small because the sample size for balls that varied in k_T was small (only four balls).

REFERENCES

[4.1] **Smith, Lloyd V. and Duris, Joseph G.** *Progress and challenges in numerically modelling solid sports balls with application to softballs.* February 15, 2009, Journal of Sports Sciences, pp. 353-360.

[4.2] **Duris, J. G.** Experimental and Numerical Characterization of Softballs. *Unpublished Master's Thesis, Washington State University.* 2004.

[4.3] **Cruz, C. M.** Characterizing Softball Bat Modifications and Their Resulting Performance Effects. s.l. : MS Thesis, Washington State University, May 2005.

Chapter Five

Summary

5.1. Summary

The main focus of this work was reducing the effect of ball properties and understanding the mechanisms in bat performance measurements.

The three properties of the ball that effected bat performance were the weight, elasticity, and stiffness. The ball was non-linear and being such the ball was temperature, humidity, and strain-rate dependent. The metrics for elasticity and stiffness used in this study reflect a high-speed impact. Using a high-speed ball cannon the elasticity and stiffness were successfully categorized in context of a bat-ball collision through CCOR and dynamic stiffness.

Three bats of differing performance were used: a low performance wood bat, a medium performance composite bat and a high performance composite bat. The bats were tested with a range of balls with properties varying in weight, CCOR and dynamic stiffness. Normalizing was performed on the bats through the normalized collision efficiency, e_{AN}. The nominal value for CCOR was 0.37 and for dynamic stiffness was 5800 lb/in. It was found that CCOR normalizing works better than dynamic stiffness normalizing.

It was discovered that with balls of low dynamic stiffness and balls of low CCOR and high dynamic stiffness $e_T \approx e_{0T}$ causing r_N to become large and in some cases negative, making the correction for dynamic stiffness small.

From the experimental data it was recommended that for the bat performance test e_T be between 0.33 and 0.38 and k_T be between 5600 lb/in and 7000 lb/in. When the properties of the ball were in between these values the range of BBS with the low performing bat was 3.8 mph,

the range with the medium performing bat was 1.8 mph and the range of the high performing bat was 2.5 mph, however all three bats normalized to ± 0.6 mph of the BBS for the standard ball (e_{0N} = 0.37, k_N = 5800 lb/in).

Using the finite element modeling program, LS-DYNA, the ball and bat were modeled using a visco-elastic material for the ball and elastic material for the bat. In the FEA program the BBS performance test was modeled and the results were normalized. To isolate competing effects balls of varying CCOR and constant dynamic stiffness and balls with varying dynamic stiffness and constant CCOR were modeled. The normalizing procedure corrected the BBS for ball CCOR but did not correct enough for dynamic stiffness. In further analysis it was found that the bat stiffness changes with ball dynamic stiffness and not with CCOR. The changing bat stiffness was normalized and the correction in BBS became much better. It was also concluded that there was more energy loss in the bat then the normalizing procedure assumes.

5.2. Future Work

The work presented here was able to provide a comprehensive analysis the normalizing procedure for BBS. However, there were multiple issues that arose in the course of this investigation.

The FEA ball contact time closely match the experimental data in the dynamic stiffness simulation. However, the model had a significantly different force-time curve then in the experimental data. It was unclear how much of an effect this has on the normalizing procedure but probably affects the energy loss during the bat-ball impact. Having an FEA model that matches the experimental data better may address this issue.

The FEA model showed that the bat stiffness decreases with ball stiffness. For balls that have typical stiffness used in experimental testing (~6000 lb/in) the bat stiffness did not significantly change. A procedure was developed to normalize for changing bat stiffness. Having a way to find bat stiffness experimentally would account for these changes. Also it was unclear how the bat stiffness changes along the length of the barrel and how much of an effect that has on normalizing.

The normalizing procedure assumes that there was no energy loss in the bat upon impact or that the bat coefficient of restitution, e_1, was one. The FEA model showed that it was not one and for some cases it was rather low, particularly for balls with low dynamic stiffness. It was unclear how much a factor the model has on e_1 and if the strain rate was closer to experimental data if e_1 would become closer to one.

The normalizing procedure was built by assuming that the ball behaves like a linear spring. However, the ball was made from polyurethane a non-linear material, it was suggested that if the normalizing procedure was formulated around a non-linear spring then the BBS would normalized.

APPENDIX ONE

Standard Test Ball Data

Table A1.1: Standard test ball static and dynamic properties.

WSU Code	Manufacturer	Model	Avg Comp (lb)	COR	Dyn Stiff	CCOR
N1440	DeMarini	A9044 ASA WR	374	0.443	5890	0.372
N1511	DeMarini	A9044 ASA WR	373	0.449	5707	0.372
N1529	DeMarini	A9044 ASA WR	374	0.443	5614	0.373
N1547	DeMarini	A9044 ASA WR	368	0.444	5551	0.372
N1551	DeMarini	A9044 ASA WR	362	0.445	5659	0.372
N1561	DeMarini	A9044 ASA WR	375	0.439	5756	0.372
N1562	DeMarini	A9044 ASA WR	367	0.438	5614	0.372
N1584	DeMarini	A9044 ASA WR	366	0.442	5693	0.372
N1585	DeMarini	A9044 ASA WR	367	0.443	5852	0.373
N1586	DeMarini	A9044 ASA WR	369	0.443	5692	0.370
N1587	DeMarini	A9044 ASA WR	374	0.444	5791	0.375
N1588	DeMarini	A9044 ASA WR	372	0.444	5616	0.375
N1589	DeMarini	A9044 ASA WR	374	0.443	5967	0.376
N1590	DeMarini	A9044 ASA WR	374	0.442	5920	0.377
N1591	DeMarini	A9044 ASA WR	363	0.444	5952	0.377
N1592	DeMarini	A9044 ASA WR	365	0.444	5892	0.376
N1596	DeMarini	A9044 ASA WR	374	0.445	5784	0.375
N1597	DeMarini	A9044 ASA WR	375	0.442	5856	0.378
N1599	DeMarini	A9044 ASA WR	373	0.445	5816	0.371
N1600	DeMarini	A9044 ASA WR	361	0.437	5626	0.375
N1601	DeMarini	A9044 ASA WR	353	0.445	5702	0.375
N1602	DeMarini	A9044 ASA WR	367	0.438	5767	0.371
N1603	DeMarini	A9044 ASA WR	365	0.437	5745	0.374
N1604	DeMarini	A9044 ASA WR	370	0.445	5971	0.377
N1605	DeMarini	A9044 ASA WR	359	0.439	5879	0.374
N1608	DeMarini	A9044 ASA WR	359	0.445	5586	0.371
N1609	DeMarini	A9044 ASA WR	372	0.440	5693	0.372
N1610	DeMarini	A9044 ASA WR	361	0.444	5586	0.371
N1611	DeMarini	A9044 ASA WR	363	0.441	5471	0.365
N1612	DeMarini	A9044 ASA WR	365	0.440	5637	0.372
N1613	DeMarini	A9044 ASA WR	369	0.442	5472	0.375
N1614	DeMarini	A9044 ASA WR	364	0.435	5932	0.375
N1615	DeMarini	A9044 ASA WR	358	0.437	5948	0.370
N1617	DeMarini	A9044 ASA WR	362	0.435	5661	0.370
N1618	DeMarini	A9044 ASA WR	374	0.441	5727	0.373
N1619	DeMarini	A9044 ASA WR	360	0.438	5704	0.373
N1620	DeMarini	A9044 ASA WR	366	0.439	5645	0.374

N1621	DeMarini	A9044 ASA WR	363	0.441	5546	0.374
N1623	DeMarini	A9044 ASA WR	362	0.444	5658	0.373
N1625	DeMarini	A9044 ASA WR	365	0.438	5875	0.375
N1627	DeMarini	A9044 ASA WR	365	0.443	5781	0.375
N1628	DeMarini	A9044 ASA WR	375	0.445	5513	0.377
N1629	DeMarini	A9044 ASA WR	362	0.443	5791	0.375
N1632	DeMarini	A9044 ASA WR	361	0.435	5714	0.370
N1633	DeMarini	A9044 ASA WR	373	0.441	5881	0.373
N1634	DeMarini	A9044 ASA WR	367	0.445	5660	0.373
N1636	DeMarini	A9044 ASA WR	372	0.444	5673	0.374
N1637	DeMarini	A9044 ASA WR	351	0.445	5989	0.376
N1638	DeMarini	A9044 ASA WR	363	0.443	5697	0.375
N1639	DeMarini	A9044 ASA WR	362	0.443	5589	0.375
N1641	DeMarini	A9044 ASA WR	360	0.443	5720	0.376
N1642	DeMarini	A9044 ASA WR	354	0.445	5531	0.373
N1649	DeMarini	A9044 ASA WR	361	0.442	5669	0.375
N1650	DeMarini	A9044 ASA WR	365	0.441	5577	0.368
N1651	DeMarini	A9044 ASA WR	363	0.440	5596	0.368
N1652	DeMarini	A9044 ASA WR	373	0.442	5636	0.371
W260	Worth	SX44RLA3	351	0.445	5910	0.373
W261	Worth	SX44RLA3	373	0.445	5968	0.373
W266	Worth	SX44RLA3	363	0.442	5897	0.372
W269	Worth	SX44RLA4	360	0.442	5805	0.370
W275	Worth	SX44RLA3	363	0.444	5722	0.373
W278	Worth	SX44RLA3	371	0.443	5967	0.373
W284	Worth	SX44RLA3	351	0.445	5966	0.375
W294	Worth	SX44RLA3	351	0.450	5595	0.371
W305	Worth	SX44RLA3	367	0.443	5801	0.373
W307	Worth	SX44RLA3	354	0.443	5867	0.371
W309	Worth	SX44RLA3	352	0.445	5782	0.373
W310	Worth	SX44RLA3	357	0.444	5625	0.365
W312	Worth	SX44RLA3	358	0.444	5777	0.374
W314	Worth	SX44RLA3	361	0.445	5808	0.375
W315	Worth	SX44RLA3	354	0.440	6174	0.374
W321	Worth	SX44RLA3	352	0.445	6127	0.375
W326	Worth	SX44RLA3	353	0.443	5859	0.371
W331	Worth	SX44RLA3	357	0.442	6068	0.376
W332	Worth	SX44RLA3	356	0.444	6033	0.371
W333	Worth	SX44RLA3	352	0.443	6100	0.374
W335	Worth	SX44RLA3	355	0.442	6130	0.377
W336	Worth	SX44RLA3	351	0.443	6080	0.374
W337	Worth	SX44RLA3	350	0.441	5883	0.374
W338	Worth	SX44RLA3	352	0.443	6182	0.374
W345	Worth	SX44RLA3	365	0.442	5870	0.372
W348	Worth	SX44RLA3	360	0.440	5710	0.366
W350	Worth	SX44RLA3	360	0.444	5753	0.370
W351	Worth	SX44RLA3	356	0.443	5655	0.373

W352	Worth	SX44RLA3	355	0.444	5579	0.377
W353	Worth	SX44RLA3	359	0.445	5557	0.369
W357	Worth	SX44RLA3	352	0.443	5855	0.373
W365	Worth	SX44RLA3	347	0.442	5795	0.372
W366	Worth	SX44RLA3	360	0.444	5784	0.372
W367	Worth	SX44RLA3	355	0.445	5782	0.373
W368	Worth	SX44RLA3	353	0.441	5519	0.368
W369	Worth	SX44RLA3	353	0.442	5562	0.371
W372	Worth	SX44RLA3	353	0.444	5736	0.370
W374	Worth	SX44RLA3	366	0.440	5543	0.369
W376	Worth	SX44RLA3	356	0.443	5820	0.373
W377	Worth	SX44RLA3	364	0.445	5711	0.377
W378	Worth	SX44RLA3	362	0.441	5775	0.374
W379	Worth	SX44RLA3	356	0.440	5882	0.373
W380	Worth	SX44RLA3	351	0.445	5858	0.373
W381	Worth	SX44RLA3	369	0.438	5435	0.370
W382	Worth	SX44RLA3	367	0.442	5769	0.373
W383	Worth	SX44RLA3	353	0.445	5728	0.371
W384	Worth	SX44RLA3	359	0.440	5535	0.370
W386	Worth	SX44RLA3	356	0.442	5488	0.369
W393	Worth	SX44RLA3	364	0.438	5684	0.369
W394	Worth	SX44RLA3	352	0.438	5580	0.368
W395	Worth	SX44RLA3	357	0.438	5718	0.371
W396	Worth	SX44RLA3	357	0.441	5700	0.370
W397	Worth	SX44RLA3	363	0.443	5791	0.370
W398	Worth	SX44RLA3	359	0.444	5930	0.371
W400	Worth	SX44RLA3	358	0.445	5756	0.369
W401	Worth	SX44RLA3	353	0.443	5473	0.369
W402	Worth	SX44RLA3	357	0.444	5606	0.367
W403	Worth	SX44RLA3	357	0.441	5540	0.366
		Average	**362**	**0.442**	**5755**	**0.372**
		max	**375**	**0.450**	**6182**	**0.378**
		min	**347**	**0.435**	**5435**	**0.365**
		std	**7**	**0.003**	**166**	**0.003**

APPENDIX TWO

Sample pre-processor input code used for the dynamic stiffness model.

```
$---+----1----+----2----+----3----+----4----+----5----+----6----+----7----+----8
$ LS-DYNA(970) DECK WRITTEN BY : eta/FEMB-PC version 28.0
$ TEMPLATE #: 20040810
$  ENGINEER :
$   PROJECT :
$     UNITS : IN, LB*SEC^2/IN, SEC, LB
$      TIME : 12:29:50 PM
$      DATE : Monday, November 21, 2008
$---+----1----+----2----+----3----+----4----+----5----+----6----+----7----+----8
*KEYWORD
$---+----1----+----2----+----3----+----4----+----5----+----6----+----7----+----8
*TITLE
LS-DYNA USER INPUT
$---+----1----+----2----+----3----+----4----+----5----+----6----+----7----+----8
$                                                                              $
$                                  CONTROL CARD                                $
$                                                                              $
$---+----1----+----2----+----3----+----4----+----5----+----6----+----7----+----8
*CONTROL_TERMINATION
$   ENDTIM    ENDCYC     DTMIN    ENDENG    ENDMAS
    0.0030         0       0.0       0.0       0.0
$---+----1----+----2----+----3----+----4----+----5----+----6----+----7----+----8
$                                                                              $
$                           DATABASE CONTROL FOR ASCII                         $
$                                                                              $
$---+----1----+----2----+----3----+----4----+----5----+----6----+----7----+----8
*DATABASE_NODOUT
$        DT    BINARY
  0.000010         1
*DATABASE_RCFORC
$        DT    BINARY
  0.000010         1
$---+----1----+----2----+----3----+----4----+----5----+----6----+----7----+----8
$                                                                              $
$                            DATABASE HISTORY CARDS                            $
$                                                                              $
$---+----1----+----2----+----3----+----4----+----5----+----6----+----7----+----8
*DATABASE_HISTORY_NODE
$^HISTORY_1
$     NID1      NID2      NID3      NID4      NID5      NID6      NID7      NID8
      1943
$---+----1----+----2----+----3----+----4----+----5----+----6----+----7----+----8
$                                                                              $
$                                  PART CARDS                                  $
$                                                                              $
$---+----1----+----2----+----3----+----4----+----5----+----6----+----7----+----8
*PART
BALL
$      PID     SECID       MID     EOSID      HGID      GRAV    ADPOPT      TMID
         2         1         1         0         0         0         0         0
*PART
CYLINDER
$      PID     SECID       MID     EOSID      HGID      GRAV    ADPOPT      TMID
         3         1         2         0         0         0         0         0
$---+----1----+----2----+----3----+----4----+----5----+----6----+----7----+----8
$                                                                              $
$                                SECTION CARDS                                 $
$                                                                              $
$---+----1----+----2----+----3----+----4----+----5----+----6----+----7----+----8
*SECTION_SOLID_TITLE
P-1
$    SECID    ELFORM       AET
         1         1         0
$---+----1----+----2----+----3----+----4----+----5----+----6----+----7----+----8
$                                                                              $
$                                MATERIAL CARDS                                $
$                                                                              $
$---+----1----+----2----+----3----+----4----+----5----+----6----+----7----+----8
*MAT_VISCOELASTIC_TITLE
```

```
M-1
$      MID        RO      BULK         G0         GI      BETA
         1 0.00003971.0000E+07   20000.0    1000.0   68000.0
*MAT_ELASTIC_TITLE
M-2
$      MID        RO         E         PR         DA         DB
         2  0.0007363.0000E+07       0.30        0.0        0.0
$---+----1----+----2----+----3----+----4----+----5----+----6----+----7----+----8
$                                                                              $
$                              SEGMENT SET CARDS                               $
$                                                                              $
$---+----1----+----2----+----3----+----4----+----5----+----6----+----7----+----8
*SET_SEGMENT_TITLE
```

Master and Slave Node Information

```
$---+----1----+----2----+----3----+----4----+----5----+----6----+----7----+----8
$                                                                              $
$                                NODE SET CARDS                                $
$                                                                              $
$---+----1----+----2----+----3----+----4----+----5----+----6----+----7----+----8
*SET_NODE_LIST_TITLE
```

Nodes and Node Sets Information

```
$---+----1----+----2----+----3----+----4----+----5----+----6----+----7----+----8
$                                                                              $
$                              BOUNDARY SPC CARDS                              $
$                                                                              $
$---+----1----+----2----+----3----+----4----+----5----+----6----+----7----+----8
*BOUNDARY_SPC_NODE_ID
```

Boundary Condition Information

```
$---+----1----+----2----+----3----+----4----+----5----+----6----+----7----+----8
$                                                                              $
$                            INITIAL VELOCITY CARDS                            $
$                                                                              $
$---+----1----+----2----+----3----+----4----+----5----+----6----+----7----+----8
*INITIAL_VELOCITY
$     NSID    NSIDEX     BOXID    IRIGID
         1         0         0
$       VX        VY        VZ       VXR       VYR       VZR
       0.0   -1408.0       0.0       0.0       0.0       0.0
$---+----1----+----2----+----3----+----4----+----5----+----6----+----7----+----8
$                                                                              $
$                                CONTACT CARDS                                 $
$                                                                              $
$---+----1----+----2----+----3----+----4----+----5----+----6----+----7----+----8
*CONTACT_SURFACE_TO_SURFACE
$^CONTACT1
$      SSID      MSID     SSTYP     MSTYP    SBOXID    MBOXID       SPR       MPR
         1         2         0         0         0         0         0         0
$       FS        FD        DC        VC       VDC    PENCHK        BT        DT
       0.0       0.0       0.0       0.0       0.0         0 0.01.0000E+20
$      SFS       SFM       SST       MST      SFST      SFMT       FSF       VSF
       1.0       1.0       0.0       0.0       1.0       1.0       1.0       1.0
$---+----1----+----2----+----3----+----4----+----5----+----6----+----7----+----8
$                                                                              $
$                              NODE INFORMATION                                $
$                                                                              $
$---+----1----+----2----+----3----+----4----+----5----+----6----+----7----+----8
```

Node Information

```
$---+----1----+----2----+----3----+----4----+----5----+----6----+----7----+----8
$                                                                              $
$                            ELEMENTS INFORMATION                              $
$                                                                              $
$---+----1----+----2----+----3----+----4----+----5----+----6----+----7----+----8
$---+----1----+----2----+----3----+----4----+----5----+----6----+----7----+----8
$                                                                              $
$                              SOLID ELEMENTS                                  $
$                                                                              $
$---+----1----+----2----+----3----+----4----+----5----+----6----+----7----+----8
*ELEMENT_SOLID
```

Sample pre-processor input code used for the bat model.

```
$---+----1----+----2----+----3----+----4----+----5----+----6----+----7----+----8
$ LS-DYNA(970) DECK WRITTEN BY : eta/FEMB-PC version 28.0
$ TEMPLATE #: 20040810
$  ENGINEER :
$   PROJECT :
$     UNITS : IN, LB*SEC^2/IN, SEC, LB
$      TIME : 04:48:52 PM
$      DATE : Thursday, September 29, 2008
$---+----1----+----2----+----3----+----4----+----5----+----6----+----7----+----8
*KEYWORD
$---+----1----+----2----+----3----+----4----+----5----+----6----+----7----+----8
*TITLE
LS-DYNA USER INPUT
$---+----1----+----2----+----3----+----4----+----5----+----6----+----7----+----8
$                                                                               $
$                                  CONTROL CARD                                 $
$                                                                               $
$---+----1----+----2----+----3----+----4----+----5----+----6----+----7----+----8
*CONTROL_TERMINATION
$   ENDTIM    ENDCYC     DTMIN    ENDENG    ENDMAS
    0.0030         0       0.0       0.0       0.0
$---+----1----+----2----+----3----+----4----+----5----+----6----+----7----+----8
$                                                                               $
$                           DATABASE CONTROL FOR ASCII                          $
$                                                                               $
$---+----1----+----2----+----3----+----4----+----5----+----6----+----7----+----8
*DATABASE_NODOUT
$       DT    BINARY
  0.000010         1
*DATABASE_RCFORC
$       DT    BINARY
  0.000010         1
*DATABASE_ELOUT
$       DT    BINARY
  0.000010         3
$---+----1----+----2----+----3----+----4----+----5----+----6----+----7----+----8
$                                                                               $
$                          DATABASE CONTROL FOR BINARY                          $
$                                                                               $
$---+----1----+----2----+----3----+----4----+----5----+----6----+----7----+----8
*DATABASE_BINARY_D3PLOT
$  DT/CYCL      LCDT      BEAM     NPLTC
   0.00010         0         0         0
$    IOOPT
         0
$---+----1----+----2----+----3----+----4----+----5----+----6----+----7----+----8
$                                                                               $
$                             DATABASE HISTORY CARDS                            $
$                                                                               $
$---+----1----+----2----+----3----+----4----+----5----+----6----+----7----+----8
*DATABASE_HISTORY_NODE
$^HISTORY_1
$     NID1      NID2      NID3      NID4      NID5      NID6      NID7      NID8
    168239    106060    132389
*DATABASE_HISTORY_TSHELL
$^HISTORY_2
$     TID1      TID2      TID3      TID4      TID5      TID6      TID7      TID8
     60357     60358     60481
$---+----1----+----2----+----3----+----4----+----5----+----6----+----7----+----8
$                                                                               $
$                                  PART CARDS                                   $
$                                                                               $
$---+----1----+----2----+----3----+----4----+----5----+----6----+----7----+----8
*PART
BALL
$      PID     SECID       MID     EOSID      HGID      GRAV    ADPOPT      TMID
         2         2         4         0         0         0         0         0
*PART
KNOB
$      PID     SECID       MID     EOSID      HGID      GRAV    ADPOPT      TMID
         5         1         1         0         0         0         0         0
*PART
BAT
$      PID     SECID       MID     EOSID      HGID      GRAV    ADPOPT      TMID
```

```
         6         1         2         0         0         0         0         0
*PART
ENDCAP
$      PID     SECID       MID     EOSID      HGID      GRAV    ADPOPT      TMID
         7         1         3         0         0         0         0         0
$---+----1----+----2----+----3----+----4----+----5----+----6----+----7----+----8
$                                                                               $
$                                SECTION CARDS                                  $
$                                                                               $
$---+----1----+----2----+----3----+----4----+----5----+----6----+----7----+----8
*SECTION_TSHELL_TITLE
P-1
$    SECID    ELFORM      SHRF       NIP     PROPT   QR/IRID     ICOMP
         1         1       1.0         2       1.0         0         0
*SECTION_SOLID_TITLE
P-2
$    SECID    ELFORM       AET
         2         1         0
$---+----1----+----2----+----3----+----4----+----5----+----6----+----7----+----8
$                                                                               $
$                                MATERIAL CARDS                                 $
$                                                                               $
$---+----1----+----2----+----3----+----4----+----5----+----6----+----7----+----8
*MAT_ELASTIC_TITLE
Knob
$      MID        RO         E        PR        DA        DB
         1  0.0002551.0000E+07      0.30       0.0       0.0
*MAT_ELASTIC_TITLE
Bat
$      MID        RO         E        PR        DA        DB
         2  0.0002551.0000E+07      0.30       0.0       0.0
*MAT_ELASTIC_TITLE
Endcap
$      MID        RO         E        PR        DA        DB
         3   0.00179  500000.0      0.28       0.0       0.0
*MAT_VISCOELASTIC_TITLE
Ball
$      MID        RO      BULK        G0        GI      BETA
         4 0.00003971.0000E+07   20000.0    1000.0   68000.0
$---+----1----+----2----+----3----+----4----+----5----+----6----+----7----+----8
$                                                                               $
$                              SEGMENT SET CARDS                                $
$                                                                               $
$---+----1----+----2----+----3----+----4----+----5----+----6----+----7----+----8
```

Master and Slave Node Information

```
$---+----1----+----2----+----3----+----4----+----5----+----6----+----7----+----8
$                                                                               $
$                                NODE SET CARDS                                 $
$                                                                               $
$---+----1----+----2----+----3----+----4----+----5----+----6----+----7----+----8
```

Nodes and Node Set Information

```
$---+----1----+----2----+----3----+----4----+----5----+----6----+----7----+----8
$                                                                               $
$                              BOUNDARY SPC CARDS                               $
$                                                                               $
$---+----1----+----2----+----3----+----4----+----5----+----6----+----7----+----8
*BOUNDARY_SPC_NODE_ID
$       ID
         5
$      NID       CID      DOFX      DOFY      DOFZ     DOFRX     DOFRY     DOFRZ
    114401         0         1         1         0         0         0         0
         6
    114405         0         1         1         0         0         0         0
         7
    132257         0         1         1         0         0         0         0
         8
    132261         0         1         1         0         0         0         0
$---+----1----+----2----+----3----+----4----+----5----+----6----+----7----+----8
$                                                                               $
$                            INITIAL VELOCITY CARDS                             $
$                                                                               $
$---+----1----+----2----+----3----+----4----+----5----+----6----+----7----+----8
*INITIAL_VELOCITY
```

```
$     NSID    NSIDEX     BOXID    IRIGID
         2         0         0
$       VX        VY        VZ       VXR       VYR       VZR
       0.0   -1936.0       0.0       0.0       0.0       0.0
$---+----1----+----2----+----3----+----4----+----5----+----6----+----7----+----8
$                                                                              $
$                                CONTACT CARDS                                 $
$                                                                              $
$---+----1----+----2----+----3----+----4----+----5----+----6----+----7----+----8
*CONTACT_SURFACE_TO_SURFACE
$^CONTACT1
$     SSID      MSID     SSTYP     MSTYP    SBOXID    MBOXID       SPR       MPR
         1         2         0         0         0         0         0         0
$       FS        FD        DC        VC       VDC    PENCHK        BT        DT
       0.0       0.0       0.0       0.0       0.0         0  0.01.0000E+20
$      SFS       SFM       SST       MST      SFST      SFMT       FSF       VSF
       1.0       1.0       0.0       0.0       1.0       1.0       1.0       1.0
$---+----1----+----2----+----3----+----4----+----5----+----6----+----7----+----8
$                                                                              $
$                              NODE INFORMATION                                $
$                                                                              $
$---+----1----+----2----+----3----+----4----+----5----+----6----+----7----+----8
```

Node Numbers and Coordinate Information

```
$---+----1----+----2----+----3----+----4----+----5----+----6----+----7----+----8
$                                                                              $
$                            ELEMENTS INFORMATION                              $
$                                                                              $
$---+----1----+----2----+----3----+----4----+----5----+----6----+----7----+----8
$---+----1----+----2----+----3----+----4----+----5----+----6----+----7----+----8
$                                                                              $
$                                MASS ELEMENTS                                 $
$                                                                              $
$---+----1----+----2----+----3----+----4----+----5----+----6----+----7----+----8
```

Mass Information

```
$---+----1----+----2----+----3----+----4----+----5----+----6----+----7----+----8
$                                                                              $
$                                SOLID ELEMENTS                                $
$                                                                              $
$---+----1----+----2----+----3----+----4----+----5----+----6----+----7----+----8
```

Solid Node Information

```
$---+----1----+----2----+----3----+----4----+----5----+----6----+----7----+----8
$                                                                              $
$                            THICK SHELL ELEMENTS                              $
$                                                                              $
$---+----1----+----2----+----3----+----4----+----5----+----6----+----7----+----8
```

Thick Shell Node Information